DEVELOPMENT OF HEMP FIBER-REINFORCED FIRE-RESISTANT COMPOSITES FOR SUSTAINABLE MINING VENTILATION SYSTEMS

A Thesis Submitted to the College of Graduate and Postdoctoral Studies

in Partial Fulfillment of the Requirements

for the Degree of Master of Science

In the Department of Mechanical Engineering

University of Saskatchewan

Saskatoon, Saskatchewan

Canada

By

Sadman Sakib

PERMISSION TO USE

In presenting this thesis in partial fulfillment of the requirements for a Postgraduate degree from the University of Saskatchewan, I agree that the Libraries of this University may make it freely available for inspection. I further agree that permission for copying of this thesis in any manner, in whole or in part, for scholarly purposes may be granted by the professor or professors who supervised my thesis work or, in their absence, by the Head of the Department or the Dean of the College in which my thesis work was done. It is understood that any copying or publication or use of this thesis or parts thereof for financial gain shall not be allowed without my written permission. It is also understood that due recognition shall be given to me and to the University of Saskatchewan in any scholarly use which may be made of any material in my thesis.

Requests for permission to copy or to make other use of material in this thesis in whole or part should be addressed to:

Head of Mechanical Engineering
57 Campus Drive
University of Saskatchewan
Saskatoon, Saskatchewan S7N 5A9, Canada

Dean
College of Graduate and Postdoctoral Studies
University of Saskatchewan
116 Thorvaldson Building, 110 Science Place
Saskatoon, Saskatchewan S7N 5C9, Canada

ABSTRACT

Saskatchewan's economy thrives on two critical sectors: agriculture and mining. With an increasing focus on sustainability, this research aligns with Saskatchewan's growing emphasis on agricultural waste management and sustainable mining operations. The hemp industry, in particular, has seen a significant rise in production within Saskatchewan and across Canada, creating opportunities to utilize hemp fibers in innovative ways. The sustainable development of materials for the ventilation duct for underground mining operation could have far-reaching impacts on both the agricultural and mining sectors in Saskatchewan, which is an important goal of this research.

To achieve the goal, the hemp fibers were treated with different concentrations of sodium hydroxide (NaOH) to improve their surface properties and compatibility with polymers. In addition, ammonium polyphosphate (APP) was applied in various combinations to further enhance fire resistance. The effectiveness of these treatments was verified through Scanning Electron Microscopy (SEM) analysis, which provided insights into the fiber surface modifications. The treated hemp fibers were used to fabricate nonwoven hemp fiber fabrics. These fabrics underwent a series of mechanical and physical tests, including tensile tests, water absorption tests, and flammability assessments, to determine their suitability for further composite fabrication.

A hand layup method was employed to develop hemp fiber-reinforced polymer composites, with bio-based epoxy resin serving as the matrix. The fiber-to-matrix ratio was maintained at 30:70. A comprehensive range of tests was then conducted on the resulting composites, including tensile, flexural, and Izod impact tests, as well as water absorption tests, density measurements, and flame resistance evaluations using the UL94 vertical and horizontal flame tests. Additional performance assessments, such as cone calorimeter tests, thermal conductivity evaluations, and Thermogravimetric Analysis (TGA), were performed to further investigate the material's thermal stability and fire resistance properties. These tests provided a thorough understanding of the mechanical, thermal, and fire-resistant capabilities of the developed composites.

To optimize the manufacturing parameters for the hemp fiber-reinforced polymer composites, a Taguchi L9 orthogonal array was used for the experimental design. Linear regression analysis was carried out using MINITAB software to develop predictive equations for key performance indicators. Among these equations, the most influential ones were identified and subsequently applied to a multi-objective optimization process using genetic algorithm (GA) in MATLAB Global Optimization Tool. The optimization process focused on improving the composite's mechanical and thermal performance by fine-tuning the manufacturing parameters, including fiber treatment concentrations and resin formulations.

This research presents a sustainable pathway for utilizing hemp fiber in the development of fire-resistant composites, particularly for underground mining applications. By combining agricultural waste management with innovations in material science, the study not only contributes to reducing environmental impact but also offers a practical solution for creating safer and more sustainable mining operations.

ACKNOWLEDGEMENT

I am deeply grateful to my supervisors, Professor Chris Zhang and Dr. Satyanarayan Panigrahi. Professor Zhang's unwavering faith in me, invaluable lessons, and constant support throughout this journey have been instrumental in my academic growth. Dr. Panigrahi, a true mentor, provided exceptional guidance, expert opinions, and the resources and funding that made this research possible. His insights have been a cornerstone of my work, and I am truly appreciative of his support.

I sincerely thank Professsor Venkatesh Meda for his guidance and administrative support, which were crucial in navigating the complexities of this project.

I would like to express my sincere gratitude to Professor Assem Hedayat for his invaluable support and guidance as the external examiner. His expertise, insightful feedback, and encouragement have significantly contributed to the quality of this work.

I would like to express my heartfelt gratitude to the faculty, staff, and technical personnel of the College of Engineering for their tremendous support throughout my research journey. Their invaluable technical assistance, guidance, and access to advanced machinery and equipment have been instrumental in the successful completion of my work. The collaborative environment and unwavering encouragement provided by the College of Engineering have significantly enriched my academic experience. I am truly grateful for the generosity, expertise, and continuous support, which have played a crucial role in my research and professional growth.

Special thanks to Dr. G. Liu for his invaluable help with microscopy at the Microscopy Core Facility, Department of Biology, University of Saskatchewan.

I would like to extend my sincere gratitude to NRC-IRAP and the Agricultural Development Funding of Saskatchewan for their invaluable financial support, which has significantly contributed to the success of my research. I am also deeply appreciative of Saskatchewan Polytechnic's Innovative Manufacturing Centre (IMC) and the Biomaterials Testing and

Prototyping (B-TAP) facilities—including the B-TAP fiber processing center in Hafford, SK, and the B-TAP certified testing center in Saskatoon, SK—for providing access to state-of-the-art equipment, technical expertise, and research facilities. Their support has played a crucial role in advancing my work on natural fiber-based composites, and I am truly grateful for their commitment to fostering innovation and sustainable material development.

I would like to express my sincere appreciation to Engineer Faria Binta Amin for her support in mold making and fiber processing. Her expertise and insightful recommendations have greatly contributed to the refinement of my research methodology and the successful execution of key fabrication processes.

Finally, I thank my parents for their inspiration, love, and encouragement, which have been the foundation of my perseverance and success.

TABLE OF CONTENT

LIST OF TABLES

LIST OF FIGURES

LIST OF ABBREVIATIONS

ATH	Aluminum trihydrate
APP	Ammonium polyphosphate
AFP	Automated fiber placement
DOE	Design of experiment
DSC	Differential scanning calorimetry
FCBPSS	F: Function, C: Context, B: Behavior, P: Principle, S: Sate, S: Structure
FBS	Function-Behaviour-State
GA	Genetic algorithms
T_g	Glass transition temperature
GHG	Greenhouse gas
HRR	Heat release rate
$Mg(OH)_2$	Magnesium hydroxide
CH_4	Methane
NFC	Natural fiber composites
N_2O	Nitrous oxide
PHRR	Peak heat release rate
RTM	Resin transfer molding
SEM	Scanning electron microscopy
NaOH	Sodium hydroxide
TGA	Thermal gravimetric analysis
THR	Total heat release
TSM	Towards sustainable mining
VOD	Ventilation-on-demand
WMI	Whitehorse mining initiative
WPC	Wood-plastic composites
ZB	Zinc borate

CHAPTER 1

INTRODUCTION

1.1 Overview

Agriculture and mining are two cornerstone industries in Saskatchewan, playing vital roles in the province's economy. In the region, agriculture contributes a significant amount to GDP, with crops such as hemp emerging as sustainable resources. However, the management of agricultural waste poses environmental challenges. On the other hand, the mining sector, which underpins Saskatchewan’s resource economy, is under increasing pressure to adopt environmentally responsible and safer practices. The integration of these two industries offers a unique opportunity to develop innovative solutions, fostering sustainability and safety while addressing pressing environmental issues.

Underground mining operations depend heavily on efficient ventilation systems to ensure the safety of workers and machinery. Ventilation ducts, a critical component of these systems, facilitate the circulation of air, maintaining a breathable and safe working environment. Traditionally, these ducts have been made from synthetic materials, which have a number of drawbacks, including severe flammability, limited recyclability, and significant environmental impact. The need for an eco-friendly, durable, and fire-resistant alternative to synthetic ventilation ducts is urgent.

Agricultural byproducts like hemp fiber provide a sustainable solution to this challenge. Hemp fibers, with their high strength, availability, and ease of modification, are ideal candidates for developing bio-based composites. By combining these fibers with flame-retardant additives like ammonium polyphosphate (APP), it is possible to produce fire-resistant materials with superior mechanical and thermal properties. This study explores the potential of hemp fiber-reinforced polymer composites as a sustainable alternative for mining ventilation ducts, addressing both environmental and safety concerns.

The motivation behind this research stems from multiple factors. First, Saskatchewan's agricultural industry produces large quantities of hemp byproducts, which remain underutilized. Transforming this agricultural waste into high-value composites aligns with the principles of circular economy and sustainable development. Second, the mining industry faces increasing regulatory and societal demands for environmentally friendly practices. Developing bio-based ventilation ducts not only reduces reliance on synthetic materials but also enhances mining safety through improved fire resistance and mechanical performance. Finally, the abundance and modifiability of hemp fibers make them an excellent resource for engineering applications .

The study employs a systematic approach, starting with the preparation of nonwoven hemp mats treated with varying concentrations of NaOH and APP. The chemical treatments modify the fiber surface, enhancing bonding with the matrix and imparting flame retardancy. The treated fibers are then incorporated into epoxy resin using the hand layup method, a widely used composite fabrication technique. The resulting composites are subjected to rigorous mechanical, thermal, and flame resistance tests to evaluate their suitability for underground mining applications.

1.2 Motivation

Sustainability lies at the core of this research, addressing the pressing need to minimize the environmental footprint of industrial processes. By utilizing hemp fibers, a renewable and biodegradable resource, the study provides a sustainable alternative to synthetic fibers traditionally used in composite materials. This approach aligns with global efforts to mitigate climate change by reducing reliance on petrochemical-based polymers and minimizing industrial waste. Moreover, the research transforms agricultural by-products into high-value materials, contributing to circular economy practices. The incorporation of bio-based epoxy resin further emphasizes the commitment to eco-friendly material solutions, showcasing a pathway toward sustainable manufacturing and resource utilization.

This research has significant implications for Saskatchewan's economy, which thrives on agriculture and mining. With the rise of hemp production in the province, the study leverages a locally abundant resource to create innovative materials, stimulating growth in the agricultural sector. By connecting agriculture with mining through the development of advanced composites

for industrial applications, the study fosters economic diversification and job creation in Saskatchewan. Furthermore, promoting the use of locally sourced and processed materials reduces transportation costs and carbon emissions, providing both environmental and economic benefits. This research not only strengthens Saskatchewan's position as a leader in sustainable materials innovation but also supports regional industries in adapting to global sustainability trends.

Safety in mining operations is a critical concern, and this research addresses it by developing fire-resistant composite materials for underground ventilation systems. Mining environments are prone to fire hazards, making the development of materials with enhanced thermal stability and flame resistance an essential priority. By treating hemp fibers with sodium hydroxide and ammonium polyphosphate, the research ensures the composites can withstand high temperatures and resist ignition, thereby protecting miners and reducing the risk of catastrophic incidents. Additionally, the lightweight yet durable properties of the composites contribute to safer and more efficient installation and maintenance in underground operations. This advancement not only enhances worker safety but also promotes the adoption of sustainable practices in an industry often challenged by environmental and safety concerns.

1.3 Objectives

The goal of this research is to develop and optimize sustainable, fire-resistant hemp fiber-reinforced polymer composites for use in underground mining ventilation ducts. To achieve this goal, the following objectives were pursued:

Objective 1: To develop effective treatment methods for hemp fibers to improve their surface properties and compatibility for nonwoven fabric production.

Description: The objective is to enhance the surface properties and compatibility of hemp fibers with the polymer matrix through effective sodium hydroxide (NaOH) treatment. This involves achieving a substantial reduction in lignin and hemicellulose content to improve fiber bonding characteristics and increase surface roughness and wettability. These improvements will be assessed through Scanning Electron Microscopy (SEM) analysis to observe surface modifications and contact angle analysis to

evaluate enhanced surface energy. The treatment aims to produce fibers with significantly improved chemical and physical properties for use in high-performance composite materials.

Objective 2: To fabricate and evaluate hemp fiber-reinforced polymer composites for fire-resistant underground mining ventilation ducts.

Description: The objective is to fabricate hemp fiber-reinforced polymer composites using a bio-based epoxy resin with an optimized fiber-to-matrix ratio, ensuring the material meets stringent performance requirements for underground mining applications. The composites are designed to achieve high fire resistance, while maintaining excellent mechanical properties such as tensile and flexural strength. Additionally, the materials are developed to exhibit low water absorption, ensuring durability and stability in harsh operating environments. These performance metrics are critical for validating the suitability of the composites for demanding industrial applications.

Objective 3: To optimize the manufacturing parameters of hemp fiber-reinforced polymer composites through performance analysis and advanced optimization technique.

Description: The objective is to optimize the manufacturing parameters for hemp fiber-reinforced polymer composites by employing a systematic experimental design approach, such as the Taguchi method, to evaluate the effects of varying chemical treatments and fiber-to-matrix ratios on performance. The optimization process focuses on enhancing key mechanical properties, including tensile and flexural strength, while simultaneously improving thermal and fire-resistant characteristics. Predictive regression models are developed to accurately estimate performance outcomes, and experimental validation ensures the composites meet or exceed established benchmarks. Multi-objective optimization is used to identify efficient trade-offs among mechanical, thermal, and fire-resistance properties, resulting in a balanced and high-performing material.

The major contribution is to identify an economical method for managing agricultural waste and to develop a material through a systematic approach that meets the performance requirements of mining ventilation systems.

1.4 Organization of the thesis

CHAPTER 1: INTRODUCTION

This chapter provides an overview of the research topic, emphasizing the importance of sustainable materials and the challenges faced in agricultural waste management and mining operations. The chapter discusses the motivation behind using hemp fiber-reinforced polymer composites as a solution for underground mining ventilation ducts. Additionally, it outlines the research objectives and contributions

CHAPTER 2: LITERATURE REVIEW

This chapter presents an extensive review of the existing literature. Key areas covered include:

i. Agricultural waste management and sustainable practices
ii. Mining ventilation systems and their material requirements
iii. The mechanical, thermal, and flame-resistant properties of natural fiber composites
iv. Treatment methods for fibers, including alkaline and fire retardant treatments
v. An overview of ammonium polyphosphate and bio-based epoxy resins as key materials for the study

CHAPTER 3: A SYSTEMATIC APPROACH TO NEW MATERIAL DEVELOPMENT AND OPTIMIZATION

This chapter focuses on a structured and systematic approach to new material development, emphasizing optimization techniques and analytical methods to improve material performance in real-world applications. Key areas covered include:

i. A systematic Approach to New Material Development
ii. Taguchi Optimization in Design of Experiment
iii. Regression Analysis
iv. Genetic Algorithm in Parameter Optimization

CHAPTER 4: MATERIALS AND EXPERIMENTAL METHODS

This chapter details the materials, methods, and processes used in the research. It includes:

i. Preparation of hemp fiber and its treatments.
ii. Fabrication techniques, such as the hand layup process for composites.

iii. Description of tests performed to evaluate mechanical, thermal, and flame resistance properties of the composites.
iv. Analytical techniques, including SEM and thermal analysis, used for material characterization

CHAPTER 5: RESULTS AND DISCUSSION

This chapter presents the findings of the research and their interpretations. Key topics include:

i. Mechanical property analysis (tensile, flexural, and impact tests).
ii. Thermal behavior and decomposition characteristics.
iii. Flame resistance performance based on UL94 tests.
iv. Comparison of treated and untreated fibers and the impact of treatments on composite properties.
v. Statistical optimization using experimental data.

CHAPTER 6: CONCLUSIONS AND RECOMMENDATIONS

The final chapter summarizes the key outcomes of the research, highlighting the potential of hemp fiber-reinforced composites for mining ventilation ducts. It also provides recommendations for future research, including improvements in material treatments and further exploration of bio-based materials for industrial applications

CHAPTER 2

LITERATURE REVIEW

2.1 Introduction

The increasing global emphasis on sustainability and resource efficiency has driven research into innovative uses of renewable materials to address critical industrial challenges. Natural plant-based fibers constitute a significant portion of agricultural waste, offering substantial potential for sustainable utilization, yet their utilization in high-performance industrial applications remains underexplored. This research is motivated by the need to develop a new process for producing nonwoven fabrics from natural plant-based fibers, enabling their use in advanced composite materials. By harnessing the structural strength and availability of these fibers, the study aims to provide a sustainable and cost-effective alternative to synthetic materials in industrial applications.

Another key motivation is the systematic transformation of agricultural waste into valuable, high-performing materials suitable for demanding environments, such as underground mining. Agricultural by-products, including bast fibers, often go underutilized or discarded, representing a missed opportunity for sustainable material development. This research focuses on utilizing these renewable resources to develop composite materials for mining ventilation systems, which require exceptional mechanical, thermal, and fire-resistant properties. The integration of agricultural waste into high-value applications not only aligns with circular economy principles but also addresses pressing environmental concerns by reducing waste and reliance on non-renewable resources.

The need to improve the fire resistance and thermal stability of bioplastics in an economically viable way further drives this research. As industries increasingly adopt bio-based polymers for sustainability, enhancing their performance remains a significant challenge, particularly in applications where fire resistance and thermal properties are critical. By combining natural fibers with advanced treatments and bio-based resins, this research aims to develop composites that meet stringent safety and performance requirements without significantly increasing production

costs. Together, these motivations underscore the significance of this study in advancing sustainable material development for industrial applications.

2.2 Overview of sustainable practices in agricultural waste management

Agriculture in Canada produces a lot of waste, such as leftover crops, animal manure, and byproducts from agricultural industries (Friesen, 2019). If this waste is not handled properly, it can cause serious environmental problems, like polluting the soil and water, increasing greenhouse gases, and harming wildlife. Conversely, sustainable agricultural waste management can transform waste into valuable resources like bioenergy, compost, and bioproducts, contributing to a circular economy (Awasthi et al., 2022). In Saskatchewan, the extensive agricultural sector heightens the importance of waste management (Agriculture Sector Overview, n.d.). Proper practices enhance soil health and crop productivity, supporting the long-term viability of the agricultural industry while mitigating environmental impacts Proper practices enhance soil health and crop productivity, supporting the long-term viability of the agricultural industry while mitigating environmental impacts (Koul et al., 2022).

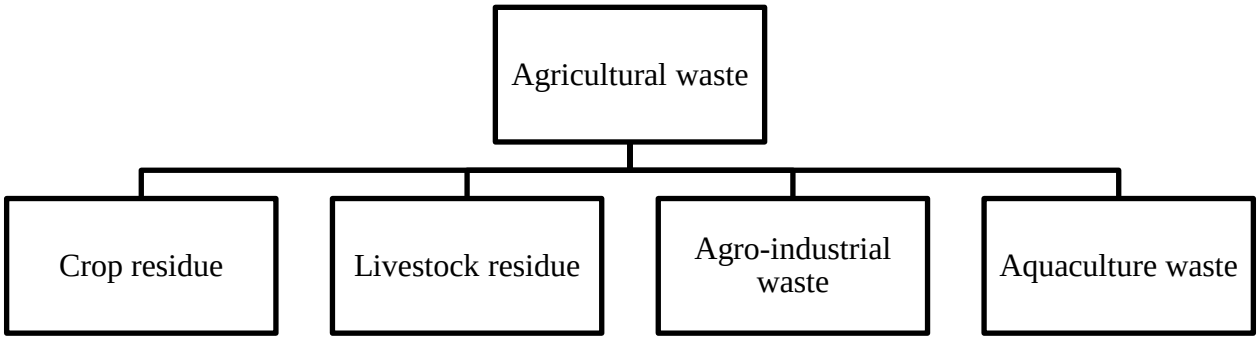

Figure 2.1 Sources of agricultural waste (Nagendran, 2011)

Despite its importance, agricultural waste management in Canada and Saskatchewan faces numerous challenges. Technically, collecting, processing, and transporting agricultural waste is complex and resource-intensive, with variability in waste composition and quantity adding to the difficulty (Cong et al., 2023). Economically, the high initial investment for waste management infrastructure and technologies can be prohibitive, and there is often insufficient market demand for products derived from agricultural waste (Gontard et al., 2018). Innovation to transform agricultural waste into valuable products is also a significant challenge (Haque et al., 2023).

Regulatory and policy challenges, including gaps and inconsistencies in regulations, hinder effective waste management, with enforcement and compliance issues further complicating the situation (Mmereki et al., 2016). Additionally, social and cultural factors, such as the attitudes and perceptions of farmers and communities towards waste management, can impede the adoption of sustainable practices (Rodriguez et al., 2008). Addressing these challenges requires enhanced regulatory frameworks, increased economic incentives, and comprehensive education and awareness campaigns. Successful case studies and initiatives in Saskatchewan highlight the potential benefits of effective waste management, but broader implementation and innovation are essential for significant progress.

Agricultural waste management is critical for achieving environmental sustainability and maximizing resource utilization. The agro wastes are now being handled in different ways as represented in Figure 2.2

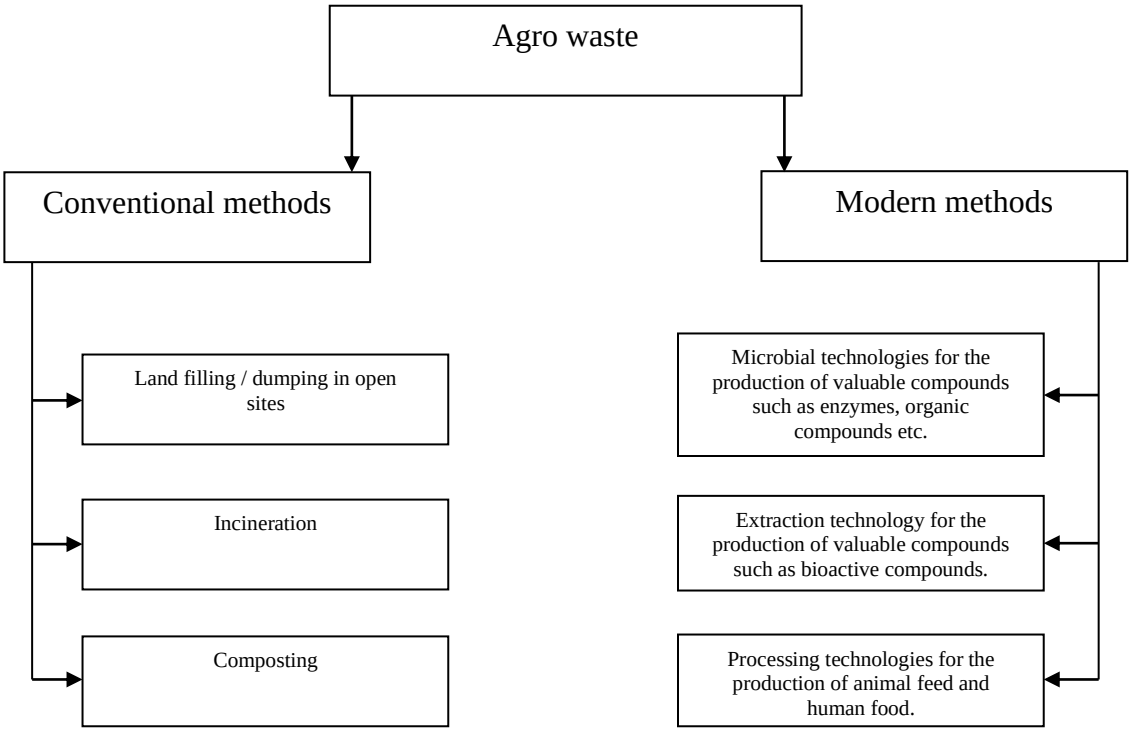

Figure 2.2: Different Management Process of Agro by-products (Ajila et al. 2011)

One of the primary environmental benefits of effective agricultural waste management is the reduction of greenhouse gas (GHG) emissions (Yu et al., 2023). Agricultural activities are significant sources of methane (CH_4) and nitrous oxide (N_2O), potent GHGs (Mishra et al., 2012). Properly managing animal manure through anaerobic digestion can capture methane to produce biogas, a renewable energy source (Obileke et al., 2020). This process not only reduces methane emissions but also generates energy that can replace fossil fuels, further lowering GHG emissions.

Improper disposal of agricultural waste, such as open burning of crop residues and uncontrolled dumping of animal manure, can lead to soil and water pollution. Open burning releases harmful pollutants, including particulate matter and volatile organic compounds, which degrade air quality and contribute to respiratory diseases (Estrellan & Iino, 2010). Moreover, runoff from improperly managed manure can contaminate water bodies with nutrients and pathogens, causing eutrophication and harming aquatic ecosystems (Tiwari & Pal, 2022). Composting and anaerobic digestion are effective practices that stabilize organic waste, reduce pathogen levels, and minimize nutrient leaching, thereby protecting soil and water quality.

Agricultural waste can be a valuable resource for producing bioenergy. Technologies such as anaerobic digestion, gasification, and pyrolysis convert organic waste into biogas, bio-oil, and syngas, respectively (Tao et al., 2022). These renewable energy sources can be used for heating, electricity generation, and transportation fuels, reducing dependence on fossil fuels and enhancing energy security. In regions with abundant agricultural residues, such as Saskatchewan, bioenergy production from agricultural waste presents a significant opportunity for sustainable energy development.

Agricultural residues are rich in cellulose, hemicellulose, and lignin, making them suitable for producing various value-added products. For example, natural fibers from crop residues like flax, hemp, and jute can be used to create biodegradable composites, textiles, and paper products (Murali et al., 2022). These materials offer environmentally friendly alternatives to synthetic fibers and plastics, reducing pollution and resource depletion. Additionally, agricultural waste

can be processed into bio-based chemicals, bioplastics, and pharmaceuticals, creating new economic opportunities and promoting the circular economy (Priya et al., 2023).

Recycling agricultural waste into organic fertilizers is a sustainable way to enhance soil fertility. Composting transforms crop residues and animal manure into nutrient-rich compost, which can be applied to fields to improve soil structure, increase nutrient availability, and promote healthy plant growth (Siedt et al., 2021). Using organic fertilizers reduces the reliance on chemical fertilizers, which can degrade soil health over time. By returning organic matter to the soil, agricultural waste management practices help maintain long-term soil productivity and sustainability.

2.3 Sustainable mining operation

Sustainable mining involves practices that ensure mining operations are conducted in a manner that balances economic, environmental, and social considerations (Veiga et al., 2001). This concept, often referred to as the "triple bottom line," focuses on making mining economically viable while being environmentally responsible and socially acceptable (Alhaddi, 2015) . Sustainable practices include minimizing environmental impact through effective resource management, ensuring proper mine closure and rehabilitation, and maintaining profitability to support ongoing operations.

Moreover, sustainable mining necessitates active engagement with local communities, respecting cultural values and enhancing community development (Hamann, 2003). This approach also involves rigorous adherence to environmental regulations to prevent long-term ecological damage, such as pollution and habitat destruction (Fonseca et al., 2014). By integrating these principles, mining operations aim to preserve the integrity of the environment and improve the quality of life for adjacent communities, ensuring that resources are available for future generations.

Figure 2.3 Basic elements of a sustainable mining operation (Laurence, 2011)

Fitzpatrick et al. (2011) examined the evolution of sustainable mining within the Mining Association of Canada, tracing the shift from the broad, inclusive Whitehorse Mining Initiative (WMI) of the early 1990s to the more focused, performance-oriented Towards Sustainable Mining (TSM) strategy of 2010. It highlights the limitations of voluntary initiatives in achieving sustainability without governmental regulations, stressing the need for continuous learning, policy adaptation, and collaboration among all stakeholders. It also highlights the importance of integrating environmental, economic, and social factors throughout the mining process, from exploration and extraction to the post-mining management of minerals.

Gorman and Dzombak (2018) reviewed the shift in the mining industry's focus from managing the lifecycle of a mine to addressing the entire lifecycle of the mineral, advocating for a holistic approach to sustainability that integrates environmental, economic, and social factors. They elaborated on strategies to enhance sustainability in mining, discuss challenges in their implementation, and underscore the need for embedding sustainable practices throughout the mineral lifecycle to promote responsible resource management.

2.4 Mining in Canada

Mining is a cornerstone of Canada's economy, with the industry contributing significantly to GDP, exports, and employment, especially in rural and Indigenous communities. Mining industry is categorized into three main groups: metals, non-metals, and coal. Major mined resources include gold, coal, iron ore, potash, copper, and nickel, each contributing significantly to the economy. In 2022, Canada’s minerals sector produced 60 minerals from nearly 200 mines and 6,500 quarries, valued at $74.6 billion, with potash leading at $16.8 billion. Mineral exports

reached $153.2 billion, representing 26% of total merchandise exports. Contributing $109 billion directly and $40 billion indirectly to GDP, the sector employed 694,000 people, including 17,300 Indigenous workers, who make up 11% of the mining workforce. Exploration spending was $4.1 billion, and Canadian mining assets totaled $285.8 billion globally, with $195.9 billion outside Canada (*Minerals and the Economy*, 2024)

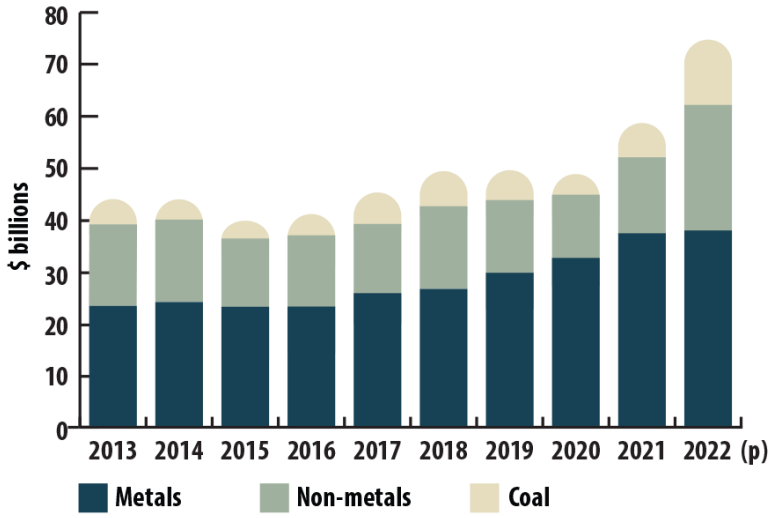

Figure 2.4 Mineral production, by commodity group, 2013-2022 (p) (*Minerals and the Economy*, 2024)

In 2023, Saskatchewan's mining industry significantly contributed to the local economy through jobs, taxes, and investments. The sector directly employed over 11,000 individuals, with an average annual salary of $113,516, nearly twice the provincial average. Additionally, it indirectly created jobs in mining support and services. Taxes from mining operations generated over $2.7 billion in revenue at the federal, provincial, and municipal levels, supporting vital public services. The industry invested $3.7 billion in capital projects and procured over $2.8 billion in goods and services from Saskatchewan suppliers, with $670 million from Indigenous-owned businesses, enhancing local and Indigenous economies (*Saskatchewan Minerals*, 2024).

Saskatchewan is the world's top potash producer, accounting for 33% of global production and generating $10.9 billion in sales in 2023. This sector employed 6,300 direct workers and 7,500 long-term contractors, collectively earning $1.1 billion in salaries. The province's potash mines

procured $4 billion in goods and services, including $424 million from Indigenous suppliers. Known for its low greenhouse gas intensity, Saskatchewan's potash production is 50% less carbon-intensive than the global average, making it a more sustainable choice for supporting global food security and various industrial applications (*Saskatchewan Potash Nourishing the Earth*, 2024).

Saskatchewan's uranium industry plays a critical role in the clean energy transition, producing 20% of the world's uranium in 2023. Led by companies like Cameco and Orano, the sector generated $1.6 billion in sales and employed 2,192 direct workers, with an additional 1,228 contractors. The industry prioritized Indigenous and northern community partnerships, investing $6.4 million in social initiatives. Saskatchewan's uranium mines procured $502 million from local businesses and $222 million from Indigenous-owned enterprises, supporting economic resilience in northern regions (*Saskatchewan Uranium Energizing the World*, 2024).

2.5 Ventilation duct in mining

Modern mining operations rely heavily on robust ventilation systems to maintain safe working conditions in underground environments. Primary ventilation systems provide the main flow of fresh air into the mine, while secondary systems deliver additional airflow to specific areas where equipment and personnel are concentrated (Shriwas & Pritchard, 2020). Researchers have increasingly focused on ventilation-on-demand (VOD) technology, which uses real-time data from sensors to adjust airflow dynamically (Ihsan et al., 2024). This approach minimizes energy consumption by delivering airflow only where and when it's needed. Studies indicate that implementing VOD can reduce energy costs significantly, sometimes by up to 50%, depending on the mine's layout and the level of automation used. Alongside this, advancements in fan technology and duct design have improved airflow efficiency and reduced operational costs, further reinforcing the role of ventilation systems in modern mining (Yeboah et al., 2023).

Ventilation ducts are crucial components of secondary ventilation systems, directing air to specific underground areas that primary ventilation might not adequately reach. Ducts allow for targeted airflow, especially in deep or remote sections, which is essential for removing localized hazards such as dust, diesel exhaust, and heat from machinery (Phuong & Ito, 2012). Proper duct

design and placement improve airflow efficiency, reduce pressure losses, and ensure that fresh air reaches the most critical areas without wastage. Research suggests that using high-quality materials and innovative duct designs, such as flexible, flame-resistant, and anti-static ducts, enhances durability and efficiency in the harsh mining environment (Lu, 2018). Literature emphasizes that poorly maintained or improperly sized ducts can lead to inadequate ventilation, resulting in dangerous conditions and increased operational costs due to airflow losses (Mosaad et al., 2017).

One of the main challenges with ventilation ducts is maintaining their durability and efficiency within the harsh underground mining environment, where they are often exposed to high dust levels, moisture, and corrosive gases (Yang et al., 2022). Studies show that duct degradation, leaks, and blockages can significantly reduce the efficiency of ventilation systems, leading to increased energy consumption as more power is required to maintain adequate airflow (Irshad et al., 2015). Recent research has focused on materials and designs that can withstand these harsh conditions, such as reinforced flexible ducts and anti-static coatings that prevent dust buildup. Innovations like modular duct systems also enable faster and more efficient installations and repairs (Huang et al., 2011). With these advancements, mines can achieve more effective ventilation, reducing downtime and maintaining safe air quality standards.

2.6 Natural fibers in composite material

Natural fibers have gained significant interest in the field of composite materials due to their renewable nature and favorable mechanical properties. These fibers, sourced from plants, animals, and minerals, offer a range of benefits over traditional synthetic fibers. Plant fibers such as flax, hemp, jute, and sisal are particularly noteworthy for their high tensile strength and good flexural properties. For example, flax fibers exhibit tensile strengths comparable to glass fibers, while being lighter in weight (Yan et al., 2014). Animal fibers like wool and silk also contribute unique properties, such as excellent insulation and high elasticity (Mann et al., 2023). The incorporation of these fibers into polymer matrices results in composites that are not only strong and durable but also environmentally friendly. The biodegradability and lower carbon footprint of natural fibers make them an attractive option for reducing the environmental impact of composite materials.

Table 2.1 Chemical composition of various natural fibers (John & Anandjiwala, 2007)

Fiber	Cellulose (wt%)	Hemicellulose (wt%)	Lignin (wt%)	Waxes (wt%)
Abaca	56–63	20–25	7–9	3
Alfa	45.4	38.5	14.9	2
Bagasse	55.2	16.8	25.3	-
Bamboo	26–43	30	21–31	-
Banana	63–64	19	5	-
Coir	32–43	0.15–0.25	40–45	-
Cotton	85–90	5.7	-	0.6
Curaua	73.6	9.9	7.5	-
Flax	71	18.6–20.6	2.2	1.5
Hemp	68	15	10	0.8
Henequen	60	28	8	0.5
Isora	74	-	23	1.09
Jute	61–71	14–20	12–13	0.5
Kenaf	72	20.3	9	-
Kudzu	33	11.6	14	-
Nettle	86	10	-	4
Oil palm	65	-	29	-
Piassava	28.6	25.8	45	-
Pineapple	81	-	12.7	-
Ramie	68.6–76.2	13–16	0.6–0.7	0.3
Sisal	65	12	9.9	-
Sponge gourd	63	19.4	11.2	3
Straw (Wheat)	38–45	15–31	12–20	-
Sun hemp	41–48	8.3–13	22.7	-

When comparing natural fibers to synthetic fibers such as glass and carbon, several key differences emerge. Synthetic fibers are known for their superior mechanical properties, including higher tensile strength and stiffness, which make them ideal for high-performance applications (Rajak et al., 2022). However, these advantages come at a cost. The production of

synthetic fibers involves significant energy consumption and the use of non-renewable resources, resulting in a larger carbon footprint (Amarakoon et al., 2022). Additionally, synthetic fibers are not biodegradable, leading to long-term environmental concerns. In contrast, natural fibers, while generally having lower mechanical properties than synthetic fibers, offer significant environmental benefits. They are derived from renewable sources, require less energy to produce, and are biodegradable. Furthermore, natural fibers are lighter, which can lead to weight savings in composite applications (Ahmad et al., 2014). The trade-off between mechanical performance and environmental impact is a crucial consideration when selecting fibers for composite materials.

Natural fiber-reinforced composites exhibit a range of properties that make them suitable for various applications. The mechanical properties of these composites are influenced by the type of natural fiber used, the matrix material, and the processing methods. For instance, flax fiber-reinforced polypropylene composites have demonstrated high specific strength and stiffness, making them suitable for automotive interior components (More, 2021). The impact resistance of natural fiber composites is another significant advantage, as these materials can absorb and dissipate energy effectively (Meredith et al., 2012). This property is particularly beneficial in applications where impact performance is critical, such as in packaging and protective gear. Additionally, natural fiber composites offer good thermal and acoustic insulation properties, which can be advantageous in building and construction applications (Hassan et al., 2020). In the consumer goods sector, natural fiber composites are employed in products such as furniture, sports equipment, and packaging (Azman et al., 2021). Their environmental benefits, combined with good performance characteristics, make them suitable for sustainable product design. Additionally, there is growing interest in using natural fiber composites in advanced applications, such as aerospace and renewable energy, where their weight savings and environmental benefits can offer significant advantages (Balakrishnan et al., 2016).

2.7 Hemp fiber

Industrial hemp *(Cannabis Sativa),* distinct from its psychoactive relative due to low THC levels, has been cultivated primarily for fiber and seed. In Canada, hemp production resumed in 1998 after decades of restriction, with a focus on varieties containing THC levels below 0.3% (Health

Canada, 2018). Hemp thrives in Saskatchewan's Dark Brown and Black soil zones, particularly in well-structured soils with moderate rainfall, where it can grow between 1.5 to 4 meters tall (Mooleki et al., 2013). While its cultivation for fiber is limited due to processing constraints, hemp seeds have gained significant market traction due to their nutritional value, particularly in omega-3 and omega-6 fatty acids, and their use in cosmetics and cooking oils.

Agronomic practices for hemp in Saskatchewan require specific considerations due to its unique growth needs and challenges (Parvez et al., 2021). Farmers are advised to plant hemp between May 1 and May 31 to optimize biomass yield, although seeding rates vary depending on whether the crop is grown for fiber or grain. Due to hemp's sensitivity to day length, the timing of flowering and maturity is influenced by natural light cycles (Zhang et al., 2021). For optimal results, nitrogen fertilization is essential, yet excessive levels can adversely impact fiber quality. Weed management is critical in early growth stages, as hemp competes effectively once established. However, pest control remains challenging, as no herbicides, fungicides, or insecticides are registered for hemp in Canada. As a result, hemp is best suited to regions where organic practices are feasible, enhancing its appeal as an eco-friendly crop.

The industrial market for hemp in Canada is still developing, particularly for fiber, which lacks the infrastructure necessary for large-scale processing (Cherney & Small, 2016). Grain production, however, has grown steadily, with consistent demand and prices. Harvesting for fiber requires specialized equipment due to the fibrous nature of the stalks, which can pose challenges such as wrapping around machinery parts. The process of retting, essential for fiber extraction, is particularly challenging in dry regions like Saskatchewan, where field retting is less reliable (Sisti et al., 2017). Despite these logistical hurdles, the economic prospects for hemp remain positive, with growing interest in both conventional and organic hemp for seeds, and potential for future expansion into fiber markets as processing technology advances.

2.8 Nonwoven fabrics

Nonwovens, recognized by their distinct lack of weaving or knitting, are engineered fabrics known for their versatility and cost-effectiveness in applications ranging from hygiene products to geotextiles. These fabrics, referred to as "Vliesstoffe" in German, may often be confused with

other materials due to their ambiguous naming. Defined formally by ISO 9092 and adopted by various standardization bodies such as CEN and DIN, nonwovens are fabrics made from fibers that are consolidated in various ways without the necessity of being spun into yarn. They can be made from short, unspinnable fibers similar to those used in the paper industry or from long, synthetic fibers extruded directly from polymers (Albrecht et al., 2003). The structure of nonwovens is not defined by the interlacing of yarn but by the physical and chemical bonds between the fibers, which are enhanced through processes such as bonding and thermal consolidation. Their inherent properties allow for the creation of products with specific attributes like absorbency, breathability, flame resistance, and filtration efficiency, which opens them up to a wide range of applications.

In practical terms, nonwovens are found in everyday items across various sectors including personal care, healthcare, clothing, automotive, and construction, to name a few. They are used in everything from baby diapers and surgical gowns to automotive filters and roofing materials. There are three primary methods for forming nonwoven webs: the drylaid system, which utilizes carding or airlaying; the wetlaid system; and the polymer-based system, featuring processes like spunlaid (spunbonding) and advanced techniques such as meltblown or flashspun. The bonding of fibers plays a crucial role in reinforcing the web's structure, a key stage in nonwoven manufacturing. This bond, essential due to insufficient natural friction, heavily impacts the fabric's ultimate characteristics and should be tailored to suit specific applications. The web can be consolidated through various methods. Chemical methods involve the uniform or intermittent application of binders via impregnation, coating, or spraying. Thermal techniques like cohesion bonding, achieved through calendering or through-air blowing, help meld the fibers together. Additionally, mechanical processes such as needling, stitching, or water-jet entangling are employed to enhance the fabric's structural integrity and its functional qualities. Despite their wide-ranging utility, the origins of nonwovens are humble, often involving the recycling of industrial fiber waste or the innovative use of raw material shortages. This background highlights the industry’s ability to innovate and repurpose materials, further enhancing the sustainability and economic viability of nonwovens in global markets. Despite their wide-ranging utility, the origins of nonwovens are humble, often involving the recycling of industrial fiber waste or the innovative use of raw material shortages. This background highlights the industry’s ability to

innovate and repurpose materials, further enhancing the sustainability and economic viability of nonwovens in global markets.

2.9 Fiber treatment and effect

Alkaline treatment, predominantly using sodium hydroxide (NaOH), is a common method to enhance the properties of natural fibers. When NaOH is dissolved in water, it exhibits a pH value ranging from 6.5% to 8.5%, ensuring that it does not harm the environment even if the treated water is discharged onto the land (Prabhu et al., 2021). The treatment disrupts the packed crystalline cellulose structure in the fibers, creating an amorphous region that allows NaOH to react more effectively with the fibers (Sahu & Gupta, 2019). The process breaks down hydroxyl groups between molecules as they react with water molecules present in the fibers, converting the hydrophilic nature of the fibers into a hydrophobic one. This chemical modification enhances the strength of natural fiber composites. However, it is crucial to maintain the optimal alkali percentage, as exceeding this limit can damage the fibers (Yan et al., 2016). Treating sugar palm fiber by submerging it in a 0.25M NaOH solution for 1 hour enhances the tensile strength of sugar palm/epoxy composites (Bachtiar et al., 2008). Submerging jute fiber in a 25% NaOH solution for 20 minutes significantly enhances the tensile strength of jute/epoxy composites (Gassan & Bledzki, 1999). Similarly, treating coir fiber by submerging it in a 2% NaOH solution for 1 hour at 300^{o}C significantly enhances both the tensile and flexural strength of coir/polyester composites (Rout et al., 2001).

$$\text{Fiber} - \text{OH} + \text{NaOH} \rightarrow \text{Fiber} - \text{O} - \text{Na} + \text{H}_2\text{O} \quad (2.1)$$

Silane compounds, with the chemical formula SiH_4, are widely used as coupling agents to improve the adhesion between natural fibers and polymer matrices, thereby stabilizing composite materials (Zhou et al., 2016). In the presence of moisture, hydrolysable alkoxy groups on silanes form silanols, which then react with the hydroxyl groups of the fibers to create strong covalent bonds on the cell walls. This interaction enhances the fiber-matrix adhesion and provides hydrocarbon chains that resist fiber swelling by creating a cross-linked network through covalent bonds. This treatment not only stabilizes the composite but also significantly improves its mechanical properties by enhancing the interface between the fiber and the polymer matrix.

Treating pineapple fiber with a 5% solution of amino silane significantly enhances the mechanical properties (strength and tensile modulus) of pineapple/polylactic acid composites (Huda et al., 2008). Similarly, treating kenaf fiber with a 4% solution of glycidoxypropyl silane significantly improves the mechanical properties of kenaf/polylactic acid composites, increasing tensile strength by 20% (Nishino et al., 2006). The reaction schemes are given as follows (Li et al., 2007).

$$CH_2CHSi(OC_2H_5)_3 + H_2O \rightarrow CH_2CHSi(OH)_3 + 3C_2H_5OH \quad (2.2)$$

$$CH_2CHSi(OH)_3 + Fiber - OH \rightarrow CH_2CHSi(O - Fiber)(OH)_2 + H_2O \quad (2.3)$$

Chemical modification using acetic anhydride (CH_3-C(=O)-O-C(=O)-CH_3) is another effective method to alter the properties of natural fibers. This process involves substituting the polymer hydroxyl groups on the cell walls with acetyl groups (CH_3COO-), which makes the fibers hydrophobic (John & Anandjiwala, 2007). This hydrophobic nature is beneficial for the composites as it reduces moisture absorption, leading to improved dimensional stability and durability. By altering the fiber's surface properties, acetic anhydride treatment enhances the compatibility between the fibers and the polymer matrix, thereby improving the mechanical properties of the resulting composite materials. The reaction of acetic anhydride with fiber is shown as (Li et al., 2007).

$$Fiber - OH + CH_3–C(=O)–O–C(=O)–CH_3 \rightarrow Fiber - OCOCH_3 + CH_3COOH \quad (2.4)$$

Benzoyl chloride is frequently used in fiber treatments due to its ability to decrease the hydrophilic nature of fibers and improve their interaction with hydrophobic matrices. The inclusion of benzoyl groups ($C_6H_5C=O$) on the fibers significantly improves fiber-matrix adhesion. Benzoylation enhances the composite's strength, reduces water absorption, and improves thermal stability (Sherwani et al., 2021). This treatment method creates a more uniform and stable interface between the fibers and the matrix, resulting in composites with superior mechanical and thermal properties. By employing these chemical modifications, the performance and durability of natural fiber-reinforced composites are substantially improved, making them more suitable for various applications in industries seeking sustainable and high-performance

materials. The reaction between the cellulosic hydroxyl group of the fiber and benzoyl chloride is shown in Equations 2.5 and 2.6 (Li et al., 2007).

$$\text{Fiber} - \text{OH} + \text{NaOH} \rightarrow \text{Fiber} - \text{O}^{-}\text{Na}^{+} + \text{H}_2\text{O} \quad (2.5)$$

$$\text{Fiber} - \text{O}^{-}\text{Na}^{+} + \text{ClC}_6\text{H}_4\text{C}(=\text{O}) \rightarrow \text{Fiber} - \text{O}-\text{C}(=\text{O})-\text{C}_6\text{H}_4 + \text{NaCl} \quad (2.6)$$

The thermal properties of composites, including thermal stability, decomposition temperature, and thermal conductivity, are also positively influenced by fiber treatments. Alkaline treatment, primarily using sodium hydroxide, has been shown to improve the thermal stability of natural fibers by removing hemicellulose, which lowers thermal degradation onset temperatures (Asim et al., 2020). This treatment exposes more cellulose, enhancing the thermal stability and potentially the flame retardancy of the composite (Taib et al., 2022). Silane treatment can enhance the thermal stability of the composites by improving the interfacial bonding, which contributes to less heat generation at the interface during thermal decomposition (Atiqah et al., 2017). Acetylation with acetic anhydride contributes to better thermal resistance, as less moisture typically means less thermal degradation pathway initiation in the composite material (Nurazzi et al., 2021). Benzoyl chloride treatment can enhance thermal stability by reducing the presence of free hydroxyl groups, which are prone to degradation at elevated temperatures.

2.10 Bio-based epoxy resins

Thermosetting polymers, which include well-known types such as epoxies, polyesters, polyurethanes, and phenolics, are formed from a resin and a compatible hardener or curing agent (Baroncini et al., 2016). These components undergo a chemical reaction to cure, typically at room temperature, with the option to heat them to enhance cross-linking until fully cured. This results in a highly cross-linked, relatively rigid and brittle structure. Thermosets, being amorphous polymers, do not have a melting temperature but instead exhibit a glass transition temperature (T_g) (Hale et al., 1991). They can be categorized as either synthetic, based on petroleum, or bio-based, depending on their raw material sources.

Epoxy resins stand out among thermosetting polymers for their ability to create high-performance composites adaptable to various processing techniques, demonstrating excellent

strength and high-temperature performance. Synthetic epoxy resins, which dominate the market, are primarily synthesized from petrochemicals such as diglycidyl ether of bisphenol-A (DGEBA), trifunctional epoxy resins, cycloaliphatic epoxies, or diglycidyl ethers of novolac resins (Tator, 2015). DGEBA alone accounts for about 90% of the epoxy precursors used globally, with over 67% of its molar mass reliant on fossil resources (Yuan et al., 2024; Nikafshar et al., 2017). These resins find extensive applications in sectors like aerospace, electronics for circuit board packaging, high-performance adhesives in transportation, and decorative flooring (Forsdyke & Starr, 2002).

In contrast, bio-based epoxy resins are derived from renewable natural sources like linseed oil, corn, soybean oil, pine, and other vegetable oils, addressing the environmental impacts of synthetic epoxies (Wang & Schuman, 2014). For instance, plant oils used in biodiesel production are processed to extract glycerol, which is initially in a crude form contaminated with biodiesel byproducts. This glycerol undergoes rigorous multi-stage purification until it is 99.5% pure with minimal water content. Subsequently, this purified glycerol is converted into an elementary epoxide, a crucial precursor for producing bio-based epoxy resins. This approach not only utilizes bio-renewable resources but also significantly reduces dependency on fossil-based materials, promoting environmental sustainability.

2.11 Ammonium polyphosphate as a fire retardant

Fire retardants are crucial for enhancing the safety of fiber-reinforced polymer composites, with various chemicals being used to slow or inhibit the spread of fire. Common powder forms of fire retardants (FRs) that are compatible with epoxy resins include Ammonium polyphosphate (NH_4PO_3) (APP), Aluminum trihydrate (ATH), and Magnesium hydroxide ($Mg(OH)_2$) (Budd & Cree, 2018). APP is particularly advantageous as a fire retardant due to its low required filler loadings, cost-effectiveness, and minimal impact on the mechanical properties of polymers (Hörold, 1999). These qualities make APP, essential for improving the fire resistance of polymer composites while maintaining their structural integrity and performance.

Ammonium polyphosphate (APP) starts to decompose at approximately 165°C, leading to the formation of phosphoric acid, phosphorus oxides, water, and ammonia (Lim et al., 2016). The

phosphoric acid then solidifies into a char on the polymer surface, creating a barrier that insulates the underlying material and inhibits the escape of volatile compounds (García et al., 2009). Additionally, phosphorus radicals produced during decomposition interact with hydrogen and hydroxide radicals in the flame, effectively disrupting the combustion process by diluting the fuel mixture (Chapple & Anandjiwala, 2010). According to existing studies, APP significantly reduces smoke production and smoldering, prevents flame spread, and lowers the Peak Heat Release Rate (Zhang et al., 2024). Another benefit of APP is its efficiency; it requires only small concentrations, is cost-effective, and minimally impacts the mechanical properties of the polymer or fiber-reinforced polymer (Hörold, 1999). Typically, APP is incorporated at concentrations ranging from 5–10 wt. % in various polymers. Research involving epoxy resins has explored additions of APP between 5–17 wt.%, finding that a 15 wt.% loading of APP yields the most effective fire retardancy.

According to Matkó et al. (2005), APP significantly enhanced the flame retardancy of biocomposites with various matrices such as polypropylene, polyurethane, and biodegradable starch, each demonstrating unique synergistic effects in flame retardant mechanisms. Notably, silylation improved the compatibility and thermal stability of wood flakes in polypropylene composites, while PUR composites benefitted from the combined flame retardant actions of matrix and fillers, and starch-based composites achieved effective flame retardation with just 10% ammonium polyphosphate.

In an effort to compare several FR additives by Stark et al. (2010), wood-plastic composites (WPCs) made of wood flour and polyethylene were evaluated for fire performance using oxygen index and cone calorimeter tests, revealing their characteristics in comparison to unfilled polyethylene and solid wood. The addition of magnesium hydroxide and ammonium polyphosphate significantly enhanced the fire resistance of WPCs, whereas bromine-based retardants and zinc borate showed minimal improvement.

Lim et al. (2016) has shown the application of Ammonium polyphosphate (APP) across various commodity and engineering thermoplastics, including polyethylene, polypropylene, polystyrene, poly(methyl methacrylate), poly(ethylene terephthalate), acrylonitrile-butadiene-styrene,

polyamides, and poly(vinyl alcohol). This phosphorous-based compound enhances the fire resistance of these composites by facilitating char formation when decomposed, acting as a thermal barrier that shields the underlying materials from heat and flame. Its efficacy is optimized through strategic combinations with additives like montmorillonite, pentaerythritol, and various types of layered double hydroxide, which not only improve the mechanical properties and morphologies of these plastics but also boost thermal properties. Enhancements in limiting oxygen index values, cone calorimetry, and thermogravimetric analysis outcomes are evident, particularly when APP is synergized with intumescent flame retardant systems involving melamine.

To enhance the flame retardancy of wood flour/polypropylene composite (WPC), Guan et al. (2015) introduced a modified version of ammonium polyphosphate (APP), known as ETA-APP, was developed through an ion exchange reaction with ethanolamine. Testing through limiting oxygen index (LOI), UL-94 vertical burning test, and cone calorimeter revealed that ETA-APP significantly improved the flame retardant properties of WPC, increasing the LOI by 71.6% to 43.0% compared to WPC treated with standard APP.

Khalili et al. (2017) explored various epoxy/hardener compositions with added flame retardants (FRs) to produce natural fiber composites using the resin infusion technique. They examined the impact of natural fibers (NF), ammonium polyphosphate (APP), alumina trihydrate (ATH), and a hybrid of ATH/APP on the flammability, thermal, and mechanical properties of the composites. Their findings indicated that the combination of 10 wt% ATH and 5 wt% APP exhibited superior flame retardancy, characterized by self-extinguishing capabilities, the lowest gross heat release, and the highest char residue among the tested formulations.

Similarly, Khalili et al. (2019) studied the flame retardancy of empty fruit bunch (EFB) fiber reinforced epoxy composites containing 10 wt% ammonium polyphosphate (APP) and 5 wt% zinc borate (ZB). They found that this composition achieved the highest level of flame retardancy in the 12-second vertical Bunsen burner test and demonstrated promising results regarding burn length, drip flame time, and total flame time, as assessed by the 60-second vertical Bunsen burner test.

2.12 Scanning electron microscopic analysis

Scanning Electron Microscopy (SEM) is a powerful imaging technique used to observe surface morphologies at high magnification and resolution, offering a detailed understanding of fiber surface characteristics and microstructural features (Rout et al., 2000). In SEM analysis, a focused electron beam scans the sample surface, generating high-resolution images that reveal structural details and surface topography. This imaging technique is critical in materials science for studying natural fibers, as it helps characterize fiber surface roughness, porosity, fiber fracture mechanisms, and the effects of chemical or physical treatments on fibers (Gholampour & Ozbakkaloglu, 2019).

SEM analysis of natural fibers, such as hemp, flax, jute, and sisal, provides valuable insights into their morphology, which directly influences their mechanical performance in composite applications (Chaudhary et al., 2017). Natural fibers typically have a complex microstructure, with various layers and cell wall compositions that contribute to their overall properties. SEM helps researchers visualize these structures and identify features like lumen (central hollow space in fibers), surface fibrils, cracks, and defects. The analysis often reveals irregularities and roughness on the fiber surface, which can enhance fiber-matrix adhesion in composite materials. SEM also enables the examination of treated fiber surfaces, where treatments like alkaline (NaOH) or chemical modifications alter surface characteristics (Verma & Goh, 2021). These treatments often remove non-cellulosic components like hemicellulose and lignin, thereby increasing surface roughness and improving compatibility with polymer matrices.

When applied to fiber composites, SEM is essential for assessing fiber-matrix interactions, delamination, and interfacial bonding, which are critical for composite performance (Lee et al., 2021). Images obtained from SEM analysis reveal how well the fibers are embedded in the matrix, showing either strong adhesion or gaps at the fiber-matrix interface. For instance, treated natural fibers typically exhibit enhanced bonding with matrices, leading to improved mechanical properties like tensile strength and modulus. Furthermore, SEM is used to observe fracture surfaces after mechanical testing, allowing researchers to investigate the failure mechanisms within the composites (Greenhalgh, 2009). By analyzing fiber pull-out, matrix cracking, and

fiber breakage, SEM provides essential information for optimizing composite design, making it an indispensable tool in developing high-performance, bio-based materials.

2.13 Fabrication methods for composites

The hand lay-up method is a traditional and widely used technique in the field of thermoset composite manufacturing, celebrated for its simplicity and the minimal cost of equipment. It involves placing a dry reinforcement fabric, such as woven or stitched materials, into a mold—typically a single-sided, female mold (Middleton, 2016). Technicians manually apply a resin, often of low viscosity to aid the process, using tools like rollers or brushes (Cairns & Shramstad, 2000). This method requires precise manual dexterity to correctly drape and shape the fabric to fit the mold's contours, making the skill level of the operator crucial to achieving high-quality results (Middleton, 2016).

This method offers several advantages that make it attractive for various applications. It is particularly cost-effective due to the low initial investment in equipment, and the simplicity of the tooling allows for a broad range of part sizes, unrestricted by machine capabilities (Elkington et al., 2015). This makes it ideal for constructing large-scale items such as boat hulls and wind turbine blades (Edwards, 2009). Additionally, the versatility of the hand lay-up process enables the incorporation of different types of core materials, facilitating the production of complex shapes and composite structures like sandwich panels.

However, the hand lay-up method also presents significant limitations. The quality of the final product can vary considerably, dependent largely on the operator's expertise, which introduces inconsistencies in production outcomes (Bai, 2013). The process is also labor-intensive and features long cure times as composites solidify at room temperature, which can extend the production cycle significantly (Phiri et al., 2024). Moreover, thoroughly impregnating heavier fabrics or achieving a high fiber volume fraction with resin is challenging, which can compromise the mechanical properties of the finished product (Islam et al., 2024). These factors make the hand lay-up method less suitable for applications requiring high volume production or uniform product quality.

Composite manufacturing encompasses a diverse array of techniques, each tailored to meet specific production needs with varying degrees of automation, precision, and scale. Spray Lay-Up and Vacuum Bagging expand on the basic hand lay-up process by mechanizing resin application and using vacuum pressure to enhance laminate quality, respectively (Xiao et al., 2015, Abdurohman et al., 2018). More advanced methods like Resin Infusion and Resin Transfer Molding (RTM) allow for greater control over resin distribution and fiber placement, leading to more consistent and high-quality outputs (Agwa et al., 2020). Techniques such as Compression Molding, Stamp Forming, and Automated Fiber Placement (AFP) are geared towards high-volume production, with automated processes reducing labor intensity and increasing repeatability (Middleton, 2016). For specialized applications, processes like Autoclave, Injection Molding, Extrusion, Pultrusion, and Filament Winding offer solutions for high-performance composites, with precise control over material properties and part geometry (Debnath & Singh, 2017).

In research experiments, the hand lay-up technique is often selected due to its simplicity, cost-effectiveness, and the high degree of control it offers over the fabrication process (Iqbal et al., 2024). This manual method allows researchers to easily adjust the orientation, placement, and volume of reinforcement materials, making it ideal for testing various hypotheses with different fiber types or resin formulations. Additionally, its low-cost requirements make it accessible for academic or small-scale industrial research with limited budgets. Hand lay-up also provides valuable hands-on experience and facilitates detailed observations of the effects of specific material manipulations, which is crucial for educational and exploratory studies in composite manufacturing.

2.14 Mechanical properties of natural fiber composites

Natural fiber composites (NFCs) have emerged as a compelling alternative to synthetic fiber-reinforced composites, driven by their sustainability, biodegradability, and relatively good mechanical properties. These composites incorporate fibers derived from natural sources—such as plants, animals, or minerals—into a matrix material, typically a polymer, to enhance mechanical strength and other physical properties (Benin et al., 2020).

For natural fiber-reinforced polymer composites used in ventilation ducts for underground mines, critical mechanical tests include tensile testing to assess maximum strength and elongation under tension, ensuring ducts can handle stretching and repositioning as mines expand (Ku et al., 2011). Flexural tests evaluate bending strength and modulus, important for ducts navigating tight underground spaces and resisting external loads that may cause bending (Asma et al., 2020). Impact tests determine the composite's resilience to sudden shocks from falling debris or equipment, crucial for maintaining the safety and longevity of the ducts in the harsh mining environment (Masud & Chorzepa, 2016).

Density measurement is vital for assessing natural fiber-reinforced polymer composites (NFCs) used in applications like ventilation ducts in underground mines, as it ensures material consistency and quality. Variations in density can reveal irregularities in fiber distribution or voids, affecting the composite's mechanical properties such as stiffness and strength, which are crucial for the ducts to support their weight, resist deformation, and withstand underground conditions (Mehdikhani et al., 2018). A gas pycnometer, using helium to measure the true volume by accounting for even tiny pores, provides accurate density values, essential for ensuring that NFCs meet design, performance, and safety standards necessary for their successful deployment in mining operations (Lowell et al., 2004).

Several factors influence the mechanical properties of NFCs. As noted by Khalid et al. (2021), the mechanical properties of NFCs can differ based on the type of natural fiber used, with factors such as cellulose content and fiber purity playing significant roles. Chemical treatments such as alkali treatment enhance fiber-matrix bonding, leading to better mechanical properties (Aravindh et al., 2022). The orientation and length of the fibers critically affect the mechanical strength. Longer, aligned fibers contribute to higher tensile and flexural strengths (Fu & Lauke, 1996). The process used to form NFCs impacts their internal structure and mechanical properties.

However, NFCs have challenges too, such as varying quality of natural fibers and how they hold up to moisture and sunlight (Kamarudin et al., 2022). Overcoming these challenges is important for making these materials more reliable for widespread use. Researchers are working on

improving these composites with better fiber treatments and combining different materials to enhance their properties, aiming to make them viable for more demanding applications.

2.15 Thermal properties of natural fiber composites

Thermal analysis is a critical aspect of material science, especially in the study and application of composite materials. Composites, made from two or more constituent materials with differing physical or chemical properties, are used widely in industries due to their enhanced mechanical properties, lightweight nature, and cost-effectiveness. Understanding the thermal properties of these materials is essential for their application in environments with fluctuating temperatures or in thermal management systems (Gholampour & Ozbakkaloglu, 2019). Techniques such as Differential Scanning Calorimetry (DSC), Thermal Gravimetric Analysis (TGA), and thermal conductivity analysis using a heat flow meter are commonly employed to assess the thermal behavior of composite materials (Asyraf et al., 2023, YÜKSEL, 2016). These methods provide insights into phase transitions, thermal stability, decomposition patterns, and heat transfer characteristics, which are crucial for the design and optimization of composite materials in various applications.

Differential Scanning Calorimetry (DSC) is a powerful thermal analysis technique used to study the heat flow associated with material transitions as a function of temperature (Menczel et al., 2008). This method is significant in analyzing the thermal properties of composites, as it helps identify phase transitions such as melting, crystallization, and glass transition temperatures (Mutlur, 2004). In the context of composites, DSC can be used to determine the compatibility and interactions between the matrix and the reinforcement materials (Chen et al., 2016). It also provides valuable data on the specific heat capacity and enthalpy changes during these transitions, which are critical for understanding the thermal stability and performance of composite materials under different temperature conditions (Losada-Pérez et al., 2011). The information gained from DSC analysis is vital for optimizing the processing conditions and predicting the service life of composites (Hayaty et al., 2011).

Thermogravimetric Analysis (TGA) is another essential technique used in the thermal analysis of composites. TGA measures the mass change of a material as a function of temperature or time

under a controlled atmosphere (Menczel & Prime, 2008). This method is particularly useful for evaluating the thermal stability and composition of composite materials. TGA can identify the decomposition temperatures of different components in a composite, providing insights into the thermal degradation processes. For natural fiber composites, TGA is crucial in understanding how the organic fibers behave at elevated temperatures, which is important for applications where thermal resistance is a key factor (Asim et al., 2020). Additionally, TGA can help in determining the moisture content, filler content, and other volatile components in composites, which can influence their thermal and mechanical properties.

Thermal conductivity analysis using a heat flow meter is an important method for assessing the heat transfer characteristics of composite materials. This technique measures the rate at which heat is transferred through a material, which is a critical property for composites used in thermal management applications (Ruuska et al., 2016). The significance of thermal conductivity analysis lies in its ability to provide insights into the efficiency of heat dissipation in composites, which is particularly important in electronics, aerospace, and automotive industries (Chen et al., 2016). By understanding the thermal conductivity of composites, engineers can design materials that either insulate or conduct heat effectively, depending on the application requirements. This analysis also helps in identifying the influence of different fillers, fibers, and matrix materials on the overall thermal performance of the composite.

The thermal stability of natural fiber composites has been a subject of extensive research due to the growing interest in sustainable and environmentally friendly materials. Previous studies have shown that natural fibers, such as jute, flax, and hemp, can significantly influence the thermal behavior of composites. For instance, research has indicated that natural fiber composites generally exhibit lower thermal stability compared to synthetic fiber composites, primarily due to the organic nature of the fibers (Asim et al., 2020). However, treatments and modifications of natural fibers have been shown to enhance their thermal stability, making them more suitable for high-temperature applications (Kalia et al., 2009). Moreover, the incorporation of flame retardants and other additives has been explored to improve the thermal resistance of natural fiber composites, expanding their potential use in various industries (Bachtiar et al., 2019).

The thermal analysis of composites is a vital aspect of material science that ensures the suitability of these materials for specific applications. Techniques such as Differential Scanning Calorimetry (DSC), Thermal Gravimetric Analysis (TGA), and thermal conductivity analysis using a heat flow meter provide comprehensive insights into the thermal properties of composites. These analyses are particularly important for natural fiber composites, where thermal stability is a significant concern. Previous research has highlighted the challenges and advancements in enhancing the thermal performance of natural fiber composites, contributing to their growing use in sustainable and high-performance applications. Understanding and optimizing the thermal properties of composites will continue to be a key area of research as industries seek to develop materials that can withstand increasingly demanding thermal environments.

2.16 Fire resistant properties of natural fiber composites

Fire testing of fiber-reinforced plastic composites commonly includes methods like the UL94 vertical burn test and the cone calorimeter test. These tests are critical for evaluating the fire resistance and flame retardant properties of composite materials, particularly in applications that require strict fire safety standards, such as automotive, aerospace, and construction. Fiber-reinforced plastics are generally combustible, so evaluating and enhancing their flame retardancy is essential. Researchers have developed various testing protocols to assess how composites behave in fire, focusing on parameters such as ignition resistance, flame propagation, heat release, smoke production, and the composite’s ability to self-extinguish.

The UL94 burn test, encompassing both vertical (UL94 V) and horizontal (UL94 HB) testing, is widely employed to assess the flammability of plastics and fiber-reinforced composites, offering critical insights into material performance under fire exposure. In the vertical burn test, materials are evaluated based on their self-extinguishing time and tendency to produce flaming drips, with classifications ranging from V-0 (the highest fire retardancy, extinguishing within 10 seconds without flaming drips) to V-2 (extinguishes within 30 seconds but may produce flaming drips). Conversely, the horizontal burn test measures the rate of flame spread along a horizontally positioned sample, with an HB rating indicating slower burning or self-extinguishing behavior before the flame reaches the sample's end. While the UL94 V test is suited for materials needing

high flame resistance in applications like electronics and automotive components, the HB test serves lower-risk applications. Numerous researchers have utilized the UL94 vertical and horizontal burn tests to study the burning and dripping behaviors of polymers (Wang et al., 2009; Wang et al., 2012; Marti et al., 2018).

The cone calorimeter test, based on standards, is a more advanced technique that provides comprehensive data on a material's combustion behavior, such as heat release rate (HRR), total heat release (THR), smoke production, and time to ignition. The cone calorimeter has been widely utilized by researchers and in industry to examine the fire behavior of materials (Babrauskas, 2015; Schartel et al., 2005; Schartel & Hull, 2007). In this test, samples are exposed to a controlled radiant heat flux, mimicking the conditions of a real fire. The cone calorimeter is particularly valuable for fiber-reinforced composites, as it quantifies how changes in fiber type, matrix composition, and fire retardant additives affect fire behavior. Key metrics like the peak heat release rate (PHRR) and total smoke production provide insights into the composite's flammability and toxicity levels. The HRR is crucial, as it directly correlates with fire intensity; materials with a lower HRR are less likely to contribute to fire growth. Studies on natural fiber-reinforced composites have shown that incorporating additives like ammonium polyphosphate, aluminum trihydrate, or nanoclays significantly reduces HRR and improves the fire performance of the composites. The cone calorimeter thus plays an essential role in optimizing fiber-reinforced plastics for fire safety, allowing researchers to design composites that meet regulatory requirements and perform well in real-life fire scenarios.

2.17 Conclusion

This chapter provided an in-depth review of sustainable practices in agricultural waste management, mining operations, and the application of natural fibers in composite materials. It highlighted the significant potential of agricultural by-products, such as hemp fibers, to serve as sustainable alternatives to synthetic materials, addressing both environmental and industrial challenges. The discussion on fiber properties, treatments, and applications showcased their versatility and potential for high-performance uses in various industries.

The chapter explored innovative fiber treatment methods, bio-based resins, and fire retardants, demonstrating how these advancements improve the mechanical, thermal, and flame-resistant properties of natural fiber composites. It also emphasized the importance of selecting and tailoring fabrication techniques to meet the stringent requirements of specific applications, such as mining ventilation systems.

This chapter laid a robust foundation for the systematic development of sustainable materials by integrating natural fibers into eco-friendly, high-performance composites. These insights pave the way for the systematic methodologies and optimization strategies detailed in the subsequent chapter.

CHAPTER 3
A SYSTEMATIC APPROACH TO NEW MATERIAL DEVELOPMENT AND OPTIMIZATION

This chapter explores the dynamic and interdisciplinary process of new material development, emphasizing its role as an open system that integrates scientific principles, innovative methodologies, and sustainable practices to address contemporary challenges and future demands.

3.1 Defining the new material development

New material development can be considered an open system because it continuously interacts with its external environment, incorporating resources such as raw materials, energy, and information as inputs, and producing outputs like new materials, waste products, and knowledge. The system is dynamic, meaning it adapts to external factors such as technological advancements, market demands, and regulatory changes. This adaptability is crucial for ensuring that the materials developed are not only innovative and functional but also economically viable and sustainable. The ongoing exchange of resources and information between the system and its environment underscores its open nature, enabling continuous improvement and alignment with external needs and constraints.

Figure 3.1 A representation of "A New Material Development" as an open system

3.2 A systematic framework for the New Material Development

The FCBPSS (F: Function, C: Context, B: Behavior, P:Principl, S: Sate, S: Structure) framework is both a methodology and a tool designed to develop a conceptual or domain model of dynamic systems, building upon and extending the Function-Behaviour-State (FBS) framework initially

proposed by Lin and Zhang (Zhang et al., 2011). The FBS framework was originally created to enhance the intelligence of computer programs in areas such as fault diagnosis and reasoning, with its knowledge representation known as the FBS model. Early pioneering work on the FBS model in the engineering design community includes contributions from Ulrich and Seering (1988). Later, Umeda et al. (1990) provided a more comprehensive overview of the concepts of function, behaviour, and state in machines, and demonstrated the application of the FBS model in fields like computer-aided design, simulation, and diagnosis. This model was further refined and applied to areas such as product upgrade design and large-scale software engineering projects.

The FCBPSS framework expands upon the original FBS model by introducing additional layers of conceptual depth, making it more versatile and applicable across a broader range of domains. Specifically, the FCBPSS framework includes key concepts such as (1) Structure, (2) State, (3) Behaviour, (4) Principle, (5) Function, and (6) Context. Additionally, it emphasizes the (7) relationships among these concepts (1)-(6) and (8) system decomposition, allowing for a more detailed and systematic approach to modeling and understanding complex systems. This extended framework is designed to offer a more nuanced and comprehensive tool for system design, analysis, and development, particularly in fields that require a deep integration of multiple layers of conceptual understanding.

3.2.1 The Principle of the new material development

The Principle in new material development is the foundational element that drives the entire process, anchoring it in solid scientific understanding and innovative thinking. It encompasses the fundamental science that underpins material properties and behavior, such as the atomic structure, chemical bonding, and physical interactions that define how a material behaves under different conditions. This scientific foundation is critical because it provides the basic knowledge required to predict how materials will perform in various applications, allowing developers to select or modify materials to meet specific needs.

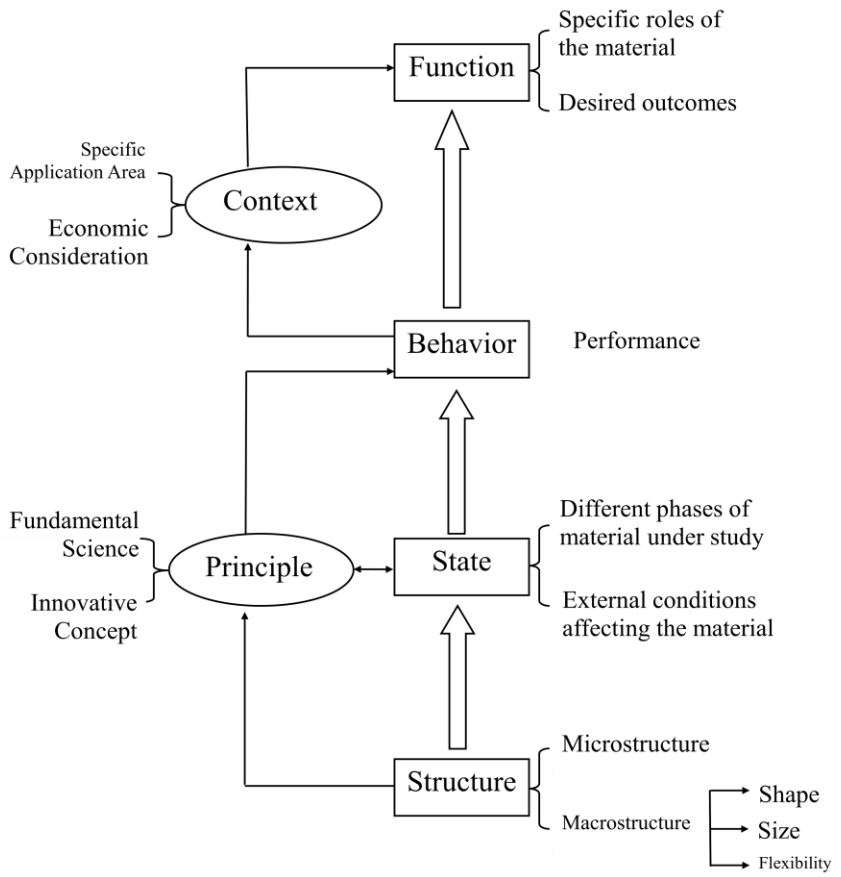

Figure 3.2 A model for "A New Material Development" inspired with W. Zhang and Wang (2016)

In addition to fundamental science, the Principle also incorporates innovative concepts that push the boundaries of material capabilities. These innovations may involve novel material compositions, advanced manufacturing techniques, or the introduction of new processes that enhance material properties or create entirely new functionalities. Innovation in material development is often driven by the need to solve specific challenges, such as increasing the strength-to-weight ratio in aerospace materials or improving the thermal conductivity in electronics. By integrating innovative concepts with fundamental science, developers can create materials that are not only theoretically sound but also practically applicable.

The Principle guides the material development process by providing a clear direction based on scientific and innovative insights. It influences decisions about material selection, processing methods, and performance optimization. For instance, understanding the principles of thermodynamics and kinetics can help in designing heat-resistant materials, while innovations in

nanotechnology might lead to the development of materials with enhanced electrical properties. This dual focus on science and innovation ensures that the material development process is both rigorous and forward-looking, capable of addressing current needs and anticipating future demands.

Finally, the Principle serves as a bridge between the theoretical and practical aspects of material development. It translates scientific knowledge into actionable strategies for creating new materials, ensuring that the resulting products are not only innovative but also viable in real-world applications. This connection between theory and practice is crucial for developing materials that meet the specific requirements of their intended context, whether in terms of performance, cost, or environmental impact. By grounding material development in strong principles, developers can create materials that are both cutting-edge and reliable, ready to meet the challenges of modern engineering and technology.

3.2.2 Structure and State of the new material development

The Structure of new material development refers to the arrangement and organization of the material at both the micro and macro levels. At the microstructural level, this involves the internal arrangement of atoms, molecules, or fibers within the material, which dictates many of its intrinsic properties such as strength, flexibility, conductivity, and thermal resistance. The microstructure can include crystalline structures, grain boundaries, phase distributions, or the alignment of fibers in composite materials. Understanding and controlling the microstructure is crucial because even small changes at this scale can significantly impact the material's overall behavior.

On the macrostructural level, the Structure pertains to the larger, observable features of the material, such as its shape, size, and overall geometry. This includes how the material is fabricated, processed, and assembled into final products. The macrostructure is important for determining how the material interacts with other components in a system, its ease of manufacturing, and its suitability for specific applications. For example, in composite materials, the alignment and distribution of fibers or particles within a matrix can greatly influence the material's mechanical properties and performance. Thus, controlling both micro and

macrostructure is key to tailoring materials for specific functions and achieving desired outcomes.

The State of the material refers to the different phases and conditions that the material might experience during its lifecycle, as well as how these factors influence its properties and performance. This includes the physical state of the material—whether it is solid, liquid, or gaseous—as well as any phase transitions it might undergo, such as melting, crystallization, or phase separation. The State also encompasses external factors like temperature, pressure, humidity, and chemical environment, which can alter the material's properties. Understanding the State of the material is essential for predicting how it will perform under different conditions and for ensuring that it remains stable and effective in its intended application.

Furthermore, the State of the material can change during processing or in response to environmental conditions, and these changes can have significant impacts on its Structure and Function. For instance, a material might be designed to exhibit certain properties at room temperature but could change behavior when exposed to high heat or stress. By carefully studying and controlling the State, material developers can ensure that the material maintains its desired properties across various conditions, thereby enhancing its reliability and durability. The interplay between Structure and State is critical in material development, as it ultimately determines the material's performance in real-world applications.

3.2.3 Behavior of the new material development

Behavior of the material is the next critical step in the development process, where the material's performance under its intended conditions of use is thoroughly evaluated. Behavior refers to how the material reacts to the specific stresses and conditions it will encounter in its application context. This could include mechanical stress, thermal fluctuations, chemical exposure, or other environmental factors. For example, if a material is designed for construction purposes, its behavior under load, resistance to weathering, and durability over time are key aspects that need to be tested and understood. The behavior is a direct outcome of the material's structure and state, as influenced by its context. By assessing the behavior, developers can identify potential issues, optimize the material's properties, and ensure that it meets the performance requirements necessary for its intended function. This evaluation is crucial in confirming that the material will

behave predictably and reliably in the conditions it will face, thereby fulfilling its role effectively in the final application.

3.2.4 Context and Function of the new material development

In the development of new materials, the Context and Function are deeply intertwined, each influencing and shaping the other throughout the design and application process.

Context refers to the specific environment or scenario in which the material is intended to be used. This includes considerations such as the application area—whether it is for aerospace, automotive, construction, or another field—as well as the economic constraints associated with its production and deployment. The context dictates the conditions the material must endure, such as temperature extremes, mechanical stresses, or exposure to chemicals. Economic considerations might include the cost of raw materials, manufacturing processes, and the overall lifecycle cost, including maintenance and disposal. In this sense, context sets the stage for what the material needs to accomplish, providing the parameters within which the material must perform.

Function, on the other hand, defines the specific roles and outcomes that the material is expected to achieve within its context. The function could include properties like durability, flexibility, thermal resistance, or any other characteristic essential to the material's intended use. It represents the ultimate goal of the material development process: to fulfill a particular need or solve a problem within the given context. For example, in the automotive industry, a material might need to be lightweight yet strong, providing both fuel efficiency and safety. The function of the material is what drives its design and dictates its required properties.

These two elements are mutually connected because the context shapes the function and vice versa. The function of a material cannot be fully understood or developed without considering the context in which it will be used. For instance, a material designed to function in high-temperature environments must be contextualized to ensure it can withstand such conditions while also being cost-effective to produce. Similarly, understanding the specific function a material must perform can lead to refinements in its context, such as adjusting the manufacturing process or exploring alternative applications that better suit the material’s strengths.

In summary, context provides the framework within which the material's function is defined and developed. The function, in turn, is the targeted outcome that must be achieved within that framework. The interplay between these two elements ensures that the material not only meets the theoretical requirements but also performs effectively and efficiently in its real-world application. This mutual connection is crucial for developing materials that are both innovative and practical, fully aligned with the specific demands of their intended use.

3.3 Integrating sustainable practices and new material development for mining operations using set theory.

In the context of integrating sustainable practices across different industries, set theory offers a structured method to explore and define the commonalities and interactions between various sustainability efforts. By defining each sustainability practice as a set of elements, we can use set theory to identify intersections—areas where practices overlap and can potentially be integrated to enhance efficiency and effectiveness. For example, in the sustainable management of agricultural waste and its utilization in mining operations, set theory helps to pinpoint precise practices that both sectors can adopt to foster greater sustainability. This clear, logical structure facilitates the development of innovative solutions that leverage strengths from multiple disciplines, driving forward the agenda of sustainable development in industrially diverse environments such as mining and agriculture.

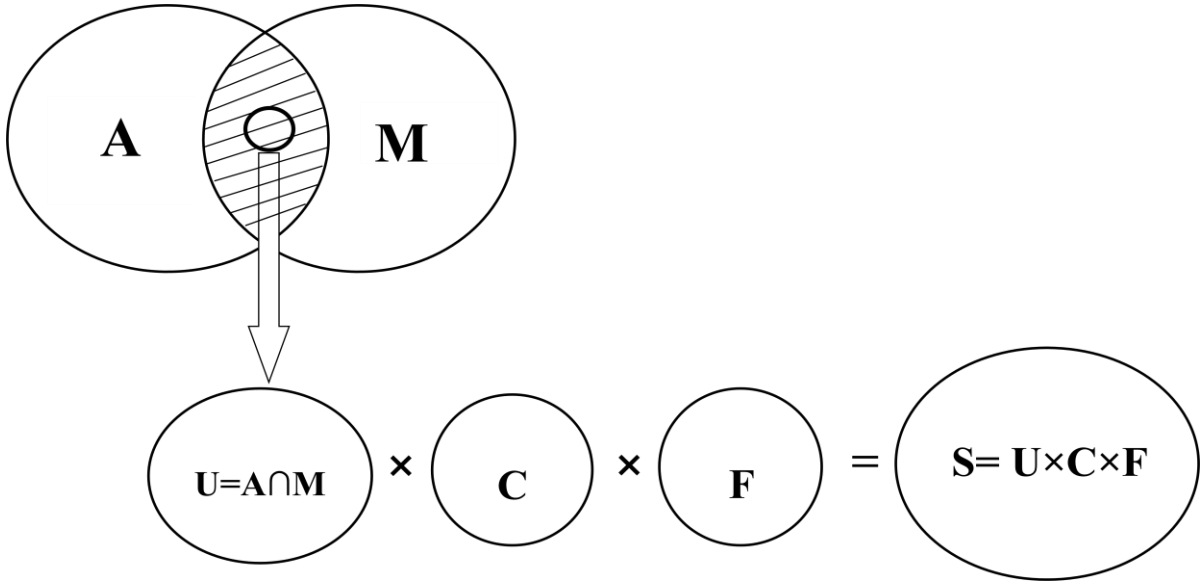

Figure 3.3 A representation of set theory of “New Material Development”

Definitions of Sets:

Let $\boldsymbol{A}$ represents the set of elements related to "Sustainable Agricultural Waste Management.

Let $\boldsymbol{M}$ represents the set of elements related to "Sustainable Agricultural Waste Management.

Let $\boldsymbol{C}$ represents the set of elements related to "Criteria for Efficient Ventilation Ducting System"

Let $\boldsymbol{F}$ represents the set of elements defined by the "FCBPSS Approach for New Material Development"

Let $\boldsymbol{S}$ represents the set of elements of "Systematic Material Development of Mining Ventilation Ducts from Agricultural Waste".

The common elements between the two sets, specifically those connected to the utilization of agricultural waste for sustainable mining operations, can be defined using set-builder notation. This allows us to construct a set based on a specific property or criterion shared by elements from both sets.

$$U = \{x \mid x \in A \text{ and } x \in M \text{ and } x \text{ pertains to the utilization of agricultural waste for mining}\}$$

Here, U is defined as the set of all elements x such that:

- x is an element of , A the set of sustainable agricultural waste management practices.
- x is also an element of , M the set of sustainable agricultural waste management practices.

x specifically relates to the use of agricultural waste in mining operations, enhancing sustainability in both fields.

Finally, the Cartesian product $U \times C \times F$ is defined as: $S = U \times C \times F = \{(u, c, f) \mid u \in U, c \in C, f \in F\}$

Each tuple (u, c, f) represents a combination where:

- u is an element from U, indicating a specific aspect of utilizing agricultural waste for mining operations.
- c is an element from C, indicating a specific criterion for efficient ventilation ducts.
- f is an element from F, indicating a specific application of the FCBPSS approach to new material development.

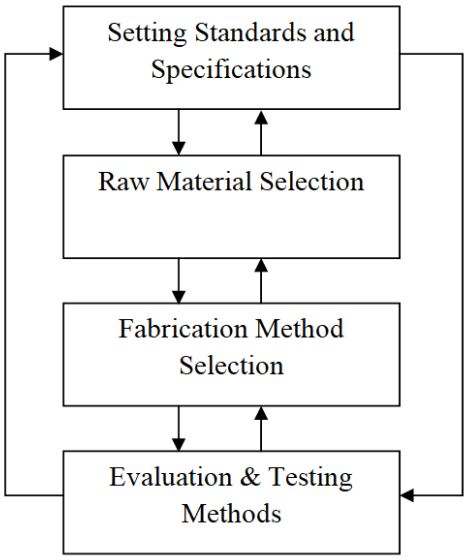

Figure 3.4 Cyclical and interdependent relationship among the four key subsets of material development

Figure 3.4 describes a cyclical and interdependent relationship among the four key subsets in the systematic material development process for mining ventilation ducts from agricultural waste. Initially, Setting Standards and Specifications establish the foundational criteria necessary for the new materials, influencing the Selection of Raw Materials, where appropriate agricultural wastes are identified to meet these standards. The selected materials then inform the Selection of the Fabrication Method, which must be capable of transforming these raw materials into the desired product effectively and efficiently. Following fabrication, the Evaluation & Testing Methods subset assesses the final product against the initial standards and specifications to ensure compliance and suitability for use in mining environments. The results of these tests may prompt revisions in the fabrication methods or even in the selection of raw materials, thereby influencing

subsequent adjustments to the standards and specifications themselves. This iterative process ensures continuous improvement and adaptation of materials and methods to achieve the best possible outcomes.

The elements for each of the four subsets in the material development process:

Subset 1: Setting Standards and Specifications:

i. Comparison with Existing Materials: Ensure compatibility and improvements over existing materials.
ii. Elimination of Existing Drawbacks: Determine if the new standards can address and eliminate known drawbacks of existing materials.
iii. Regulatory Compliance: Ensure all standards meet relevant regulatory requirements.
iv. Adherence to Safety Standards: Maintain compliance with essential safety standards.
v. Consideration of Mining Environmental Specifics: Tailor standards to the specific conditions and requirements of the mining environment.
vi. Compatibility with Raw Materials and Fabrication Methods: Guarantee that the standards are compatible with the selected raw materials and fabrication methods.

Subset 2: Raw Material Selection:

i. Regional Availability of Agricultural Waste: Evaluate the regional availability of agricultural waste.
ii. Effectiveness in Waste Management: Assess the effectiveness of the chosen material in addressing regional agricultural waste management.
iii. Environmental and Economic Impact: Analyze the environmental impact and economic viability of converting agricultural waste into a reusable raw material, including considerations of transportation, storage, and processing.
iv. Specification and Standard Compliance: Ensure the raw material meets desired specifications and standards.
v. Technology Adequacy: Determine whether existing technology is adequate or if innovation is needed.
vi. Community Benefits: Evaluate the potential benefits to the local community.

vii. Fabrication Technique Compatibility: Check compatibility with prevalent fabrication techniques.

Subset 3: Fabrication Method Selection:

i. Environmental Impact and Cost Effectiveness: Evaluate the environmental impact and cost effectiveness of transforming the raw material into the desired product.
ii. Intended Purpose of the Product: Confirm the intended purpose of the final product, whether for testing or real-world application.
iii. Performance Requirements Compliance: Ensure the chosen method meets all necessary performance requirements.
iv. Compliance with Size and Shape Specifications: Verify that the method can achieve the desired size and shape specifications.
v. Technological Sufficiency: Assess whether current technology is sufficient or if new innovations are required.
vi. Waste Reduction: Evaluate the method's effectiveness in minimizing post-production waste.
vii. Productivity Assessment: Measure the productivity of the fabrication method.

Subset 4: Evaluation & Testing Methods:

i. Crucial Specifications and Performance Evaluation: Identify and evaluate crucial specifications and performance requirements.
ii. Availability of Testing Facilities: Assess the availability and appropriateness of testing facilities and machines.
iii. Cost-Effectiveness of Testing Methods: Evaluate the cost-effectiveness of the chosen testing methods.
iv. Regulatory and Standards Compliance: Ensure that testing methods comply with local, national, and international regulations and standards.

3. 4 Design of Experiment

Design of Experiment (DOE) is a structured approach used to systematically study the effects of multiple factors on a process or product. It enables the optimization of performance and quality

by identifying critical factors and their interactions using statistical techniques like ANOVA and regression analysis. DOE is widely applied in research and industry to improve efficiency, reduce costs, and enhance product or process outcomes.

Taguchi Design of Experiment (DOE) is a robust method for optimizing processes and systems by systematically arranging experiments to assess the effects of multiple variables with minimal experimental runs (Davis & John, 2018). Developed by Dr. Genichi Taguchi, this method emphasizes creating quality by minimizing variance, even in uncontrollable environmental conditions. Taguchi's approach uses orthogonal arrays and signal-to-noise (S/N) ratios to identify optimal levels of factors and reduce process variability, making it highly effective in industrial applications (Rao et al., 2008). Numerous studies have shown Taguchi DOE's efficiency in reducing experimental costs and enhancing process performance, particularly in manufacturing and material science, where it helps in fine-tuning parameters for maximum yield or desired outcomes (Ghani et al., 2003, Mori, 2011).

The experimental design for this research was aimed to optimize the preparation of a polymer composite reinforced with hemp fiber, divided into two main fabrication stages. The first stage focused on the creation of a nonwoven hemp fiber mat from raw fiber, which would serve as the reinforcing material. In the second stage, this fiber mat was integrated into a polymer matrix to produce the final composite material. Dividing the fabrication process in this way allowed us to concentrate on the specific factors influencing both fiber mat quality and composite performance.

To streamline our experimental approach, Taguchi L9 orthogonal array was employed, which is highly effective in reducing the number of trials needed for multi-factor experiments. This method allowed us to focus on nine strategically chosen experimental runs instead of the full factorial 27 (3x3x3 combinations), significantly saving time and resources. Taguchi's orthogonal array design is valuable for capturing the main effects of each factor without the exhaustive need for every possible combination, enabling efficient analysis and optimization of the fabrication process.

Table 3.1 Design of experiment (DOE) of hemp fiber reinforced biocomposites.

Composite Sample	A	B	C
S1	0	0	0
S2	0	10	10
S3	0	20	20
S4	5	0	10
S5	5	10	20
S6	5	20	0
S7	10	0	20
S8	10	10	0
S9	10	20	10

Three factors were selected for the experiment, each with three levels representing different concentrations or combinations. The factors include: (A) treatment of the hemp fiber with NaOH solution (w/v %), which helps improve fiber-matrix adhesion; (B) treatment with ammonium polyphosphate (APP) solution (w/v %) as a flame retardant; and (C) addition of APP in the polymer matrix as a mixture with epoxy resin (w/w %). Testing these factors allowed us to assess their combined influence on the composite's mechanical and flame-retardant properties, providing insights into how each treatment impacts the overall performance.

The experiment consisted of two Design of Experiments (DOEs). The first DOE (Table 3.1) is for composite fabrication, incorporating all three factors to evaluate how the treatments influenced the properties of the final composite. A second DOE (Table 3.2) was conducted by focusing only on factors A and B to optimize the fiber processing and mat preparation, which are

essential steps before composite fabrication. In Table 3.1, the composite samples are labeled as S1 through S9, while in Table 3.2, the nonwoven fiber mat samples are labeled as F1 through F9. This dual approach allowed to isolate the effects of fiber treatment from those of polymer matrix enhancement, thus enabling a targeted optimization for each stage of the composite production process.

Table 3.2 Design of experiment (DOE) for manufacturing of hemp fiber nonwoven fabrics

Fiber Sample	A	B
F1	0	0
F2	0	10
F3	0	20
F4	5	0
F5	5	10
F6	5	20
F7	10	0
F8	10	10
F9	10	20

3. 5 Regression analysis

Regression Analysis is another widely applied method, particularly in predictive modeling and data analysis. In regression, relationships between dependent and independent variables are identified, allowing researchers to understand how variables influence one another and to predict future outcomes. Regression can be linear or nonlinear, depending on the nature of the relationship (Sarstedt & Mooi, 2018). Its applications span from economics to engineering, where it helps in quantifying the impact of design variables on system performance. Advanced

regression techniques, such as multiple regression, polynomial regression, and logistic regression, have further expanded its utility, making it an essential tool in fields that rely on statistical predictions and trends analysis (Hocking, 2013).

According to the optimized design of experiments, nine composite material samples were fabricated, with three replicates produced for each sample to ensure reliability and reproducibility of results. These samples underwent a comprehensive series of physical, mechanical, fire resistance, and thermal analyses to evaluate their performance across multiple critical parameters. For every test conducted, a corresponding set of results was generated, providing valuable data on the composite materials' properties. MINITAB 17 software was utilized to perform linear regression analysis on each dataset, facilitating the identification of relationships between the input variables and the performance metrics.

The regression analysis yielded multiple equations, each representing a predictive model for a specific property of the composite materials. Among these, the equations with the highest R-squared values were selected as the most reliable and influential for optimizing material properties. A higher R-squared value indicates that the equation provides a more accurate and reliable fit to the experimental data, capturing the relationship between factors and outcomes more effectively. The three key performance metrics identified as critical for underground ventilation duct applications included (1) the energy absorbed during the IZOD impact test, representing the material’s impact resistance, (2) the percentage of water absorption, highlighting the material's water resistance capability, and (3) the average heat release rate (HRR) density derived from Cone Calorimeter test data, which provided insights into the material’s fire performance.

These equations served as predictive tools for understanding how the composite materials would perform under the challenging conditions of underground mining. The IZOD impact test equation provided a measure of the material's ability to withstand mechanical impacts, critical for structural integrity. The water absorption equation indicated the composite’s suitability for moist or humid environments, a common concern in underground settings. Lastly, the HRR density equation addressed fire safety requirements by evaluating the material's flammability and

thermal stability. Together, these models offered a robust framework for optimizing the composite materials to meet stringent industrial standards for underground ventilation systems.

3.6 Optimization of parameters using Genetic Algorithm

Genetic Algorithms (GAs) represent a more complex, heuristic-based optimization technique inspired by natural selection principles. Developed as part of evolutionary algorithms, GAs optimize problems by generating, selecting, and recombining solutions (chromosomes) over multiple generations, gradually evolving toward an optimal solution (Painton & Campbell, 1995). GAs are particularly valuable for complex, nonlinear, and multi-objective problems where traditional optimization methods may fall short (Tamaki et al., 2002). Widely used in engineering, GAs have proven effective in optimizing design parameters, resource allocation, and scheduling problems (Norouzi & Zaim, 2014). By incorporating processes like mutation and crossover, GAs navigate large search spaces effectively, making them ideal for applications in machine learning, structural design, and network optimization, where finding global optima is crucial. Figure 3.5 illustrates the flowchart of the standard Genetic Algorithm (GA).

Optimization of the parameters was carried out using MATLAB's global optimization tools, specifically the Genetic Algorithm. The algorithm was configured with a population size of 1000, with constraints set as follows: factor A with an upper bound of 10 and a lower bound of 0, and factors B and C each with an upper bound of 20 and a lower bound of 0. This setup generated 350 optimized results, which were further analyzed through a Pareto Front graph. The Pareto Front visually demonstrated the trade-offs among the optimized properties, identifying composite formulations that best met the performance requirements for underground duct applications.

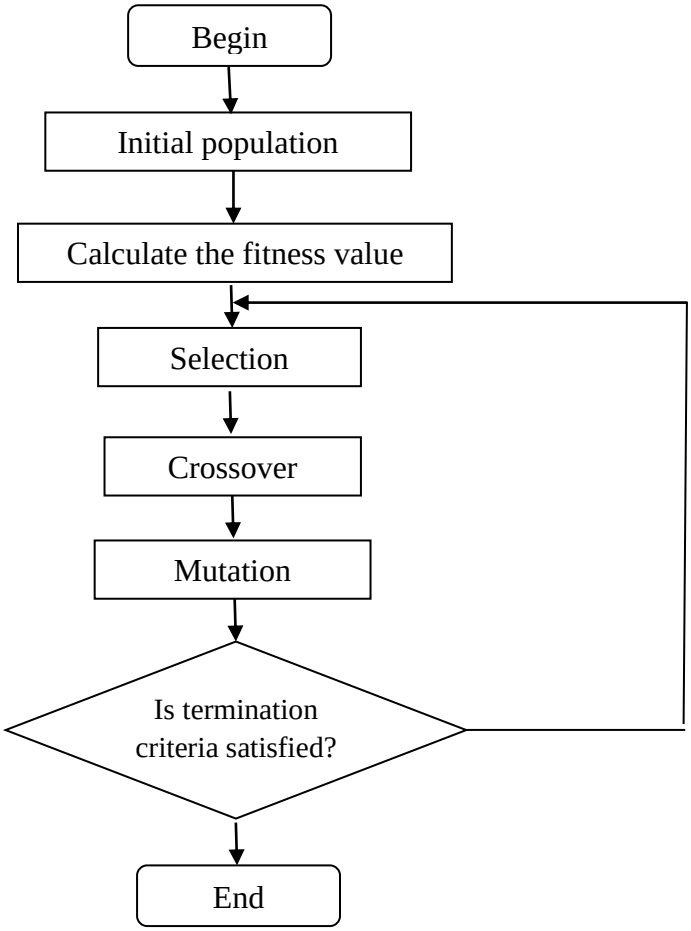

Figure 3.5 Flowchart of the standard genetic algorithm (GA)

CHAPTER 4
MATERIALS AND EXPERIMENTAL METHODS

The materials, methods and procedures adopted to achieve the objectives of this study are presented in this Chapter.

4.1 Materials

Hemp fiber was procured from Cellutech Limited in Saskatchewan, Canada. The matrix used in this study is a green bio-polymer, specifically casting epoxy and hardener, purchased from Nerpa Polymers in Calgary, Alberta, CA, which contains 31% bio-based content. The main characteristics of this polymer matrix, as obtained from the manufacturer's data sheet, are presented in Table 4.1. Sodium hydroxide (NaOH) was obtained from MilliporeSigma Canada Ltd. in Oakville, Ontario, CA (CAS Number: 1310-73-2), and ammonium polyphosphate (APP) was sourced from Shifang Taifeng New Flame Retardant Co., Ltd, China (CAS Number: 68333-79-9). Stainless steel plates for mold-making in the hand layup process were sourced from Home Depot in Saskatoon, SK, Canada.

Table 4.1 Properties of Nerpa casting epoxy resin and hardener

Properties	Bio-epoxy resin
Density (g/cm^3)	1.08
T_g (DSC, midpoint) (°C)	43.5
Mix ratio resin: hardener (by weight)	100:50
Tensile strength (MPa)	58.5
Young modulus (GPa)	2.8
Flexural strength (MPa)	96.2
Flexural modulus (GPa)	3.0

Figure 4.1 A digital image of Nerpa casting epoxy resin and hardener

4.2 Fiber processing

The production of a nonwoven hemp fiber mat from raw hemp fiber involves a series of structured steps to transform the raw material into a finished mat. Each stage is carefully designed to optimize the fiber's properties and enhance the final product's quality.

4.2.1 Washing of the crude fiber

The washing of crude fibers is a critical initial step in the preparation process for fabricating nonwoven mats. This procedure employs a commercial-grade detergent and an industrial top-loading washing machine (Figure 4.2). The use of a commercial detergent is essential as it effectively removes impurities, oils, and contaminants that naturally accumulate in raw fibers. The industrial washing machine provides the necessary robustness and capacity to handle large volumes of fiber, ensuring uniform cleaning across all materials. This thorough washing process is crucial for achieving consistent quality and properties in the subsequent stages of nonwoven mat production.

Figure 4.2 Commercial top-loading washing machine

4.2.2 Alkaline treatment

The alkaline treatment of the fiber plays a vital role in enhancing the properties of natural fibers, making them more suitable for nonwoven mat fabrication. This process involves treating the fibers with sodium hydroxide (NaOH) solutions at concentrations of 5% and 10% by weight. The NaOH used is in granular bead form, which facilitates easy handling, pouring, and precise measurement. To prepare the solution, NaOH granules are dissolved in distilled water, ensuring purity and consistency in the chemical treatment process. The amount of NaOH added is carefully calculated based on the weight of the fibers to ensure even and effective treatment across the entire batch. This alkaline treatment not only cleanses the fibers but also alters their physical structure, increasing their bondability and enhancing their overall performance in the final nonwoven product.

4.2.3 Fiber drying

After undergoing alkaline treatment, the wet fibers are subjected to a drying process to remove moisture, which is critical for preparing them for subsequent fabrication steps. Initially, the fibers are placed in a dryer (Figure 4.3) where an electric fan is used to expedite the drying process. This initial phase of rapid drying with the fan lasts for 2 hours, effectively reducing the moisture content quickly to prevent any potential degradation or microbial growth.

Figure 4.3 Dryer for natural drying

Following this accelerated drying period, the fibers are left to dry naturally over a span of 7 days at room temperature. This extended natural drying phase allows the fibers to slowly acclimate to ambient moisture levels, ensuring they retain their structural integrity and are conditioned appropriately for further processing. This two-stage drying method—combining both rapid and natural techniques—ensures the fibers are optimally prepared for the next stages of nonwoven mat production.

4.2.4 Tumbler and Picker

Samples that were washed and dried were initially processed using the Tumbler (Figure 4.4), which is a large drum covered with a mesh that rotates to agitate the fleece. As the drum rotates, the fleece inside is tumbled vigorously, which helps dislodge and remove any dirt, debris, or extraneous materials embedded within the fibers. The duration of the tumbling process varies based on several factors: the initial cleanliness of the fleece, the quantity being processed, and the fineness of the fibers. Typically, a tumbling period ranging from 5 to 45 minutes is sufficient for preliminary cleaning.

Figure 4.4 Tumbler

After the fleece was processed in the Tumbler, it was then fed into the Picker (Figure 4.5). Often called the opener, the Picker serves the initial role of loosening and separating the fleece into individual fibers, enhancing uniformity while continuing to remove any residual foreign materials embedded in the natural fiber fleece. The device features a conveyor belt that feeds the fleece into a licker drum, equipped with numerous small metal teeth that pull the fleece from the belt. Following this, a large opener drum fitted with large metal spikes lifts the fleece from the licker drum's teeth. As the fleece exits the Picker, it is ejected into a small containment chamber.

Figure 4.5 Picker

4.2.5 Operation of the De-hairer in Fiber Processing

After passing through the Picker, the fibers were then introduced into the De-hairer (Figure 4.6), which is also known as the Fiber Separator. This machine is equipped with five differently sized drums, each outfitted with metal teeth of varying sizes. The initial two drums, referred to as the lickers, measure 5.08 cm in diameter and are equipped with numerous long, sharp metal teeth. These drums serve to flatten and align the fibers as they pull them from the conveyor belt. The subsequent three drums utilize centrifugal motion to differentiate the stiff fibers from the soft, pliable ones. The fibers exit the De-hairer at the rear, where the Doffer combed them onto the final drum, producing a fluffy web. Meanwhile, any unwanted foreign particles were expelled into a waste bin located beneath the machine’s center.

Figure 4.6 De-hairer

4.2.6 Carding

Following their treatment in the De-hairer, the hemp fibers were transformed into a loose, fluffy batting. This batting was then carefully weighed and distributed evenly across the conveyor belt of the Carder (Figure 4.7). Utilizing a series of 14 drums, the Carder selectively processes the fibers, aligning and prioritizing the finer, premium-quality fibers while discarding those of lower quality. As the fibers exit the Carder, they were shaped into batting.

Figure 4.7 Carder

4.2.7 Pressing and Rubbing

Fibers shaped into batting were methodically layered in various orientations on the screw-pressing machine (Figure 4.8). After arranging the fibers and verifying the required Gram per Square Meter (GSM) which is 500, distilled water was sprayed onto the fibers. The pressing machine was then closed and activated. This machine uniquely combines pressing and rubbing actions, with the upper ramp moving in an anti-clockwise direction; the frequency of this movement is adjustable. These dual actions effectively interlock the fibers, forming a cohesive

fiber mat. After 15 minutes, the machine was turned off, and the wet mat was removed. This mat was then left to undergo natural drying for seven days.

Figure 4.8 Fiber batting on the pressing machine

4.2.8 Treatment of fiber mats with fire retardant

The treatment of fiber mats with Ammonium Polyphosphate (APP) involved preparing two concentrations of the solution and employing a natural drying process to maintain the fibers' integrity and strength. Initially, two mixtures were prepared: one with a 10% w/v concentration and the other with a 20% w/v concentration. To make these solutions, 10 grams and 20 grams of Ammonium Polyphosphate were mixed in 100 mL of distilled water at room temperature (25°C), respectively. The fiber mats, cut to a size of 100 mm x 100 mm, were then submerged in the solutions, ensuring complete immersion for thorough soaking. The mats remained in the solution for 1 hour, allowing adequate time for the treatment to take effect.

Figure 4.9 Natural drying of hemp fiber fabric after APP treatment

Following the soaking process, the fiber mats were carefully removed from the solutions and excess liquid was gently shaken off. The mats were then placed in a dryer (Figure 4.9) at room temperature, where a fan facilitated natural air circulation for drying. This natural drying process, which lasted for 7 days, was essential to preserve the fiber mats' integrity and strength, and to prevent any chemical changes that might result from artificial drying methods. By following this method, the fibers were effectively treated with Ammonium Polyphosphate while maintaining their structural and chemical properties, ensuring they remained strong and intact.

4.3 Scanning electron microscopic analysis of fiber samples

To examine the fiber surface morphology after treatments with NaOH and ammonium polyphosphate (APP), fiber samples from the nine nonwoven mats were prepared for scanning electron microscopy (SEM) analysis. Each sample was carefully cut to a specific length and securely mounted onto holders using conductive tape to ensure stability during imaging. To minimize moisture interference, the samples were thoroughly dried using a blower. Given that hemp fiber is inherently non-conductive, a gold coating was applied to each sample using the Edwards Sputter Coater S150B (Figure 4.10), which enhanced imaging quality by reducing charging effects, thereby allowing for clearer SEM imaging.

Figure 4.10 Gold coater

The surface morphology of each fiber sample was observed using a Phenom G2 scanning electron microscope (Figure 4.12) at an accelerating voltage of 2kV. For comprehensive analysis, three images were taken per sample: an initial image after focusing and adjustments, one at 500x magnification, and another at 1000x magnification. This sequence of images allowed for a detailed examination of the fiber surface, capturing both the broader texture and finer

surface features. Differences in surface topography resulting from various NaOH and APP treatments were visible in these high-resolution images, highlighting the effectiveness of these treatments in altering fiber surfaces.

(a) (b)

Figure 4.11 A digital image of fiber samples of SEM analysis (a) before gold coating (b) after gold coating

Analyzing these images provides insight into how the NaOH and APP treatments impact the fiber surface, influencing factors such as roughness, fibrillation, and potential void formation. Such morphological changes directly affect the fiber's bonding capability with polymer matrices, critical for enhancing mechanical properties in fiber-reinforced polymer composites. By observing the treated fiber surfaces, we anticipate improvements in fiber-matrix adhesion, which could lead to better load transfer and overall composite performance. The SEM images thus serve as an essential tool in understanding and optimizing treatment processes for natural fiber composites.

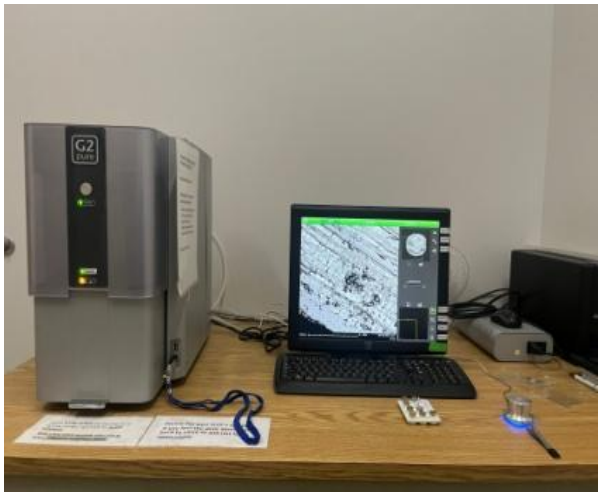

Figure 4.12 The scanning electron microscope

4.4 Flame resistance test of the nonwoven fiber fabric

The ASTM D6413 test was conducted to evaluate the flame resistance of textile samples under vertical testing conditions. All the samples were dried at room temperature (25°C) using a natural drying process to standardize moisture content before testing. Each sample, measuring 12 inches long and 3 inches wide, was mounted vertically in a specialized frame. A Bunsen burner with a controlled flame was used for the test, and the flame was applied to the lower edge of the specimen for 12 seconds. The flame had a precise length of 1.5 inches to ensure consistency during the test. The experimental setup is shown in Figure 4.13.

Figure 4.13 Experimental setup for flame resistance test of the nonwoven hemp fiber fabric

After the flame application, key measurements were taken to assess the material's fire resistance. These measurements included the afterflame time**,** which records how long the material continues to burn after the flame source is removed, and the afterglow time**,** which tracks how long the material continues to glow without flames. Additionally, the char length was recorded, indicating the extent of damage or charring caused by the flame, which is measured in inches or centimeters.

The test results offer critical insight into the flame resistance of each textile sample, particularly for applications that require high fire safety standards, such as protective clothing for industrial environments. A shorter afterflame and afterglow time, combined with a smaller char length, signifies better flame resistance, helping to determine if the material meets the necessary safety specifications for its intended use.

4.5 Tensile strength test for the nonwoven fabric

The tensile strength test for the nonwoven mats was conducted in accordance with ASTM D5035, which outlines the standard test method for determining the breaking force and elongation of textile fabrics in a strip configuration. For this test, the nonwoven mat specimens were cut into standard-sized (300mm × 200mm × 5mm) rectangular strips with a gauge length of 200 mm and conditioned in a controlled environment (25°C and 40% relative humidity) to ensure uniform moisture content before testing. Each specimen was then securely placed in the grips of an universal testing machine (Model: MTS SILENTFLO™ 515) (Figure 4.14), with the force applied longitudinally at a constant rate (10mm/min) until the specimen ruptured.

Figure 4.14 Experimental setup for Tensile strength test of the nonwoven hemp fiber fabric

During the test, the universal testing machine recorded two key parameters: Axial Force (kN) and Axial Displacement (mm). These values provide important information about the mechanical performance of the nonwoven mat. Higher tensile strength values indicate a robust material, while greater elongation reflects a more flexible structure. The tensile strengths reported are an

average value for three specimens for each fiber mat formulation to minimize the error. The tensile strength was obtained using Equation 4.1.

$$Tensile\ strength = \frac{Maximum\ load\ (N)}{Area\ (m^2)} \tag{4.1}$$

The results of the ASTM D5035 tensile strength test are critical for evaluating the durability and structural integrity of the nonwoven fabrics, particularly for use in composite materials and other applications where tensile forces are significant. A higher tensile strength combined with appropriate elongation characteristics ensures that the nonwoven fabric can meet the necessary performance standards for its intended applications, providing both strength and flexibility where required.

4.6 Preparation of mold for hand layup process

The preparation of molds for the hand layup process in the fabrication of natural fiber reinforced bio-based epoxy resin biocomposites is a critical step that determines the quality and integrity of the final product. This detailed description outlines the approach used in constructing a mold specifically tailored for such composites, utilizing robust materials and strategic design elements to ensure optimal outcomes.

The mold, crafted from two stainless steel sheets, features dimensions of 200 mm in length and width, with a substantial thickness of 10 mm. Stainless steel is an ideal choice for this application due to its durability and resistance to corrosion, which is particularly important when dealing with bio-based epoxy resins that may have corrosive properties. The thickness of the steel ensures that the mold can withstand the pressures of the hand layup process without deforming, which is crucial for maintaining the dimensional accuracy of the biocomposite.

To maintain the required thickness of the composite material consistently across the entire mold, metal washers are employed at each of the four sides of the mold. These washers act as spacers, ensuring that the distance between the two metal sheets is uniform. This setup prevents any unevenness in the thickness of the resulting composite, which can significantly affect its

mechanical properties and performance. By using washers as spacers, the mold design also allows for adjustments or replacements as needed, enhancing the mold's versatility and longevity.

An additional layer of innovation in the mold design is the use of removable polyethylene sheets that cover both metal surfaces. Polyethylene is selected for its non-stick properties and chemical inertness, making it an excellent barrier that prevents the resin from adhering to the stainless steel sheets. A mold releasing agent was applied on the polyethylene sheet to ensure easy removal of the composite samples. This choice of material ensures that the mold surfaces remain clean and free from residues, which could otherwise affect multiple production cycles.

4.7 Treatment of Resin with Fire Retardants

Ammonium Polyphosphate was incorporated into the bio-epoxy resin as filler in separate batches, with weight fractions of 10 wt.% and 20 wt.% respectively. The blending of the flame retardant (FR) into the bio-epoxy resin was carried out using a drill and mixing attachment, ensuring sufficient dispersion by mixing for 10 minutes. Following this, the hardening agent was introduced and the mixture was stirred for an additional 10 minutes. To remove any trapped air, the mixture underwent vacuum degassing at room temperature for 30 minutes. The bio-epoxy resin and hardener were combined in a ratio of 2:1 by weight. This meticulous process ensured the homogeneity of the FR within the resin matrix, crucial for the desired mechanical and thermal properties of the final composite material.

4.8 Fabrication of Fiber Reinforced Composite

To begin the composite fabrication process (Figure 4.15), the two fiber mats were weighed to determine the appropriate amount of resin needed to achieve the desired fiber-to-resin ratio of 30:70. Once the weight of the fiber mats was known, the necessary amount of bio-epoxy resin and hardener was calculated based on this ratio. The bio-epoxy and hardener were thoroughly mixed according to the calculated weight. A thin layer of the mixed resin was applied onto the mold surface using a brush. This initial layer helped create a smooth surface and enhanced the adhesion of the fiber reinforcement. The first layer of fiber reinforcement was then laid onto the

resin-coated mold, using rollers or brushes to press the fiber into the resin, ensuring it was fully wetted out and free of air bubbles for optimal adhesion and strength.

The process continued by applying resin and the second layer of fiber reinforcement, making sure each layer was thoroughly wetted with resin. Rollers were used to consolidate the layers and remove any trapped air bubbles, ensuring good adhesion between layers and a uniform distribution of resin. Once the layers were in place and consolidated, the second half of the stainless steel mold was positioned on top. The mold assembly was then placed into a pressing machine to apply uniform pressure, which helped achieve a denser and more uniform composite structure. The composite was allowed to cure at room temperature for 72 hours to ensure full polymerization and the development of the composite's mechanical properties.

(a)

(b)

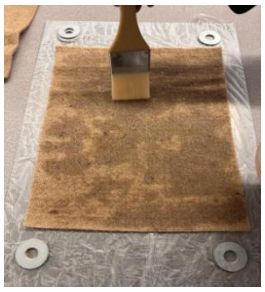

(c)

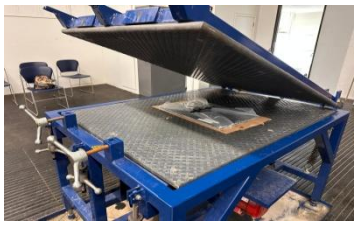

(f)

(e)

(d)

Figure 4.15 A step-by-step Process of Fabricating a Composite: (a) applying epoxy on mold surface (b) First layer of fiber fabric (c) applying epoxy on fiber fabric (d) second layer of fiber fabric (e) roller for uniform distribution of resin (f) pressing for 72 hours.

4.9 Sample preparation

After a curing period of 72 hours, the composite sheet (Figure 4.16 (a) & (b)), measuring 300 mm × 220 mm × 5 mm, was carefully prepared for testing. The sheet was demarcated according

to the recommended standard sample sizes. A band saw (Figure 4.16 (c)) was used to precisely cut the composite sheet along the marked lines, ensuring accurate dimensions for each sample. Following the cutting process, a grinder (Figure 4.16 (d)) was employed to smoothen the edges of the samples, providing uniformity and eliminating any sharp or uneven surfaces. These meticulously prepared samples were then utilized for various testing procedures to evaluate their performance and properties.

(a) (b) (c) (d)

Figure 4.16 Digital photographs of (a) composite sheet (b) demarcated composite sheet (c) Band saw (d) Grinder

4.10 Characterization of hemp fiber based biocomposite

The mechanical, physical, thermal and fire resistant properties of the composites were determined by conducting several tests such as, tensile, flexural, Izod impact toughness, composite density, water absorption, thermogravimetric analysis, thermal conductivity analysis, UL94 vertical burn test and cone calorimeter test.

4.10.1 Water absorption test

Water absorption tests were conducted over a period of 21 days on the prepared composite materials, which measured 75 mm by 25 mm by 5 mm in length, width, and thickness, respectively, following the ASTM D570-22 standard at room temperature (ASTM D570, 2022). The samples were repeatedly weighed until they reached a constant weight, indicating saturation for all composite samples. This was measured using a precision balance capable of detecting changes up to 0.0001g. Before being immersed, the samples were first dried in an oven for 12 hours at 50 °C. Subsequently, the samples were stored in a desiccator. Prior to each

measurement, the surfaces of the samples were wiped with a paper towel to eliminate any surface water. The percentage of water absorbed was calculated using Equation 4.2.

$$W\% = \frac{W_1 - W_2}{W_2} \times 100 \tag{4.2}$$

Here, W% represents the percentage of weight gain, W_1 is the weight (in grams) of the composite after absorbing water over a specific time period t, and W_2 is the initial dry weight (in grams) of the sample before it was immersed in distilled water. The data presented are the average values from three samples of each composite formulation.

4.10.2 Density measurement

Figure 4.17 illustrates the experimental setup employed for measuring the bulk density of the newly produced composites. The density tests were performed on composite samples measuring 20 mm x 20 mm x 3.2 mm (length x width x thickness). Initially, the samples were weighed in air to obtain their dry mass (M_a), and subsequently reweighed while submerged in a liquid (distilled water) to get the wet mass (M_w). The density of the samples was determined using Equation 4.3.

$$\rho_c = \frac{M_a}{M_a - M_w} \times \rho_d \tag{4.3}$$

where, $\rho_c$and ρ_d are the density of sample and liquid (g/cm^3) respectively.

Figure 4.17 Experimental setup determining composite bulk density

Additionally, the theoretical density of the composites was calculated using the Rule of Mixture (ROM), as outlined in Equation 4.4, and this theoretical value was then compared to the

experimentally measured bulk density. The weight fraction of the filler particles was converted into volume fraction employing Equation 4.5, and the volume fraction of the matrix was determined using Equation 4.6.

$$\rho_c = \rho_c V_m + \rho_p V_p \tag{4.4}$$

$$V_p = \frac{W_p}{W_p + (1 - W_p)\rho_p/\rho_m} \tag{4.5}$$

$$V_m = 1 - V_p \tag{4.6}$$

where, W_p is the weight fraction of the filler particles, ρ_c, ρ_m, ρ_p are the densities of the composite, matrix and particles, respectively. V_m and V_p are the volume fractions of the matrix and filler particles, respectively.

The void content of the composites, expressed as a percentage (%), was calculated by comparing the experimental and theoretical densities, in accordance with the ASTM D2734-23 standard, using Equation 4.7 (ASTM D2734, 2023).

$$Void\ Content\ (\%) = \frac{\rho_{theoretical} - \rho_{experimental}}{\rho_{experimental}} \tag{4.7}$$

where, $\rho_{theoretical}$ and $\rho_{experimental}$ are theoretical and experimental density, respectively.

4.10.3 Tensile tests of composites

Tensile tests were conducted on the prepared composites to assess their tensile properties under quasi-static loading conditions. These tests were carried out on dog-bone shaped samples with dimensions of 165 mm × 13 mm × 5 mm (length × width × thickness) and a gauge length of 50 mm, as depicted in Figure 4.18 (b), in accordance with the ASTM D638-22 standard (ASTM D638, 2022). A universal testing machine (Model: MARK-10 ESM1500) (Figure 4.18 (a)) was used for these tests, employing a 5 kN load cell and a cross-head speed of 10 mm/min, as illustrated in the figure. All tests were performed at room temperature with a relative humidity of 40% until the samples fractured. The reported tensile strengths are the average values from three specimens of each composite formulation to reduce variability. The tensile strength (σ_t) was calculated using equation 4.8.

$$\sigma_t = \frac{F_{max}}{A} \tag{4.8}$$

Young's modulus E(MPa) was determined by using the following equation 4.9.

$$E = \frac{\Delta\sigma}{\Delta\varepsilon} \tag{4.9}$$

where, $\Delta\sigma$ (MPa) is the change of tensile stress before the material yields, and $\Delta\varepsilon$ is the change of tensile strain before the material yields.

(a) (b) (c)

Figure 4.18 Digital images of (a) universal testing machine (b) Sample for tensile test (c) Sample for flexural test.

4.10.4 Flexural tests of composites

Flexure testing was carried out following the ASTM D790-17 standard (ASTM D790, 2017). Using the three-point bending method, the test samples were placed on two supports and loaded by a loading nose positioned midway between these supports. The samples were deflected until the outer surface reached a breaking point. Each test was conducted at a crosshead speed of 10 mm/min and repeated three times. Flexural strength and modulus values were recorded through software on a computer connected to the testing machineFlexural strength σ_f (MPa) is calculated from the following equation:

$$\sigma_f = \frac{3PL}{2bd^2} \tag{4.10}$$

where:

P = load at a given point on the load-deflection curve, N;

L = support span, mm;

b = width of beam tested, mm; and

d = depth of beam tested, mm.

Flexural modulus is determined from Equation 4.11:

$$E_B = \frac{L^3 m}{4bd^3} \tag{4.11}$$

where:

E_B = modulus of elasticity in bending, MPa;

L = support span, mm (in.);

b = width of beam tested, mm;

d = depth of beam tested, mm; and

m = slope of the tangent to the initial straight-line portion of the load-deflection curve, N/mm.

4.10.5 Izod impact tests of composites

Izod impact toughness values were measured using a HONGTUO impact tester (Model: DH-1843-5.5D), as illustrated in Figure 4.19. The tests were conducted on non-standard, un-notched specimens with dimensions of 60 mm × 20 mm × 5 mm (length × width × thickness). Un-notched samples are more suitable for detecting agglomerates and flaws in the specimens because cracks tend to initiate at these agglomerates, unlike notched samples, which are less sensitive to the presence of powder filler agglomerates in composite materials.

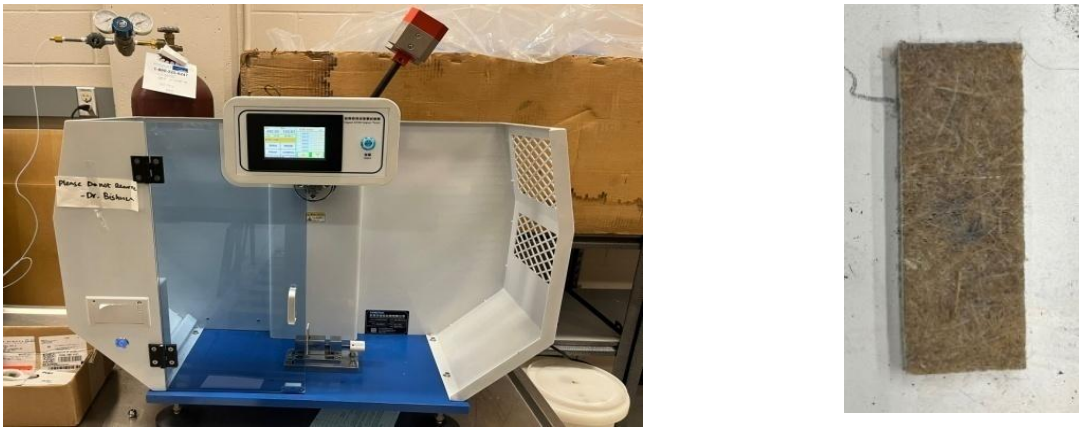

(a) (b)

Figure 4.19 Digital images of (a) Izod impact tester (b) Sample for Izod impact test

The energy absorbed by the prepared composites during fracture was measured at a temperature of 23 °C. The ASTM standard ASTM D256-24 was followed to compare the impact toughness

of the composite materials (ASTM D256, 2024). The reported values represent the average from three samples of each composite formulation tested at different temperature levels. The energy absorbed per unit area (E_a) in kJ/m² was calculated using a specific equation 4.12.

$$E_a = \frac{E}{b \times d} \tag{4.12}$$

where, E, b, and d, are energy absorbed (kJ), width (mm), and thickness (mm), respectively.

4.10.6 Thermogravimetric Analysis

The Thermogravimetric Analysis (TGA) using the Perkin Elmer TGA 8000 (Figure 4.20 (a)) was meticulously conducted, starting with careful sample preparation. Representative materials from the bulk were selected and small samples (Figure 4.20 (b)), typically weighing between 30 milligrams to 40 milligrams, were prepared to ensure uniform heating. These samples were dried as needed to remove moisture that might affect thermal properties, then precisely weighed with a microbalance. They were placed in platinum sample pans, and positioned within the TGA furnace. The experimental setup was programmed to increase the temperature from 30°C to 800°C at a rate of 20°C per minute under nitrogen atmosphere with a flow rate of 25 mL per min to prevent oxidation, along with necessary calibration and baseline adjustments for accurate readings.

(a) (b)

Figure 4.20 A digital image of (a) Thermogravimetric analyzer (b) Samples for thermogravimetric analysis

The analysis proceeded with the TGA heating the samples at the predetermined rate, continuously monitoring the mass changes. This process was closely tracked using the TGA's

software, which provided real-time data on temperature and mass variations. Upon completion of the test, the data were logged and the thermogravimetric curves were analyzed to pinpoint significant thermal events such as decomposition and moisture loss. Reports were generated, detailing key findings including the temperatures at which decomposition began, rates of weight loss, and the amounts of residue remaining. After the experiments, the apparatus was allowed to cool, and the sample pan and furnace were thoroughly cleaned to eliminate any potential contamination for future analyses. This structured and rigorous procedure ensured that the TGA provided reliable and reproducible results, which are essential for accurate material characterization and quality control.

4.10.7 Thermal conductivity analysis

The thermal conductivity measurement of materials was conducted using the Fox 314 Heat Flow Meter (Figure 4.21 (a)), adhering to ASTM C518-21 standards (ASTM C518, 2021). Samples were prepared with dimensions of 6 inches by 6 inches by approximately 0.2 inches, fitting within the maximum capacity of the machine which is 305 mm x 305 mm x 102 mm (12 in x 12 in x 4 in). This device utilizes a central measuring area of 102 mm x 102 mm (4 in x 4 in) to focus on the heat flow through the middle section of the sample. The machine, operated by WinTherm32 software, managed the setup, data acquisition, and analysis. During the test, a critical temperature difference of 25°C was maintained between the upper and lower plates, set at 10°C and 35°C, respectively.

(a)

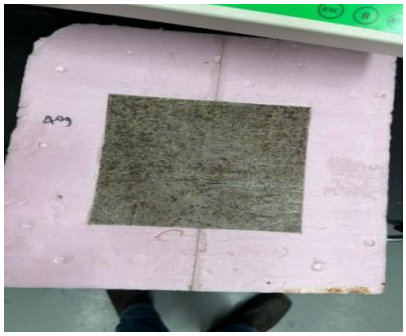

(b)

Figure 4.21 A digital image of (a) The heat flow meter (b) A sample for thermal conductivity test

The testing procedure involved positioning the specimens between the heat flow meter's upper and lower plates, where the induced temperature difference generated a heat flow from the

warmer lower plate to the cooler upper plate. The thicknesses were then recorded, tailored to the sample's rigidity. The test proceeded with the selection of temperature set points and the initiation of the test run, which captured successive data blocks until thermal equilibrium was reached, indicating consistent heat flow metrics across the sample. Post-test, the data were saved and analyzed for thermal conductivity results.

4.10.8 UL94 vertical burn test

The UL94 vertical burning test for the polymer composite was conducted using a specific experimental setup (Figure 4.22) to evaluate flame resistance (UL94, 2023). The setup included a frame and clamp to hold the sample vertically, with sample dimensions of 100 mm x 25 mm x 5 mm. A Bunsen burner producing a 20 mm blue flame was positioned at a 45° angle, 10 cm from the bottom end of the test strip. Cotton balls were placed 30 cm beneath the sample to detect any flaming particles that might drip during the test. The test proceeded in two stages: first, the flame was applied to the sample for 10 seconds and then removed to observe self-extinguishing behavior. The flame was then reapplied for another 10 seconds before final observations were recorded. Table 4.2 outlines the evaluation criteria.

Table 4.2 Criteria table for UL94 vertical burn test (V0, V1, and V2 classifications).

Criteria conditions	V0	V1	V2
Burning time of each individual test specimen (second) (after first and second flame applications)	≤10	≤30	≤30
Total burning time (second) (10 flame applications)	≤50	≤250	≤250
Burning and afterglow times after second flame application (second)	≤30	≤60	≤60
Dripping of burning specimens (ignition of cotton batting)	no	no	yes
Combustion up to holding clamp (specimens completely burned)	no	no	no

Figure 4.22 The experimental setup of UL94 vertical burn test

4.10.9 Cone Calorimeter Test

In this research, small scale heat release data was gathered from Natural Fiber Reinforced Polymer (NFRP) composite specimens using the FTT dual cone calorimeter (Fire Testing Technology, West Sussex, UK), situated in the Thermodynamics Laboratory of the Engineering Building at the University of Saskatchewan (Figure 4.24). The calorimeter is comprised of three main components: the gas analysis stack, the cone stack, and a computer system. The gas analysis stack includes a Servomex Xentra 4100 gas analyzer (Servomex Company Inc., Boston, MA), which measures the concentrations of carbon monoxide (CO), carbon dioxide (CO_2), and oxygen (O_2) in the exhaust using an IR transducer for CO and CO_2, and a paramagnetic transducer for O_2. It also houses the Agilent 34970A data acquisition system (Agilent Technologies, Mississauga, ON) that facilitates data transfer to the computer for post-processing, along with plumbing that cools and dries the exhaust gas before analysis. Prior to testing, specimens were placed in a sample conditioner for at least 24 hours that 5% RH using an aqueous solution of magnesium chloride± 5°C and 50% ±was held at 22°C with a density of 1.27 g/cm^3. The sample conditioner used for this procedure is shown in Figure 4.23.

Figure 4.23 The sample conditioner for cone calorimeter test

As seen in Figure 4.23 the sample conditioner was constructed using a cooler with wire racks installed for specimen storage. Four liters of magnesium chloride aqueous solution were placed at the bottom of the cooler. The density of the magnesium chloride solution was periodically measured using an Anton Paar DMA4500M density meter (Anton Paar GmbH, Graz Austria) between tests to maintain an appropriate concentration. To select the magnesium chloride solution density, a Vaisala HMP 233 hygrometer (Vaisala; Helsinki, Finland) with an Agilent 34972A data acquisition system was utilized to monitor the conditioner temperature and humidity to ensure that appropriate conditions could be maintained. For measuring conditioner humidity and temperature during sample conditioning, a Fisher Scientific Traceable™ relative temperature/humidity meter (Fisher Scientific Company, Ottawa, ON) was placed inside of the conditioner for the 24 hour conditioning period.

Figure 4.24 The cone calorimeter

The ambient temperature of the U of S thermodynamics laboratory was controlled by the building air handling system and varied between 19.0 and 26.7°C during the test period. The building system does not control relative humidity; however, humidity in the laboratory was only recorded to vary from 21 to 27% RH during the July 2024 cone calorimeter testing period.

After a 24-hour conditioning period, the conditioner was briefly opened to retrieve the specimen for testing. Before commencing the test, the instruments of the cone calorimeter were calibrated, and the incident heat flux was adjusted using a Schmidt-Boelter gauge (Medtherm, Huntsville AL) located at the same height as the top of the specimen, 2.5 cm beneath the cone heater element. The specimen, along with its holder, was then positioned on the cement board beneath the cone calorimeter hood, and the test began. This study analyzed the heat release rate of various specimens using a cone calorimeter set at a heat flux of 50 kW/m², a setting frequently cited in literature (Yang & Zhang, 2018). The research was structured into nine test series, with each configuration undergoing three repetitions in accordance with the recommendations of cone calorimeter testing standards, such as ASTM E 1474-22 (ASTM E1474, 2022). Consequently, a total of 27 individual tests were conducted. A sample before and after the cone calorimeter test is presented in Figure 4.25.

(a) (b)

Figure 4.25 Digital images of (a) sample before the cone calorimeter test (b) the same sample after the cone calorimeter test.

CHAPTER 5

RESULTS AND DISCUSSION

5.1 Transformation of hemp fiber

The transformation of hemp fibers through various processing operations is evident in the Figure 5.1, showcasing distinct improvements in fiber refinement and cleanliness. Initially, after washing and drying, the fibers appear rough with significant impurities. Tumbling begins to loosen and separate the fibers, making them slightly cleaner. The picker operation further breaks down the fibers, reducing clumps and enhancing uniformity. The de-hairing process effectively removes short fibers and residual impurities, yielding a cleaner and more refined material. Finally, the carding operation aligns the fibers into a uniform mat, preparing them for use in textile or composite material production. This sequential processing highlights the importance of each operation in achieving high-quality, processed hemp fibers.

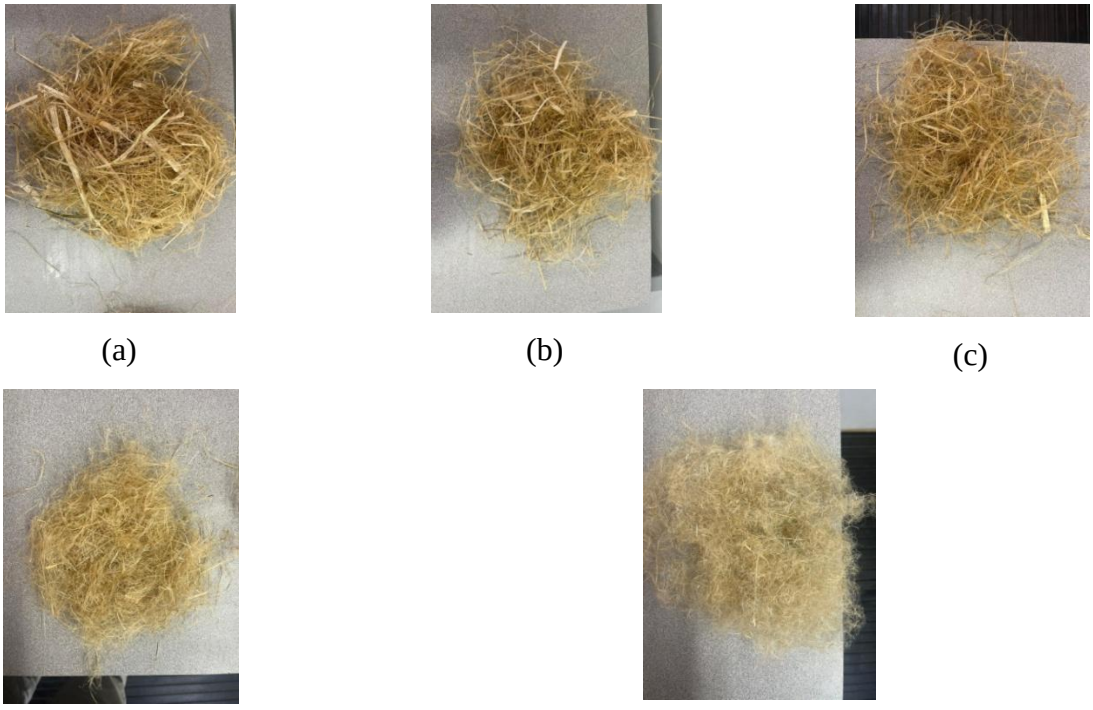

(a) (b) (c)

(d) (e)

Figure 5.1 Digital images of (a) Fiber sample after washing and drying (b) Fiber sample after tumbling operation (c) Fiber sample after picker operation (d) Fiber sample after De-Hairing operation (e) Fiber sample after carding operation

5.2 Comparative analysis of fiber sample micrographs

The findings from the scanning electron microscopic (SEM) analysis of the hemp fiber samples are presented as follows:

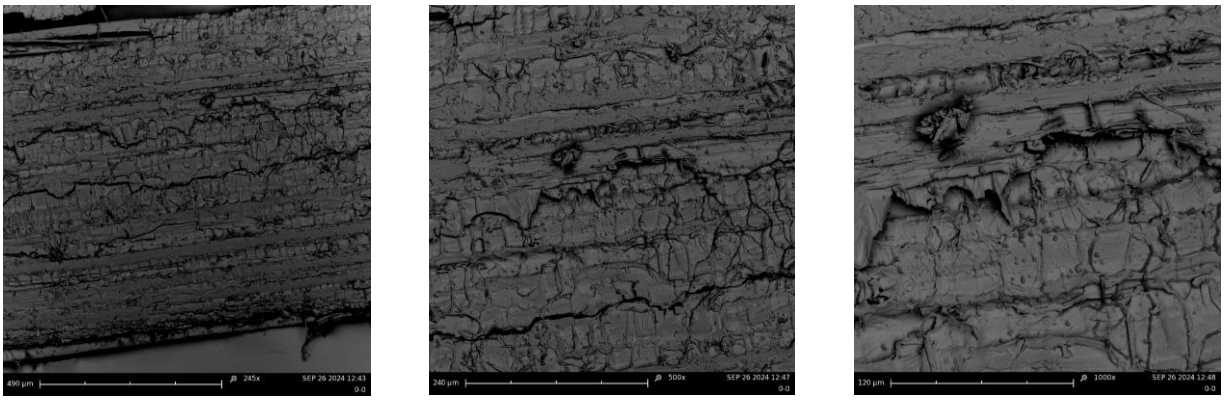

(a) (b) (c)

Figure 5.2 SEM micrographs of F1 at (a) 245x magnification, (b) 500x magnification, and (c) 1000x magnification.

These SEM images (Figure 5.2) display the surface morphology of untreated natural fibers (0% NaOH, 0% APP) at varying magnifications. The surface appears rough with visible cracks and irregular textures, indicating the natural state of the fibers without chemical treatment. The fibers show characteristic features of untreated natural fibers, including inter-fiber voids and non-uniform surfaces, which could affect their mechanical and bonding properties in composite materials.

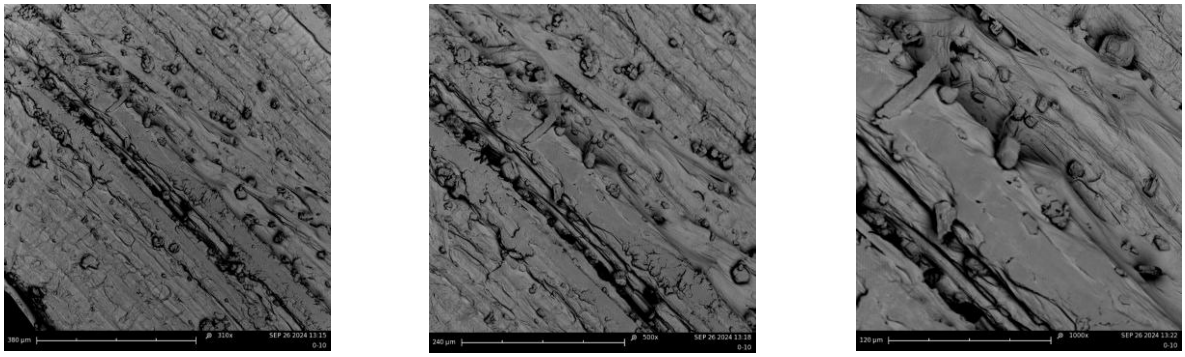

(a) (b) (c)

Figure 5.3 SEM micrographs of F2 at (a) 310x magnification, (b) 500x magnification, and (c) 1000x magnification.

These SEM images (Figure 5.3) showcase the natural fiber surface morphology after treatment with 0% NaOH and 10% APP at different magnifications. The fiber surfaces display smoother textures compared to untreated fibers, with fewer cracks and irregularities, indicating the presence of the APP coating. The globular formations observed on the surface may be due to the APP deposition, potentially enhancing the fiber's flame retardant properties but affecting the surface roughness and interfacial bonding in composite materials.

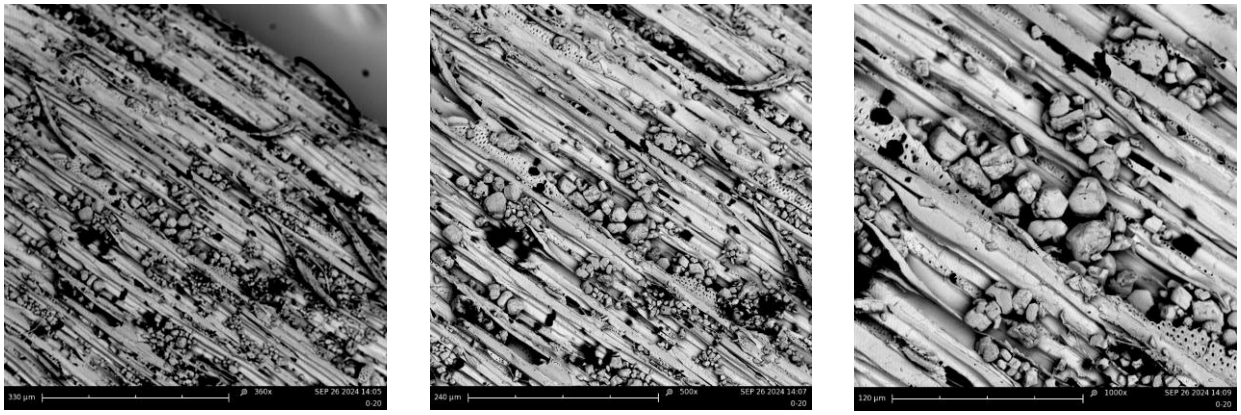

(a) (b) (c)

Figure 5.4 SEM micrographs of F3 at (a) 360x magnification, (b) 500x magnification, and (c) 1000x magnification.

These SEM images (Figure 5.4) illustrate natural fibers treated with 0% NaOH and 20% APP at various magnifications. The fiber surfaces are densely coated with irregularly shaped APP particles, showing agglomeration across the fiber structure, which is more prominent compared to lower APP concentrations. This deposition could enhance flame retardancy but might negatively impact fiber-matrix adhesion due to the uneven surface topology, potentially affecting the mechanical performance of the composite material.

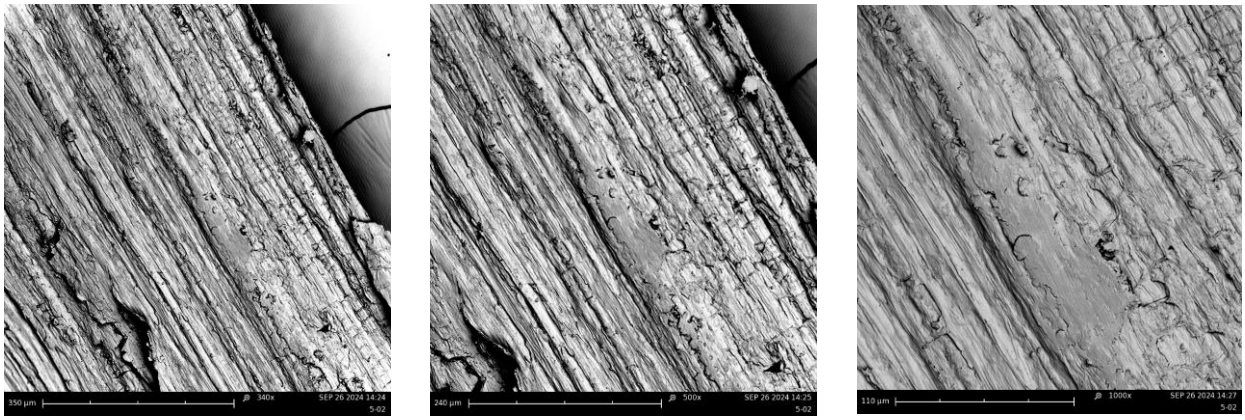

(a) (b) (c)

Figure 5.5 SEM micrographs of F4 at (a) 340x magnification, (b) 500x magnification, and (c) 1000x magnification.

These SEM images (Figure 5.5) depict fibers treated with 5% NaOH and 0% APP at various magnifications. The NaOH treatment has resulted in noticeable surface modifications, such as smoother regions and a reduction in surface irregularities, likely due to the removal of surface impurities and partial delignification. The fibers appear more distinct, with cleaner separation of fibrils, which can enhance interfacial bonding in composite applications and improve mechanical properties compared to untreated fibers

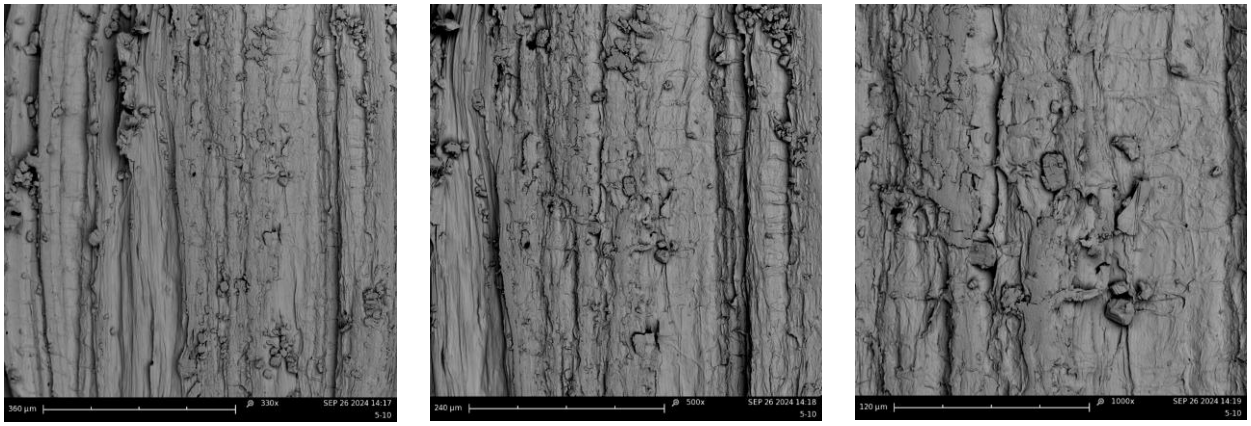

(a) (b) (c)

Figure 5.6 SEM micrographs of F5 at (a) 330x magnification, (b) 500x magnification, and (c) 1000x magnification.

These SEM images (Figure 5.6) show fibers treated with 5% NaOH and 10% APP at different magnifications. The fibers display a combination of smoother surfaces due to NaOH treatment and noticeable particle deposition from APP, creating a more textured surface. The APP particles appear to be dispersed across the fiber structure, with some agglomeration, which may enhance flame retardant properties but could affect fiber-matrix bonding in composite materials due to the non-uniform surface coverage.

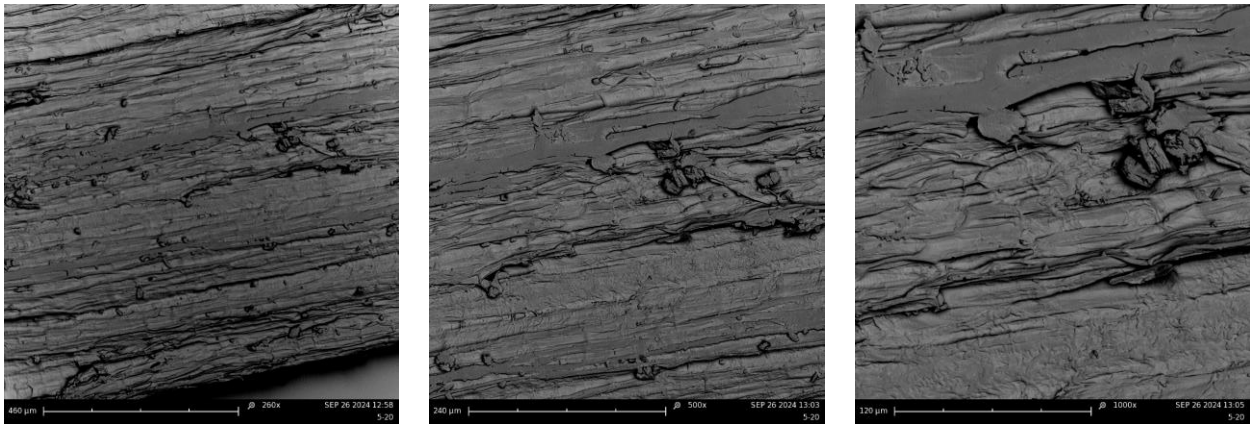

(a) (b) (c)

Figure 5.7 SEM micrographs of F6 at (a) 260x magnification, (b) 500x magnification, and (c) 1000x magnification.

These SEM images (Figure 5.7) show fibers treated with 5% NaOH and 20% APP at varying magnifications. The surface of the fibers appeared more layered and textured, with extensive APP particle deposition, forming clusters across the fiber surface. The high concentration of APP has likely increased surface roughness and particle agglomeration, which could enhance the flame retardancy but might negatively impact fiber-matrix interaction, potentially leading to reduced mechanical strength in composite materials.

These SEM images (Figure 5.8) depict fibers treated with 10% NaOH and 0% APP at different magnifications. The NaOH treatment has caused significant surface smoothing and a reduction in the natural roughness of the fibers, likely due to the more aggressive removal of surface impurities and matrix components. In some area damage to the fiber structure, surface cracking, fiber delamination, and roughened texture appeared.

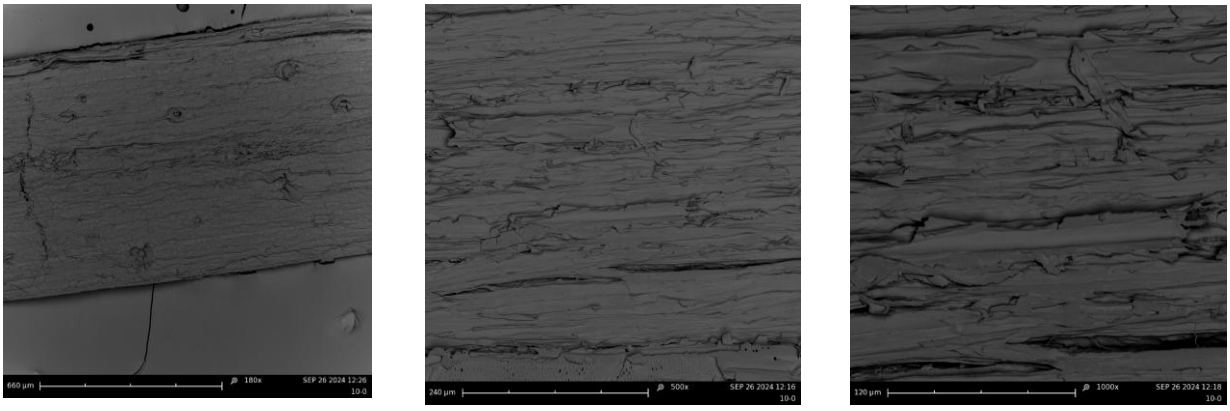

(a) (b) (c)

Figure 5.8 SEM micrographs of F7 at (a) 180x magnification, (b) 500x magnification, and (c) 1000x magnification.

The fibers exhibit distinct and clean fibril structures with less surface debris, which could improve mechanical interlocking and adhesion in composite materials on the other hand This aggressive alkali treatment likely weakened the fibers' integrity, potentially compromising their mechanical properties when incorporated into composite materials.

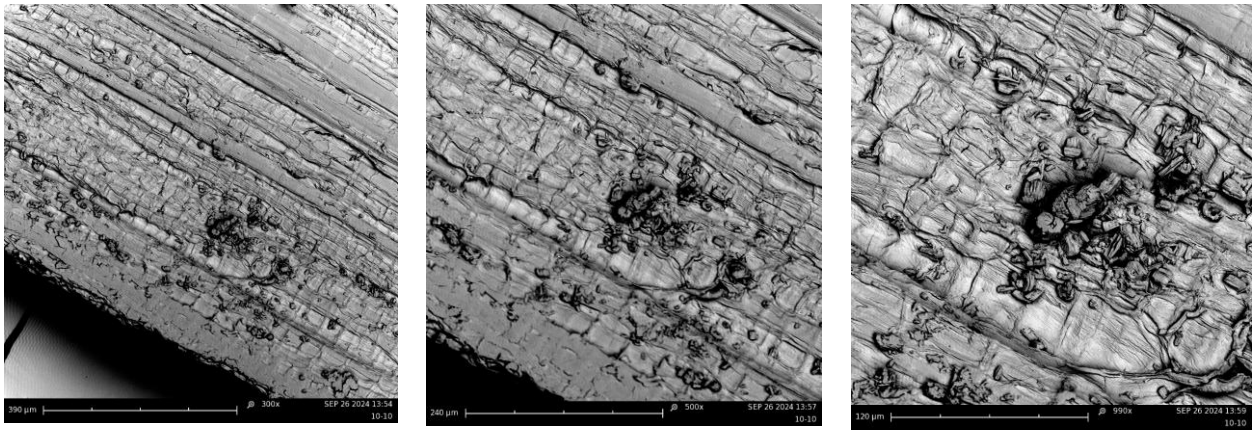

(a) (b) (c)

Figure 5.9 SEM micrographs of F8 at (a) 360x magnification, (b) 500x magnification, and (c) 1000x magnification.

These SEM images (Figure 5.9) depict fibers treated with 10% NaOH and 10% APP at different magnifications. The fibers show surface roughness with visible cracking and irregularities, which are likely due to the combined effects of the NaOH and APP treatments. APP particles can be

observed adhering to the fiber surface, potentially contributing to flame retardancy, while the damage caused by NaOH may compromise the mechanical properties by weakening the fiber structure.

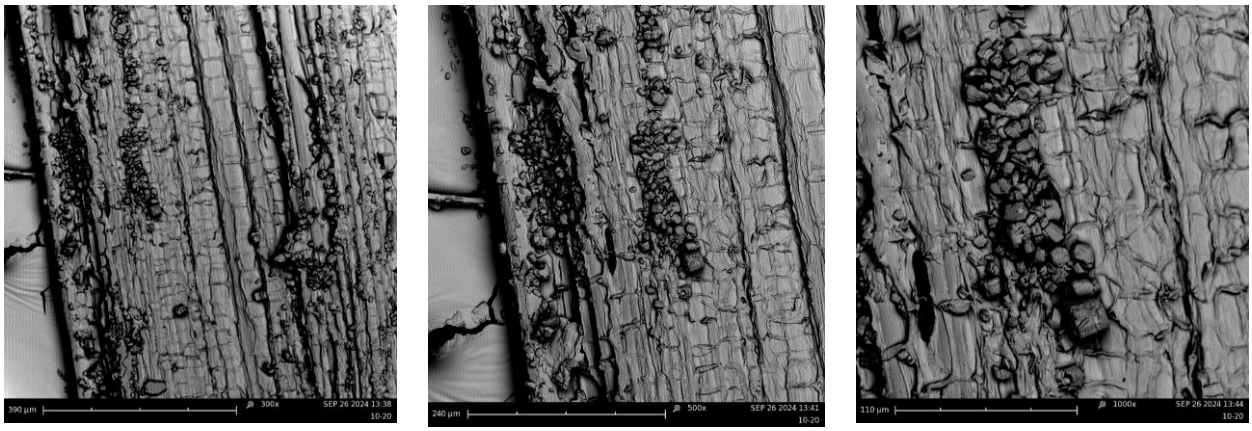

(a) (b) (c)

Figure 5.10 SEM micrographs of F9 at (a) 300x magnification, (b) 500x magnification, and (c) 1000x magnification.

These SEM images (Figure 5.10) depict fibers treated with 10% NaOH and 20% APP at different magnifications. The images show significant particle deposition, with APP particles visibly accumulated in surface cracks, indicating the tendency of APP to concentrate in these areas. This high concentration of APP within the cracks could enhance flame retardancy but may also disrupt the fiber structure, leading to compromised mechanical performance due to uneven surface coverage and potential weakening of the fiber.

5.3 Tensile strength of nonwoven hemp fiber fabric

Table 5.1 presents the tensile test results (the mean and standard deviation) of different fabric samples and Figure 5.11 presents a visual representation using bar graphs.

The tensile strength of the nine nonwoven hemp fiber samples varies based on the treatments applied, particularly the concentrations of NaOH (alkali treatment) and ammonium polyphosphate (APP). Sample F1, which received no treatment with NaOH or APP, serves as the control, with a tensile strength of 78.86 Pa. The samples treated with NaOH or APP generally exhibit improved tensile strength compared to the untreated sample, highlighting the influence of these treatments on fiber properties.

Table 5.1 Results of tensile strength test of different fiber fabric samples

Sample	Tensile Strength (Pa)	
	Mean	St. dev.
F1	78.86	1.84
F2	81.96	1.16
F3	86.59	1.11
F4	90.19	1.60
F5	94.34	1.36
F6	99.06	1.93
F7	85.12	1.61
F8	88.84	1.53
F9	92.55	0.79

The first notable comparison is between samples F1, F2, and F3, which received no NaOH treatment but increasing concentrations of APP. Sample F2, treated with 10% APP, shows a 3.93% increase in tensile strength compared to the control, reaching 81.96 Pa. Further increasing APP to 20% in sample F3 results in a 9.81% increase over F1, achieving a tensile strength of 86.59 Pa. These results indicate that APP enhances the tensile strength by improving the bonding between fibers, though the absence of NaOH limits the overall gains compared to other treated samples.

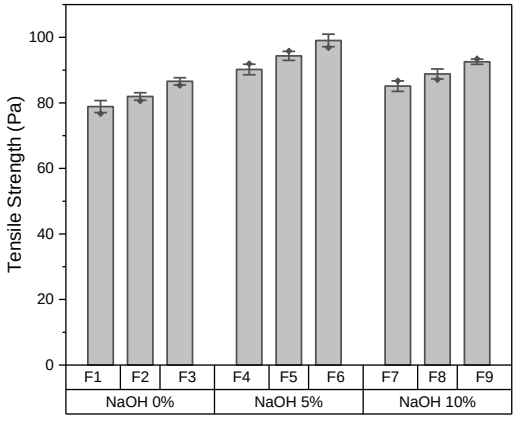

Figure 5.11 The variation in tensile strength of hemp fiber fabrics under different treatments.

Samples F4, F5, and F6 demonstrate the significant impact of NaOH treatment at 5%. Sample F4, with 5% NaOH and no APP, exhibits a tensile strength of 90.19 Pa, a 14.36% improvement over the control. This increase is largely due to NaOH removing lignin and hemicellulose from the fibers, leading to better fiber-matrix adhesion. When 10% APP is added in sample F5, the tensile strength further rises to 94.34 Pa, representing a 19.60% increase compared to F1. The highest tensile strength is observed in sample F6, which combines 5% NaOH and 20% APP, yielding 99.06 Pa—a 25.64% improvement over the control. The combination of NaOH and APP demonstrates a strong synergistic effect, optimizing fiber bonding and structural integrity.

In contrast, samples F7, F8, and F9, treated with 10% NaOH, show lower tensile strength than the corresponding 5% NaOH samples. Sample F7, with 10% NaOH and no APP, has a tensile strength of 85.12 Pa, only a 7.95% increase compared to the control, and notably lower than F4, which received 5% NaOH. The lower tensile strength is likely due to fiber degradation caused by excessive alkali treatment. Similarly, while adding 10% APP in F8 (88.84 Pa) and 20% APP in F9 (92.55 Pa) boosts tensile strength compared to F7, these values remain below those of the corresponding 5% NaOH-treated samples. This suggests that while APP helps strengthen the fibers, the negative effects of excessive NaOH treatment limit its potential.

In summary, the combination of 5% NaOH and 20% APP provides the highest tensile strength among all samples. Moderate NaOH treatment effectively purifies the fibers without causing damage, while APP enhances fiber bonding, leading to stronger nonwoven fabrics. However, excessive NaOH treatment (10%) weakens the fibers due to over-etching, reducing the benefits of APP. These findings underscore the importance of balancing the concentration of treatments to maximize tensile strength and overall fabric performance.

5.4 Mechanical characterization of the composites

The effects of different parameters of the three factors (A,B and C) on the mechanical properties of composite (tensile, flexural and Charpy test) are presented in this section.

5.4.1 Tensile properties of the composites

The tensile properties of the fiber-reinforced composites were characterized by tensile strength (σ_t) and Young's modulus (E). Table 5.2 shows the tensile strength (σ_t) and Young's modulus

(E) of the composites under varying NaOH treatment (Fiber) levels, APP concentrations in fiber, and APP concentrations in resin, highlighting the influence of these processing conditions on the mechanical properties of the materials. Figures 5.12 and 5.13 illustrate the variations in tensile strength and Young's modulus, respectively, of biocomposites under different processing conditions.

Table 5.2 Tensile properties of biocomposites at different processing conditions.

Sample	Tensile Strength σ_t (MPa)		Young's Modulus E_B (MPa)	
	Mean	St.dev.	Mean	St.dev.
S1	33.93	0.27	697.02	45.70
S2	35.36	0.89	903.27	57.20
S3	51.03	0.99	3002.09	173.07
S4	49.16	0.41	1724.88	42.15
S5	56.25	0.50	3571.11	153.44
S6	45.69	1.44	1696.18	93.21
S7	42.78	0.56	1637.08	50.10
S8	36.34	0.31	1255.87	127.183
S9	38.60	0.70	1305.56	27.50

From Table S1 (the untreated control sample) and S5 (the sample with 5% NaOH fiber treatment, 10% APP in fiber, and 20% APP in resin). S1 exhibits the lowest tensile strength (33.93 MPa) and Young's modulus (697.02 MPa), clearly showing the weakness of untreated fibers. In contrast, S5 has the highest tensile strength (56.25 MPa) and Young's modulus (3571.11 MPa), demonstrating how fiber treatment significantly enhances mechanical properties. The combination of NaOH treatment and high APP concentrations in both fiber and resin greatly strengthens the material, making S5 the most robust sample. This comparison highlights the substantial positive effect of fiber treatment and APP incorporation, which dramatically improves both strength and stiffness compared to the untreated baseline.

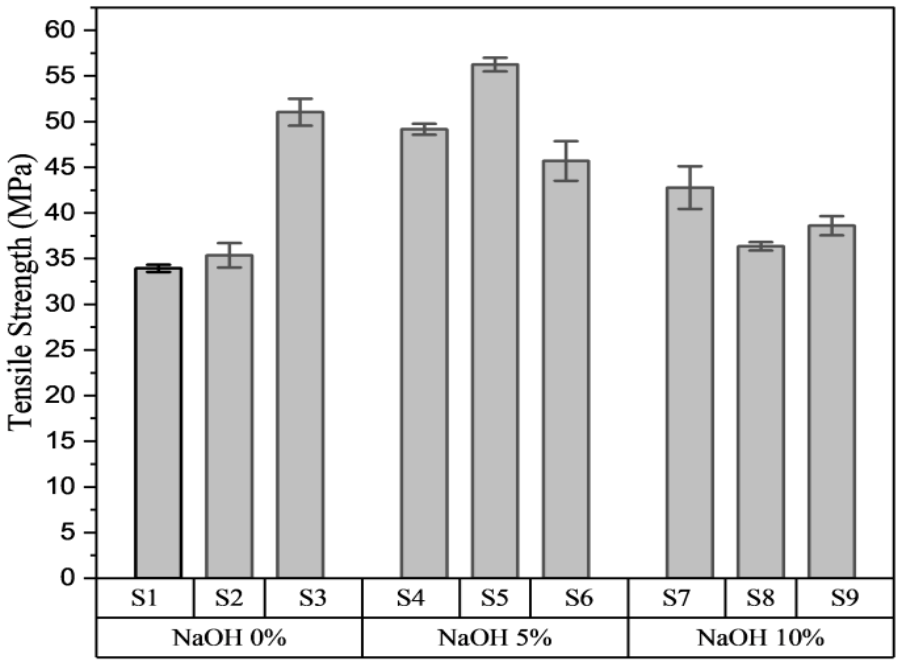

Figure 5.12 The variation in tensile strength of biocomposites of different processing conditions.

Comparing S2 and S6, both have 5% NaOH fiber treatment but differ in APP levels. S2 has 0% APP in fiber and 10% in resin, while S6 has 20% APP in fiber and none in the resin. S6 shows a higher tensile strength (45.69 MPa vs. 35.36 MPa) and Young's modulus (1696.18 MPa vs. 903.27 MPa), indicating that a higher concentration of APP in fiber has a stronger impact than APP in resin alone. However, S5, with APP in both fiber and resin, surpasses both samples in terms of mechanical properties, suggesting that the ideal scenario is to distribute APP across both phases rather than focusing on one. This demonstrates that a balanced presence of APP is essential for maximizing material performance.

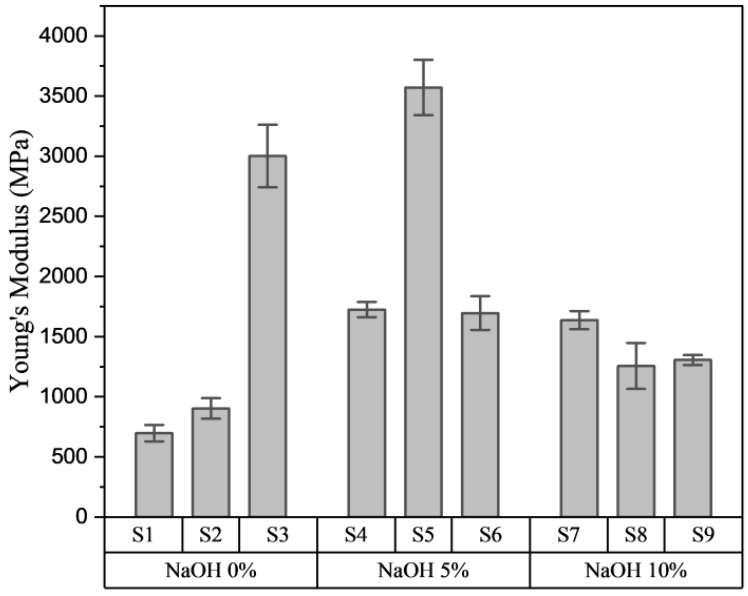

Figure 5.13 The variation in Young's modulus of biocomposites of different processing conditions.

In the comparison between S3 and S7, both of these samples have a significant concentration of APP in the resin (20%), but they differ in their NaOH fiber treatment: S3 has 0% NaOH, while S7 has 10%. Interestingly, S3 outperforms S7 in tensile strength (51.03 MPa vs. 42.78 MPa) and Young's modulus (3002.09 MPa vs. 1637.08 MPa). This suggests that increasing NaOH treatment to 10% in S7 does not improve performance and, in fact, weakens the material compared to S3, which has no NaOH treatment. The high NaOH concentration likely damages the fiber structure or reduces bonding efficiency, resulting in weaker mechanical properties. This comparison indicates that too much NaOH in fiber treatment can undermine the benefits of APP treatment in resin.

Finally, consider S4 and S9, both of which have 5% and 10% NaOH fiber treatments, respectively, with 10% APP in resin. S4 (49.16 MPa tensile strength, 1724.88 MPa Young's modulus) outperforms S9 (38.60 MPa tensile strength, 1305.56 MPa Young's modulus), suggesting that the 10% NaOH treatment in S9 is excessive, leading to reduced material performance. On the other hand, the more moderate 5% NaOH in S4 appears to enhance fiber-matrix adhesion without compromising fiber integrity, resulting in better mechanical properties.

This comparison reinforces the idea that moderate NaOH treatment improves performance, but excessive amounts can weaken the material.

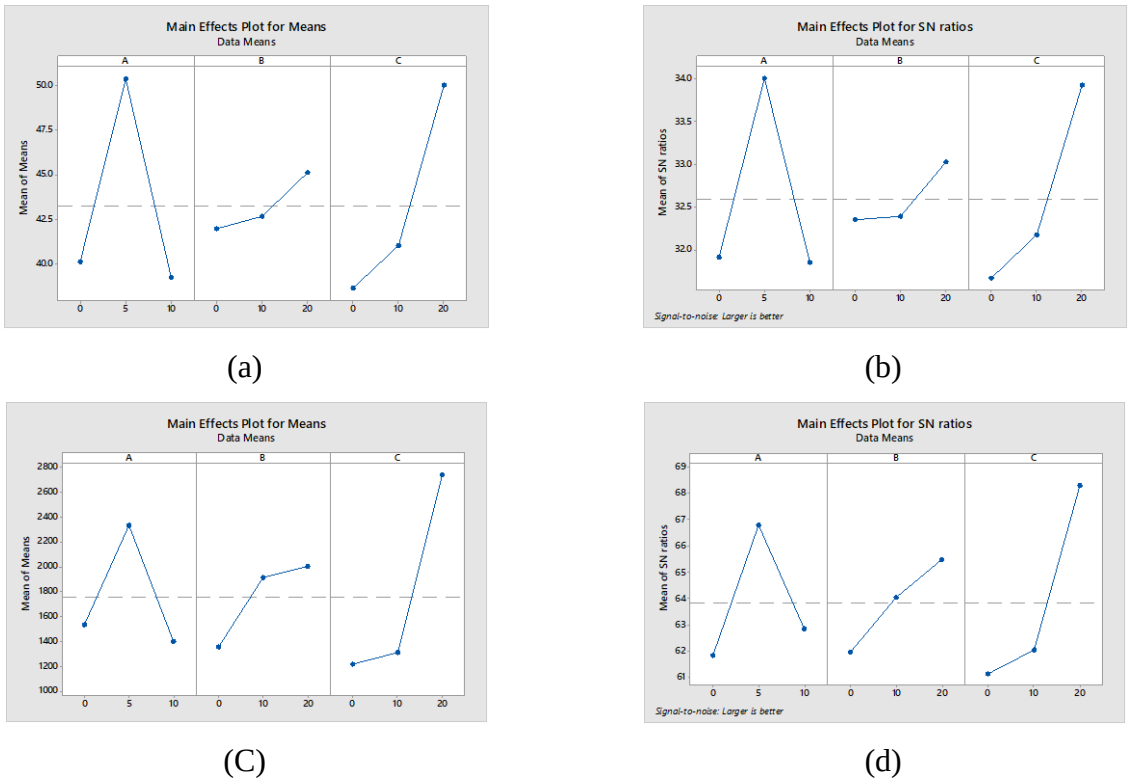

Figure 5.14 Images of (a) Main effects plot of means for tensile strength of biocomposite samples, (b) Main effects plot of signal-to-noise ratio for tensile strength of biocomposite samples, (c) Main effects plot of means for Young's modulus of biocomposite samples, and (d) Main effects plot of signal-to-noise ratio for Young's modulus of biocomposite samples.

The main effect plots (Figure 5.14 (a) & (b)) for tensile strength and Young's modulus reveal that the 5% NaOH treatment significantly improves both tensile strength and stiffness, while the 10% NaOH treatment weakens the material. This suggests that moderate NaOH treatment enhances fiber-matrix bonding, but excessive treatment leads to fiber degradation, reducing the mechanical properties. Additionally, the concentration of APP in fiber shows a gradual positive effect on both tensile strength and stiffness, though this effect is less pronounced compared to the impact of APP in resin.

The main effect plots for the SN ratios (Figure 5.14 (c) & (d)) indicate that 5% NaOH provides the most consistent and stable mechanical properties, both for tensile strength and Young's modulus, while 10% NaOH introduces variability. Increasing APP concentrations in resin significantly boosts both tensile strength and stiffness, as well as their consistency, making APP in resin a key factor in reinforcing the material and stabilizing its performance. Overall, the results suggest that a balanced approach with 5% NaOH and higher APP concentrations, particularly in the resin, yields the best mechanical performance and reliability.

The predicted models (Equation 5.1 & 5.2) were aimed to develop the relationship between the tensile properties (tensile strength and Young's modulus) of the fiber-reinforced composites and the processing conditions (NaOH treatment, APP concentration in fiber, and APP concentration in resin) by statistical tools based on the experimental data. From the foregoing discussion on the effect of processing conditions on tensile properties, it can be concluded that NaOH treatment on fiber had a variable influence on tensile strength and Young's modulus, with optimal results at 5% but weakening effects at 10%. Therefore, higher NaOH concentrations were excluded for consideration in the final mathematical model. The presence of APP, particularly in the resin, is a crucial factor in improving mechanical properties, but it must be balanced with other treatments. Linear regression models were developed between tensile strength and the concentrations of APP in fiber and resin, as well as between Young's modulus and the concentrations of APP in fiber and resin, respectively, using the commercial software MINITAB as follows:

$$Tensile\ Strength\ (MPa) = 36.41 - 0.087A + 0.158B + 0.586C \quad (5.1)$$

&

$$Young's\ Modulus\ (MPa) = 738 - 13.5A + 32.4B + 76.0\ C \quad (5.2)$$

Where,

A is Treatment of Fiber with NaOH (w/v %) solution with water

B is Treatment of Fiber with APP (w/v %) mixture with water

C is Mixture of APP (w/w %) with epoxy resin

5.4.2 Flexural properties of the composites

The flexural properties of the fiber-reinforced composites were characterized by flexural strength (σ_f) and flexural modulus (E_B). The table (Table 5.3) shows the flexural strength (σ_f) and flexural modulus (E_B) of the composites under varying NaOH treatment levels in the fiber, APP concentrations in the fiber, and APP concentrations in the resin, highlighting the influence of these processing conditions on the mechanical properties of the materials. Figures 5.15 and 5.16 illustrate the variations in flexural strength and flexural modulus, respectively, of biocomposites under different processing conditions.

Table 5.3 Flexural properties of biocomposites at different processing conditions.

Sample	Flexural Strength σ_f (MPa)		Flexural Modulus E_B (MPa)	
	Mean	St.dev.	Mean	St.dev.
S1	39.35	1.06	5209.37	78
S2	50.94	1.45	5799.57	39.16
S3	71.41	0.81	8386.27	107.12
S4	63.96	0.94	11257.74	117.4
S5	76.19	1.49	12948.47	93.91
S6	67.93	0.97	10830.84	134.95
S7	61.47	1.24	7858.68	112.81
S8	51.93	0.91	5146.92	57.68
S9	56.27	0.83	6843.06	91.33

The flexural strength and flexural modulus of the nine samples are influenced by the varying treatments of NaOH, APP, and the mixture of APP with epoxy resin. Starting with the samples without NaOH treatment (S1, S2, S3), we can observe that as the APP treatment (factor B) and the APP mixture with epoxy resin (factor C) increase, both the flexural strength and flexural modulus improve. Sample S1, with no treatment, has the lowest values for flexural strength (39.35 MPa) and flexural modulus (5209.37 MPa). With the addition of 10% APP in S2, the flexural strength increases to 50.94 MPa, and the modulus rises slightly to 5799.57 MPa. The highest values in this group are found in S3, where both B and C are increased to 20%, leading to a significant jump in flexural strength (71.41 MPa) and modulus (8386.27 MPa). This indicates a

positive correlation between APP treatments and improved flexural properties when NaOH is not used.

For the samples with 5% NaOH treatment (S4, S5, S6), the influence of APP treatments becomes more pronounced. S4, with no APP in either fiber treatment or epoxy, already shows improved flexural strength (63.96 MPa) and a substantial increase in flexural modulus (11257.74 MPa), compared to samples without NaOH treatment. Introducing 10% APP in both fiber and epoxy in S5 boosts these properties even further, reaching the highest values in this group (76.19 MPa for strength and 12948.47 MPa for modulus). Interestingly, S6, where APP was only added in fiber treatment but not in the epoxy, has lower flexural properties compared to S5 but still performs better than S4. This suggests that the combination of APP in both fiber and epoxy leads to the highest improvement in flexural properties when treated with NaOH.

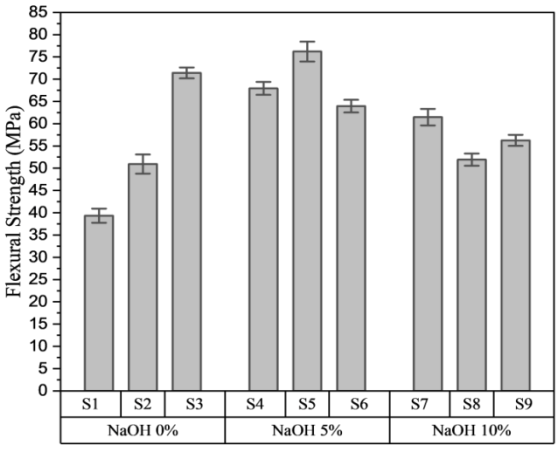

Figure 5.15 The variation in flexural strength of hemp fiber reinforced composites of different processing parameters.

For the 10% NaOH-treated samples (S7, S8, S9), the results are more variable. S7, which only has APP in the epoxy, shows good flexural properties (61.47 MPa for strength and 7858.68 MPa for modulus), though they are not as high as those seen in the 5% NaOH-treated samples. S8, with APP treatment only in the fiber and none in the epoxy, has notably lower properties (51.93 MPa for strength and 5146.92 MPa for modulus), which may suggest that APP in the epoxy plays a more critical role when NaOH is used at 10%. S9, with both APP treatments at 20%, sees

improved values compared to S8 but still does not match the high values of S5, implying that the combined effect of NaOH at higher concentrations may not always result in linear improvements.

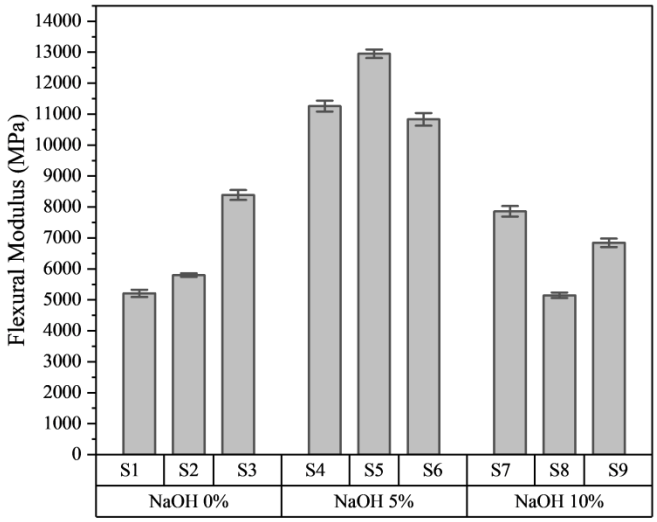

Figure 5.16 The variation in flexural modulus of hemp fiber reinforced composites of different processing parameters.

In summary, flexural strength and modulus improve with the addition of NaOH and APP treatments, but the effect depends on the combination of these treatments. Samples treated with 5% NaOH and combined with APP in both fiber and epoxy (S5) show the best overall flexural properties. Treatments with NaOH at 10% provide mixed results, and the absence of NaOH shows significant improvement with APP but doesn't reach the same levels as NaOH-treated samples. This suggests that a balanced treatment of NaOH and APP, particularly in both the fiber and epoxy, leads to the most significant improvements in flexural strength and modulus.

The main effects plots ((Figure 5.17 (a) & (b)) for flexural strength and modulus indicate that the optimal treatment for enhancing both properties is 5% NaOH (Factor A). At this level, flexural strength and modulus peak, while increasing NaOH to 10% results in a decline in performance. APP treatment of fibers (Factor B) shows a steady positive impact on both flexural strength and modulus, with higher concentrations (20%) yielding better results. The APP mixture in epoxy

(Factor C) also contributes to improved performance, with the highest concentrations consistently increasing both flexural properties.

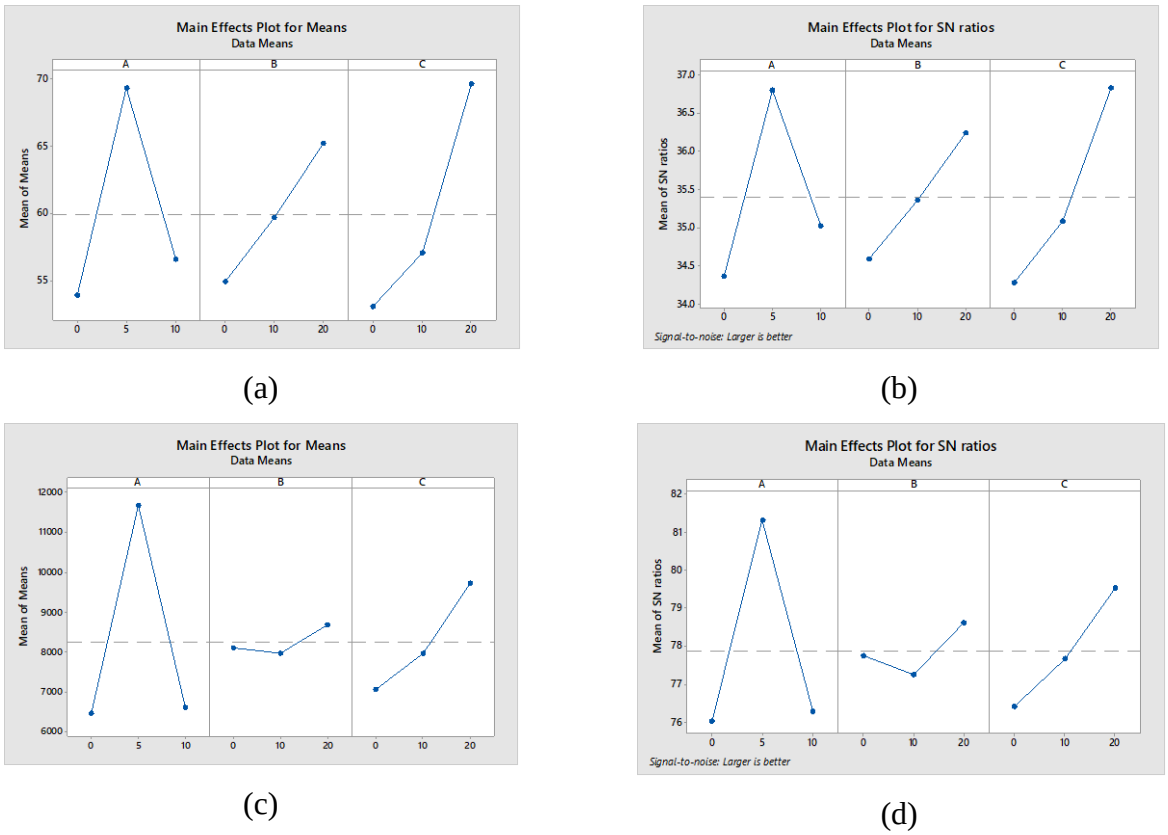

Figure 5.17 Images of (a) Main effects plot of means for flexural strength of biocomposite samples, (b) Main effects plot of signal-to-noise ratio for flexural strength of biocomposite samples, (c) Main effects plot of means for flexural modulus of biocomposite samples, and (d) Main effects plot of signal-to-noise ratio for flexural modulus of biocomposite samples.

The S/N ratio plots (Figure 5.17 (c) & (d)) for both flexural strength and modulus reinforce the idea that 5% NaOH provides the best signal-to-noise ratio, meaning that this concentration offers the most stable and reliable enhancement for these properties. Additionally, APP concentrations in both the fiber and epoxy tend to increase the S/N ratios, indicating a more consistent improvement with higher APP levels. Overall, the combined effect of 5% NaOH and increasing APP concentrations in both fiber and epoxy leads to the most significant and reliable improvements in flexural strength and modulus.

The objective of the predicted models (Equation 5.3 & 5.4) were to establish the relationship between the flexural properties (flexural strength and flexural modulus) of fiber-reinforced composites and the processing parameters, including NaOH treatment, APP concentration in the fiber, and APP concentration in the resin. These models were created using statistical tools based on experimental data. The analysis of processing conditions on flexural properties revealed that NaOH treatment had a mixed impact, with the best results occurring at a 5% concentration, while 10% NaOH had diminishing effects. As a result, higher concentrations of NaOH were excluded from the final mathematical model. The addition of APP, particularly in the resin, was found to play a key role in enhancing mechanical properties, though it must be applied in conjunction with other treatments for optimal results. Linear regression models were developed to connect flexural strength with APP concentrations in both fiber and resin, as well as flexural modulus with these concentrations, using the commercial software MINITAB 17.

$$Flexural\ strength\ (MPa) = 45.16 + 0.266A + 0.514B + 0.831C \quad (5.3)$$

&

$$Flexural\ modulus\ (MPa) = 6554 + 15A + 29B + 133C \quad (5.4)$$

Where,

A is Treatment of Fiber with NaOH (w/v %) solution with water

B is Treatment of Fiber with APP (w/v %) mixture with water

C is Mixture of APP (w/w %) with epoxy resin

5.4.3 Izod impact toughness of the composites

Table 5.4 presents data on the energy absorbed (in kJ/m²) by nine samples during Izod impact testing, along with their mean values and standard deviations and Figure 5.18 presents a visual representation using bar graphs. It provides a comparative analysis of the energy absorption capacity and variability of the samples.

Samples with NaOH treatment (A) at varying concentrations show differences in energy absorption. Samples S7, S8, and S9, treated with 10% NaOH, generally absorbed higher energy, with values ranging from 4147.40 kJ/m² (S8) to 4297.30 kJ/m² (S7). This suggests that a higher NaOH concentration may improve the fiber-matrix interaction, leading to better energy

absorption. In contrast, samples without NaOH treatment (S1, S2, S3) show slightly lower energy absorption values, with S3 being the highest among them at 4284.39 kJ/m². The intermediate NaOH concentration of 5% (S4, S5, S6) provides a balance in energy absorption, with S5 performing the best among these at 4572.64 kJ/m². This indicates that moderate NaOH treatment may provide optimal fiber bonding without over-brittling the composite.

Table 5.4 Results of izod impact testing for various composite samples

Sample	Energy absorbed (kJ/m^2)	
	Mean	St.dev.
S1	4151.74	376.45
S2	4183.11	189.28
S3	4284.39	382.71
S4	4276.18	126.41
S5	4572.64	484.62
S6	4180.74	321.73
S7	4297.30	271.37
S8	4147.40	63.54
S9	4292.42	217.13

Samples with NaOH treatment (A) at varying concentrations show differences in energy absorption. Samples S7, S8, and S9, treated with 10% NaOH, generally absorbed higher energy, with values ranging from 4147.40 kJ/m² (S8) to 4297.30 kJ/m² (S7). This suggests that a higher NaOH concentration may improve the fiber-matrix interaction, leading to better energy absorption. In contrast, samples without NaOH treatment (S1, S2, S3) show slightly lower energy absorption values, with S3 being the highest among them at 4284.39 kJ/m². The intermediate NaOH concentration of 5% (S4, S5, S6) provides a balance in energy absorption, with S5 performing the best among these at 4572.64 kJ/m². This indicates that moderate NaOH treatment may provide optimal fiber bonding without over-brittling the composite.

APP treatment on fibers (B) shows a significant impact on the composite's impact properties. Samples treated with 20% APP (S3, S6, S9) exhibit relatively higher energy absorption,

particularly S9, which absorbed 4292.42 kJ/m². However, S6 absorbed lower energy at 4180.74 kJ/m², suggesting that the interaction between APP and other factors like NaOH concentration or APP in the resin mixture plays a crucial role. Samples without APP fiber treatment (S1, S4, S7) generally absorbed comparable or slightly lower energy, especially S1 (4151.74 kJ/m²). The moderate APP fiber treatment of 10% (S2, S5, S8) shows varying results, with S5 absorbing the highest energy (4572.64 kJ/m²), indicating that 10% APP might strike a favorable balance for impact resistance.

The addition of APP to the epoxy resin (Factor C) has a mixed influence on the impact properties. Samples with 20% APP in resin (S3, S5, S7) generally show higher energy absorption, particularly S5 at 4572.64 kJ/m². This suggests that a higher percentage of APP in the resin contributes positively to impact resistance when combined with moderate NaOH and APP fiber treatments. However, sample S3 absorbed slightly less energy at 4284.39 kJ/m², which might indicate that the specific fiber treatment level affects the overall composite performance. Samples without APP in the resin (S1, S6, S8) exhibited slightly lower energy absorption, with S1 being the lowest at 4151.74 kJ/m², indicating that APP in the resin is beneficial for enhancing impact resistance.

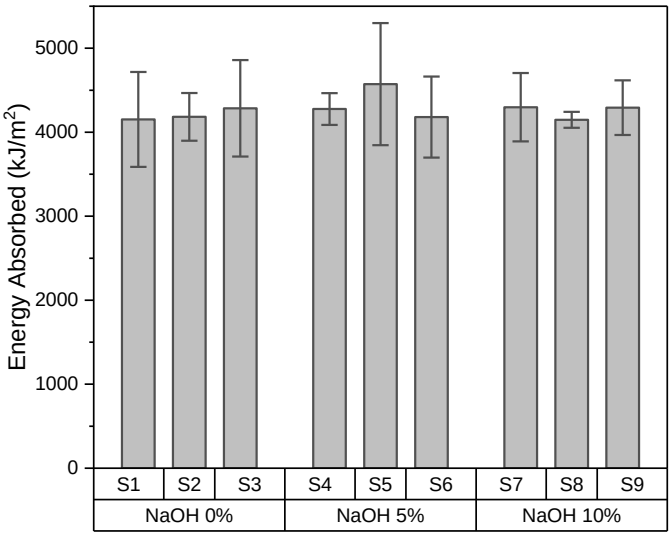

Figure 5.18 The variation in impact resistance of biocomposites of different processing parameters

In summary, the combination of NaOH treatment, APP fiber treatment, and APP in the resin mixture significantly affects the energy absorption of the composite samples. Higher NaOH concentrations generally improve the fiber-matrix bond, leading to higher energy absorption. APP treatment of fibers also plays a critical role, with moderate levels providing optimal performance. Similarly, incorporating APP into the resin mixture improves impact resistance, especially when combined with optimal fiber treatments. Sample S5, treated with 5% NaOH, 10% APP on fibers, and 20% APP in resin, demonstrated the highest energy absorption, indicating that this combination provides a favorable balance between mechanical strength and fire-retardant properties.

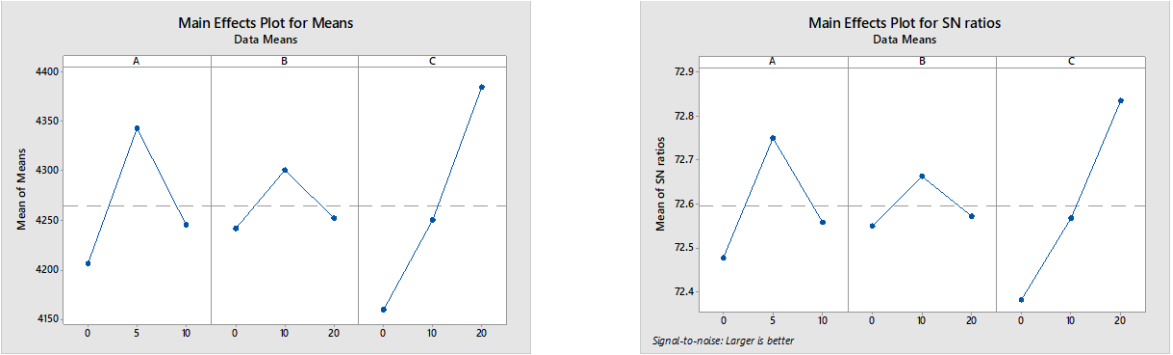

(a) (b)

Figure 5.19 Images of (a) Main effects plot of means for energy absorbed by biocomposite samples, (b) Main effects plot of signal-to-noise ratio for energy absorbed by biocomposite samples

The main effects plot for means (Figure 5.19 (a)) indicates that the flexural properties (strength and modulus) of the composites are most positively influenced by moderate NaOH treatment (5%) and the addition of APP to the resin mixture (20%). The NaOH treatment shows an increase in flexural properties at 5%, followed by a decrease at 10%, suggesting that moderate NaOH concentration optimizes fiber-matrix bonding. APP treatment of fibers shows a slight increase in flexural properties at 10% but decreases at 20%, indicating that excessive APP content in fibers may introduce brittleness. On the other hand, increasing the APP concentration in the resin (Factor C) from 0% to 20% has the most significant positive effect, showing a sharp

rise in flexural strength and modulus, likely due to improved stiffness and reinforcement of the composite.

The signal-to-noise (SN) ratio plot (Figure 5.19 (b)) for energy absorption (kJ/m²) supports similar trends, with the SN ratio peaking at 5% NaOH treatment and 10% APP fiber treatment, indicating these levels produce the most consistent and desirable energy absorption. Higher APP in the resin (20%) leads to the best robustness for impact properties, showing a sharp increase in the SN ratio, suggesting it enhances both stiffness and energy absorption. These findings suggest that a combination of moderate NaOH treatment and high APP in the resin mixture yields the best overall mechanical and impact performance.

A linear regression model (Equation 5.5) was developed in MINITAB software to predict the energy absorbed (kJ/m²) based on the three factors. The model helps quantify the relationship between these factors and energy absorption, identifying the most significant contributors to the composite's impact resistance. The regression equation is as follows:

$$Energy\ absorbed\ (kJ/m^2) = 4127.7 + 3.93A + 0.54B + 11.24\ C \qquad (5.5)$$

Where,

A is Treatment of Fiber with NaOH (w/v %) solution with water

B is Treatment of Fiber with APP (w/v %) mixture with water

C is Mixture of APP (w/w %) with epoxy resin

5.5 Physical characterization of the composites

The effects of the three factors (A, B, and C) on the physical properties of the composite, including density measurement and water absorption are presented in this section.

5.5.1 Effect of various parameters on the bulk density of hemp fiber-based polymer composites

Table 5.5 presents the experimental and theoretical densities of nine composite samples along with their void content.

Table 5.5 Density and void content analysis results of different composite samples

Sample	Experimental density (g/cm^3)	Theoretical density (g/cm^3)	Void content (%)
S1	1.082 ± 0.003	1.179	8.078
S2	1.158 ± 0.007	1.237	6.420
S3	1.219 ± 0.002	1.302	6.368
S4	1.183 ± 0.005	1.237	4.359
S5	1.251 ± 0.003	1.302	3.895
S6	1.125 ± 0.004	1.179	4.618
S7	1.257 ± 0.005	1.302	3.468
S8	1.167 ± 0.009	1.237	5.6435
S9	1.220 ± 0.002	1.302	6.336

The densities of the samples were found to vary depending on the different treatments applied, such as NaOH (Factor A), APP on fibers (Factor B), and APP in the resin mixture (Factor C). In Sample S1, the lowest experimental density of 1.082 g/cm^3 was recorded. A comparison with Sample S2, where the density reached 1.158 g/cm^3, showed a 7.02% increase, which was likely caused by the introduction of APP in the fibers and resin. This increase in matrix rigidity, due to the fiber and resin treatments, contributed to the higher density of S2. Similarly, Sample S3, with a density of 1.219 g/cm^3**,** displayed a 12.67% increase over S1, indicating that the higher APP content played a significant role in increasing the composite's density.

A comparison between Samples S4 and S5 showed that the density of S5, which was 1.251 g/cm^3, represented a 6.76% increase compared to S4, which had a density of 1.183 g/cm^3. The higher APP concentrations in both the fibers and resin of Sample S5 were likely responsible for the greater density observed. When Sample S6 was compared with S5, a 10.09% increase in density was noted in favor of S5, with the difference attributed to the higher levels of APP and NaOH in the treatment, which enhanced fiber-matrix bonding and resulted in a denser structure.

Sample S7 exhibited the highest density at 1.257 g/cm^3, which reflected an 8.44% increase over Sample S6. The combination of higher NaOH treatment and APP concentration in the resin

likely contributed to this enhanced density, as these factors promote better fiber bonding and resin integration. However, a 2.94% reduction in density was observed when Sample S7 was compared to Sample S9 (1.220 g/cm³). This reduction suggested that while APP in the resin increases density, the presence of voids or inconsistencies in treatment may slightly lower the overall density in some samples.

The differences in void content among the samples were also notable. Sample S1 had the highest void content, at 8.078%, which significantly impacted both its density and mechanical properties. The elevated void content was likely caused by insufficient NaOH or APP treatment, leading to weaker fiber-matrix adhesion. As a result, the internal structure was less compact, allowing more air pockets or voids to form, which ultimately reduced the composite's density.

In contrast, Sample S5 had the lowest void content at 3.895%**,** representing a 51.78% reduction compared to Sample S1. The significant reduction in voids in S5 was likely achieved due to a balanced NaOH treatment and higher concentrations of APP in both the fibers and the resin mixture. These treatments improved bonding between the fibers and the matrix, which helped fill gaps and reduce the formation of voids. As a result, the composite became denser and structurally more robust.

Sample S4 showed a void content of 4.359%**,** which indicated a 46.06% reduction compared to Sample S1. The moderate NaOH and APP treatments applied in S4 were likely responsible for enhancing the fiber-matrix bonding and reducing the formation of voids. However, Sample S7 had even lower void content, at 3.468%**,** suggesting that a higher APP concentration in the resin mixture played a critical role in further minimizing voids. This reduction in void content contributed to the higher density and improved structural integrity of the composite.

In Sample S8, a void content of 5.6435% was recorded, which was lower than that of Sample S2 (6.420%) but higher than that of Sample S1. This difference implied that while the addition of APP in the resin was beneficial in reducing voids, the specific fiber treatment level required optimization to balance the composite's density and void content. As seen in other samples, the

interaction between APP, NaOH treatment, and fiber bonding had a direct impact on the composite's overall void content and density.

The roles of Factors A, B, and C in influencing the density and void content of the samples were evident. The NaOH treatment (Factor A) was observed to improve fiber-matrix bonding, resulting in increased density and reduced void content. However, excessive NaOH concentrations could degrade the fibers, leading to a weaker structure. Factor B, the APP treatment of fibers, was shown to contribute to flame retardancy and improved mechanical properties. Moderate APP levels were effective in reducing void content and increasing density, but higher concentrations might induce brittleness. Factor C, the APP in the resin mixture, played a significant role in minimizing void content and increasing density, particularly in samples with higher APP concentrations. The combined effect of these treatments determined the overall quality of the composite materials.

5.5.2 Water absorption tests

Table 5.6 shows the water absorption (%) test results of different composites after 21 days of immersion in distilled water and Figure 5.20 provides a graphical representation of the variations.

Table 5.6 Water absorption of biocomposites at different processing conditions.

Sample	Water absorption (%)	
	Mean	St.dev.
S1	1.3075	0.0631
S2	1.6405	0.0459
S3	1.9728	0.1039
S4	1.1179	0.0522
S5	1.4261	0.0964
S6	1.3758	0.0511
S7	0.9112	0.0272
S8	0.8567	0.0346
S9	1.1828	0.0675

The water absorption percentages for the composite samples reveal differences based on the fiber and resin treatments. Sample S1 has a water absorption of 1.3075%**,** while Sample S2 shows a 25.47% increase in absorption at 1.6405%**.** The higher water absorption in S2 can be attributed to the inclusion of APP in both the fiber and resin treatments, which, while enhancing flame retardancy, may increase the material's hydrophilicity, making it more prone to moisture uptake. Sample S3, with 1.9728% absorption, reflects a 19.58% increase over S2, which could be linked to the higher APP concentration, further contributing to water absorption.

On the other hand, Sample S4 shows a 14.5% reduction in water absorption compared to S1, with a value of 1.1179%**.** This reduction suggests that the moderate NaOH treatment in S4 enhances fiber-matrix bonding, making the composite less permeable to water. In contrast, Sample S5 has a water absorption of 1.4261%**,** representing a 27.52% increase compared to S4. This increase in moisture uptake is likely caused by the higher concentrations of APP used in both the fibers and resin, which, while beneficial for flame resistance, contributes to greater water absorption.

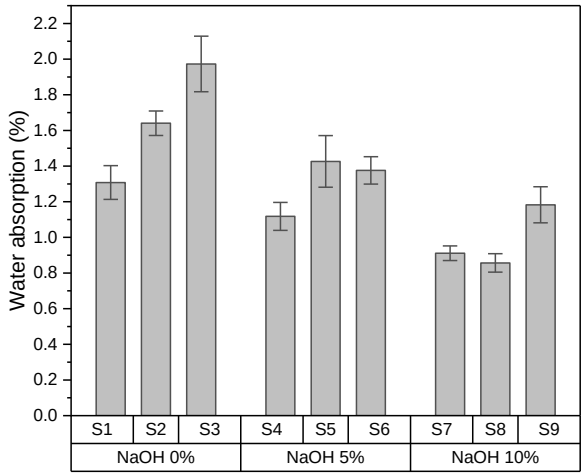

Figure 5.20 The variation in water absorption by hemp fiber reinforced composites of different processing parameters.

Sample S6**,** with 1.3758% water absorption, shows a moderate increase compared to S4, but Sample S7 exhibits a significant 33.73% reduction in absorption, reaching 0.9112%**.** The lower

absorption in S7 can be attributed to the higher NaOH treatment and the APP content in the resin, which improves the composite's resistance to moisture. The combination of these factors leads to better fiber-matrix interaction and reduced porosity, effectively lowering water absorption.

Sample S8 has the lowest water absorption of all, at 0.8567%**,** representing a 6% reduction compared to S7. This further reduction highlights the effectiveness of the APP in the resin (Factor C) in sealing the matrix and preventing moisture penetration. APP in the resin seems to play a crucial role in reducing water absorption by improving the matrix's density and minimizing porosity, especially when balanced with appropriate fiber treatments.

In Sample S9, the water absorption rises to 1.1828%**,** a 27.8% increase compared to S8. This increase may be attributed to the higher APP concentration in the fibers, which, despite its fire-retardant properties, tends to make the composite more hydrophilic, allowing more moisture to be absorbed. This pattern suggests that while APP in the resin helps reduce water absorption, APP treatment on the fibers (Factor B) can have the opposite effect, increasing the hydrophilicity of the material.

The interplay of NaOH treatment (Factor A), APP treatment of fibers (Factor B), and APP in the resin (Factor C) significantly influences water absorption in the samples. NaOH treatment improves fiber-matrix bonding and reduces water absorption by making the composite more resistant to moisture. However, excessive NaOH can weaken the fibers, leading to slight increases in absorption. APP in the fibers enhances flame retardancy but increases hydrophilicity, causing more moisture uptake, while APP in the resin helps seal the matrix and reduce water absorption by filling gaps and reducing porosity.

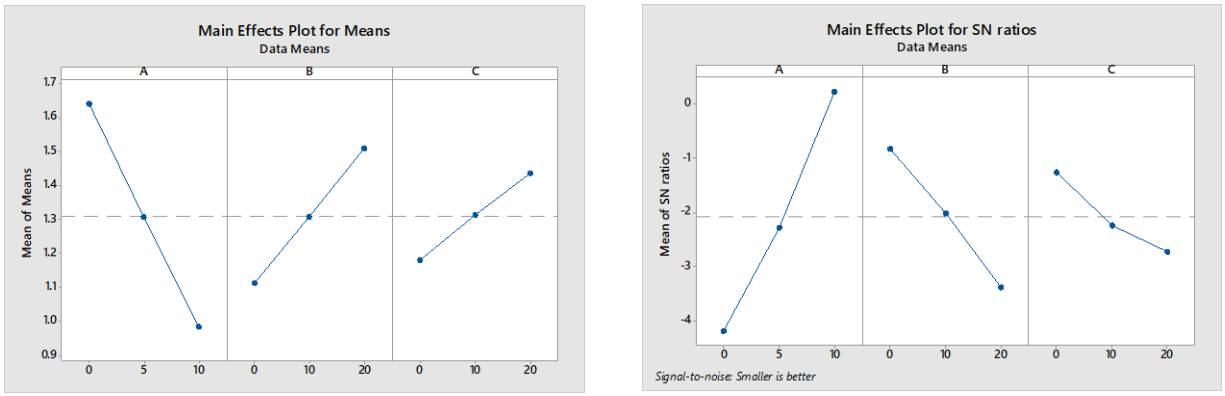

(a) (b)

Figure 5.21 Images of (a) Main effects plot of means for water absorption (%) of biocomposite samples, (b) Main effects plot of signal-to-noise ratio for water absorption (%) of biocomposite samples.

A linear regression equation (Equation 5.6) has been developed to predict water absorption (%) based on the factors A (NaOH treatment), B (APP treatment on fibers), and C (APP in resin). The equation quantifies the relationship between these factors, showing that NaOH treatment significantly decreases water absorption, while higher concentrations of APP in both the fibers and resin increase it. This model helps to understand how varying the levels of these treatments can optimize the composite's resistance to moisture. The regression model is as follows:

$$Water\ absorption\ (\%) = 1.31105 - 0.65670A + 0.019912B + 0.12833C \quad (5.6)$$

Where,

A is Treatment of Fiber with NaOH (w/v %) solution with water

B is Treatment of Fiber with APP (w/v %) mixture with water

C is Mixture of APP (w/w %) with epoxy resin

5.6 Thermal characterization of the composites

The effects of the three factors (A, B, and C) on the thermal properties of the composite, including thermal conductivity analysis and thermogravimetric analysis are presented in this section.

5.6.1 Thermal conductivity of different composite samples

Table 5.7 presents the thermal conductivity of different composite samples, determined using the heat flow meter test and Figure 5.22 presents bar graphs illustrating the variation in thermal conductivity across the nine samples.

Table 5.7 Thermal conductivity Measurements of composite samples with mean and standard Deviation

Sample	Thermal conductivity (W/m.K)	
	Mean	St.dev.
S1	0.0681	0.0093
S2	0.0667	0.0037
S3	0.0639	0.0026
S4	0.0565	0.0061
S5	0.0543	0.0035
S6	0.0565	0.0053
S7	0.0583	0.0023
S8	0.0554	0.0026
S9	0.0496	0.0069

The thermal conductivity values for the composite samples vary significantly based on the combination of treatments applied, specifically factors A (NaOH treatment), B (APP treatment on fibers), and C (APP in resin). Sample S1 has the highest thermal conductivity at 0.0681 W/m.K, indicating less effective insulation. Sample S2, with a conductivity of 0.0667 W/m.K, shows a 2.05% reduction in thermal conductivity, likely due to the introduction of APP, which improves the material's ability to resist heat transfer. Sample S3 further reduces thermal conductivity to 0.0639 W/m.K, a 4.19% decrease compared to S2, which can be attributed to the higher APP concentration in both the fibers and resin, enhancing its insulating properties.

Sample S4, at 0.0565 W/m.K, shows a significant 13.23% reduction compared to S1, suggesting that moderate NaOH and APP treatments improve the insulation of the material by limiting heat transfer pathways. Sample S5 continues this trend with an even lower thermal conductivity of

0.0543 W/m.K, representing a 3.9% decrease compared to S4. The further reduction in conductivity suggests that higher APP concentrations in both fibers and resin result in improved insulation, effectively lowering heat conduction.

Sample S6, which also has a thermal conductivity of 0.0565 W/m.K, shows similar results to S4, indicating that the levels of NaOH and APP treatments applied result in comparable thermal behavior. However, Sample S7 has a slightly higher conductivity of 0.0583 W/m.K, representing a 3.19% increase compared to S6, possibly due to a higher concentration of NaOH. While NaOH improves fiber-matrix bonding, it can slightly increase the composite's ability to conduct heat if applied in excess, as stronger bonding might enhance the transmission of thermal energy.

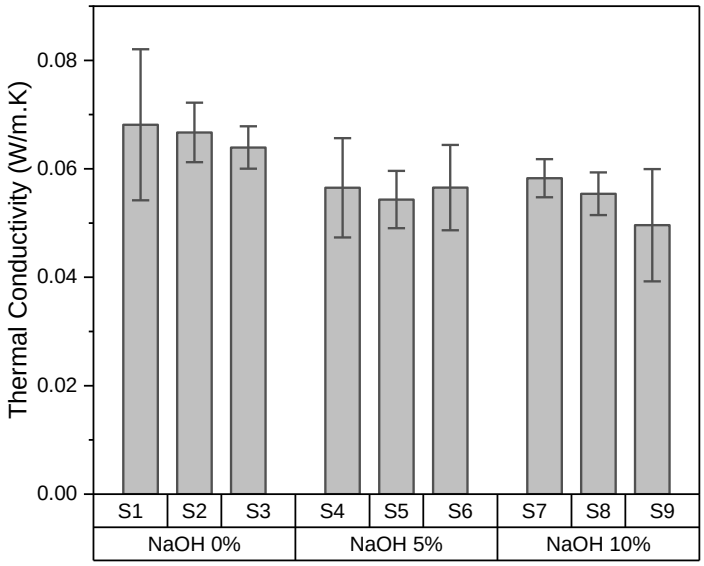

Figure 5.22 The variation in thermal conductivity of hemp fiber reinforced composites of different processing parameters.

Sample S8 reduces thermal conductivity to 0.0554 W/m.K, a 5% decrease compared to S7, showing that the combination of NaOH and APP treatments, particularly with higher APP concentrations in the resin, further minimizes heat transfer. Sample S9, with the lowest thermal conductivity at 0.0496 W/m.K**,** shows an 11.69% reduction compared to S8. This indicates that a higher concentration of APP in both the fibers and resin, along with moderate NaOH treatment,

plays a critical role in enhancing the composite's insulating properties by significantly reducing heat conduction.

Factor A (NaOH Treatment) improves fiber-matrix bonding, which typically reduces thermal conductivity by limiting heat transfer pathways. However, excessively high NaOH concentrations may slightly increase thermal conductivity, as seen in samples with denser bonding. This suggests that a balanced level of NaOH treatment is necessary to optimize insulation without increasing heat conduction through stronger bonding in the fibers.

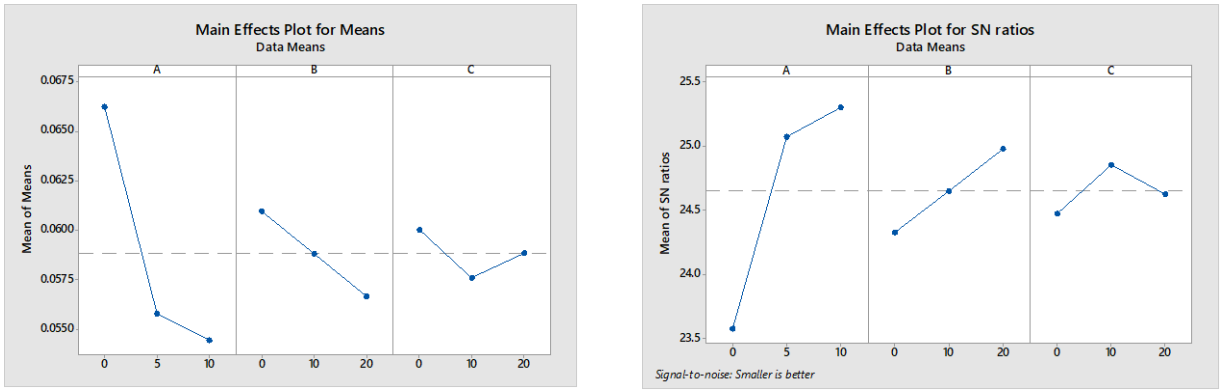

(a) (b)

Figure 5.23 Images of (a) Main effects plot of means for thermal conductivity of biocomposite samples, (b) Main effects plot of signal-to-noise ratio for thermal conductivity of biocomposite samples.

The main effects plot (Figure 5.23 (a)) for means indicates that increasing NaOH concentration (Factor A) significantly reduces water absorption, with a steep decrease seen as the concentration increases to 10%, suggesting improved fiber-matrix bonding that limits moisture uptake. Factor B (APP treatment on fibers) also shows a reduction in water absorption as APP concentration increases, though the effect is less pronounced than NaOH. On the other hand, Factor C (APP in resin) slightly increases water absorption at higher concentrations, possibly due to changes in the resin structure that allow more moisture penetration.

The SN ratio plot (Figure 5.23 (b)) for thermal conductivity shows that increasing NaOH treatment (Factor A) leads to more consistent and predictable reductions in thermal conductivity, as indicated by the rising SN ratio. Similarly, increasing APP treatment on fibers (Factor B)

improves the uniformity of thermal insulation, with a higher SN ratio reflecting better performance. However, higher APP concentrations in the resin (Factor C) show a slight dip in consistency at 20%, indicating that while APP improves insulation, too much may introduce slight variability in thermal performance.

A regression model (Equation 5.7) has been developed to predict thermal conductivity based on the three factors: NaOH treatment (Factor A), APP treatment on fibers (Factor B), and APP in resin (Factor C). The model helps quantify how these factors influence the thermal conductivity of the composite, showing that higher NaOH and APP concentrations generally reduce heat transfer. The regression is as follows-

$$Thermal\ conductivity\ (W/m.K) = 0.6744 - 0.001180A - 0.000215B - 0.000058C \quad (5.7)$$

Where,

A is Treatment of Fiber with NaOH (w/v %) solution with water

B is Treatment of Fiber with APP (w/v %) mixture with water

C is Mixture of APP (w/w %) with epoxy resin

5.6.2 Thermogravimetric analysis

The thermogravimetric analysis (TGA) and derivative thermogravimetry (DTG) results for the nine samples subjected to various treatments with NaOH (A), ammonium polyphosphate (APP) in fiber (B), and APP in epoxy resin (C) show distinct thermal degradation behaviors based on the combination and concentration of treatments. TGA tracks the weight loss as a function of temperature, while DTG provides insights into the rate of weight change, indicating the key decomposition stages of each sample (Figure 5.24 to Figure 5.32). The differences in thermal stability among the samples are influenced by the presence and levels of APP and NaOH, both known to impact fiber structure and fire-retardant properties.

Sample S1, the baseline with no NaOH or APP treatments, exhibits the typical two-stage weight loss profile common to untreated natural fiber composites. The first stage is a minor weight loss around 100°C due to moisture evaporation, followed by the primary decomposition between 300°C and 400°C**,** typical of cellulose breakdown. Without any flame retardant, the material

combusts rapidly, leaving little residual char at higher temperatures. This is reflected in the TGA graph, where the ash yield is almost negligible, indicating minimal resistance to thermal degradation.

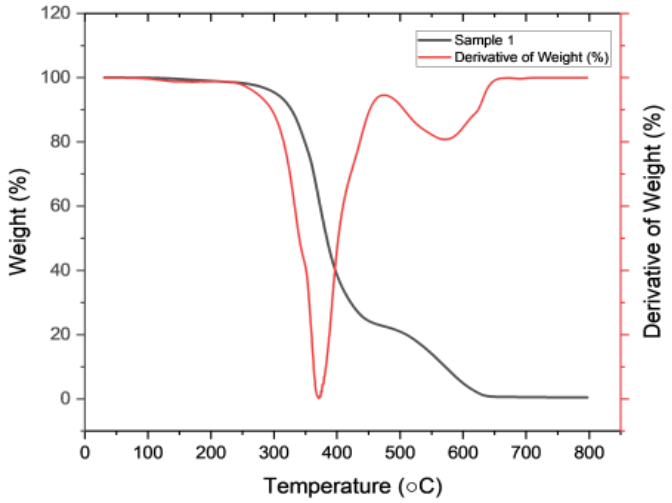

Figure 5.24 TGA and DTG Curve of composite Sample 1 (S1)

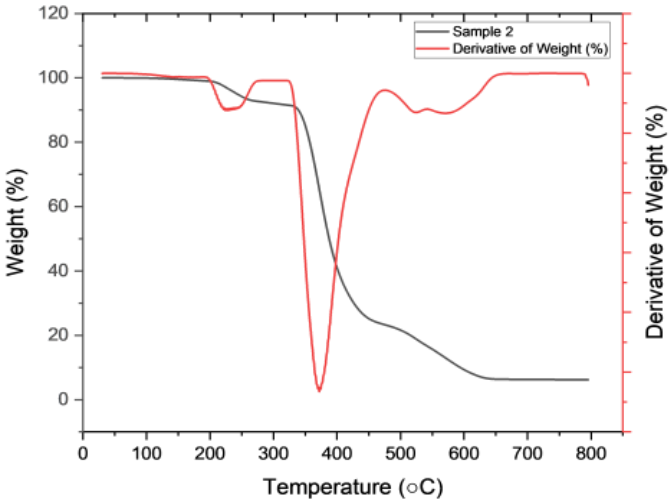

Figure 5.25 TGA and DTG Curve of composite Sample 2 (S2)

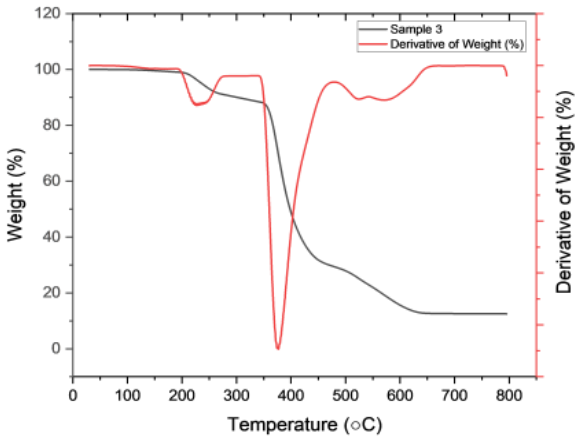

Figure 5.26 TGA and DTG Curve of composite Sample 3 (S3)

In APP-treated samples such as S2 and S3, there is a marked improvement in thermal stability compared to S1. These samples decompose more slowly, with T_{max} values of 350°C and 370°C, respectively. The inclusion of APP in the fiber promotes char formation, slowing down combustion and enhancing the material's flame resistance. S3, with a higher APP concentration, shows more residual char at the end of the test compared to S2, which correlates with its improved thermal performance. Additionally, both samples exhibit an extra weight loss step between 230°C and 260°C, a characteristic linked to the degradation of APP and its interaction with the epoxy matrix.

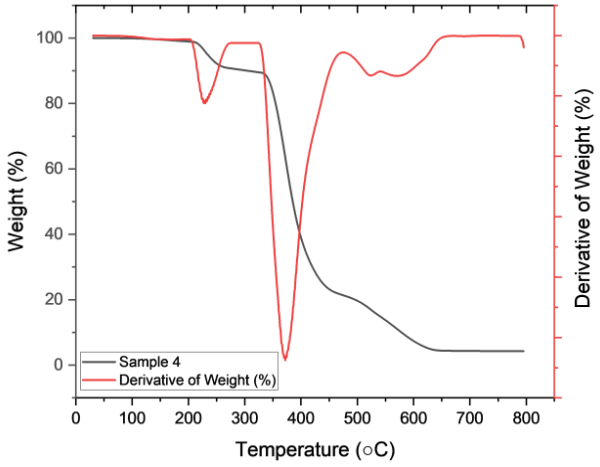

Figure 5.27 TGA and DTG Curve of composite Sample 4 (S4)

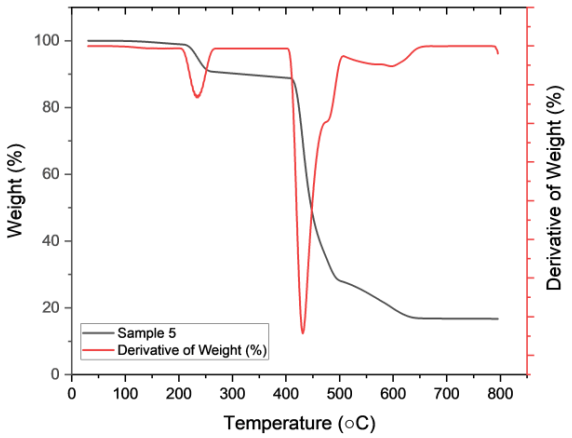

Figure 5.28 TGA and DTG Curve of composite Sample 5 (S5)

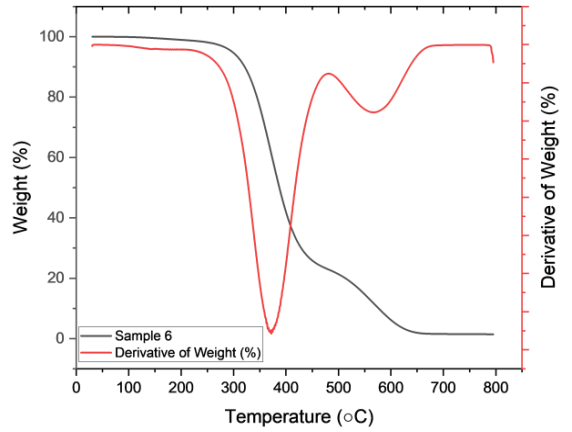

Figure 5.29 TGA and DTG Curve composite of Sample 6 (S6)

The NaOH-treated samples (S4 to S9) display significant changes in thermal behavior. The removal of hemicellulose and lignin during NaOH treatment reduces the mass loss below 300°C, as these components typically degrade at lower temperatures. The increased crystallinity of the fibers due to NaOH treatment leads to sharper decomposition peaks between 300°C and 400°C in the TGA graphs. Moreover, NaOH-treated samples exhibit a higher char yield above 600°C**,** particularly in samples where APP is also present, such as S5 and S7, resulting in better flame resistance compared to the untreated fibers in S1.

Samples S5 and S7, which contain APP in the epoxy matrix, further demonstrate the combined benefits of NaOH treatment and APP. These samples exhibit an additional degradation phase between 230°C and 260°C, not observed in samples treated only with NaOH. This phase corresponds to the interaction between APP and the epoxy, contributing to the formation of char and enhancing thermal stability. The T_{max} values for these samples are notably higher, with S5 reaching 431°C and S7 at 374°C, reflecting the dual protection offered by APP, which acts both in the fiber and the resin matrix to delay decomposition and improve flame retardancy.

Comparing 5% NaOH-treated samples (S4 to S6) with 10% NaOH-treated samples (S7 to S9) reveals some distinct differences. S4 shows a T_{max} of 372°C and 4.27% residual char, reflecting moderate improvements in thermal stability from NaOH treatment alone. S5, however, demonstrates the best thermal performance among the 5% NaOH-treated group, with T_{max} reaching 431°C and 16.71% residual char due to the combined effect of APP and NaOH treatment. On the other hand, S6, which lacks APP in the resin, has a T_{max} of 372°C and a lower char yield of 1.44%**,** indicating reduced flame resistance compared to S5.

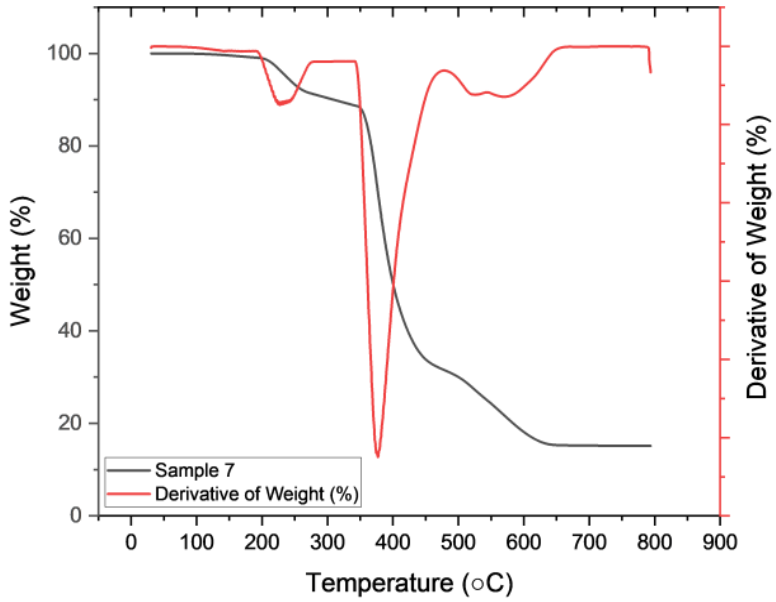

Figure 5.30 TGA and DTG Curve of composite Sample 7 (S7)

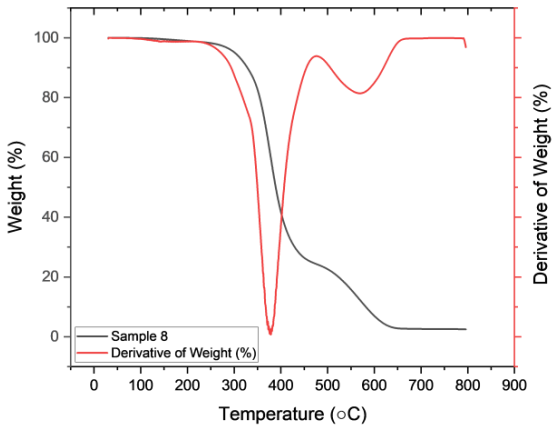

Figure 5.31 TGA and DTG Curve of composite Sample 8 (S8)

For 10% NaOH-treated samples, S7 (APP in fiber and resin) exhibits a T_{max} of 374°C and 15.14% residual char, showing strong flame retardancy. The higher NaOH concentration enhances the thermal stability of the fibers, but the higher crystallinity might lead to slightly more brittle structures, resulting in a lower T_{max} compared to S5. Similarly, S8 shows improved thermal stability with a T_{max} of 378°C and 2.49% residual char, but the absence of APP in the resin results in lower overall performance compared to S7. S9, which also lacks APP in the resin, demonstrates moderate thermal performance with a T_{max} of 373°C and 9.05% residual char, indicating that while the higher NaOH concentration improves char formation, it still falls short of samples with APP in both fiber and resin.

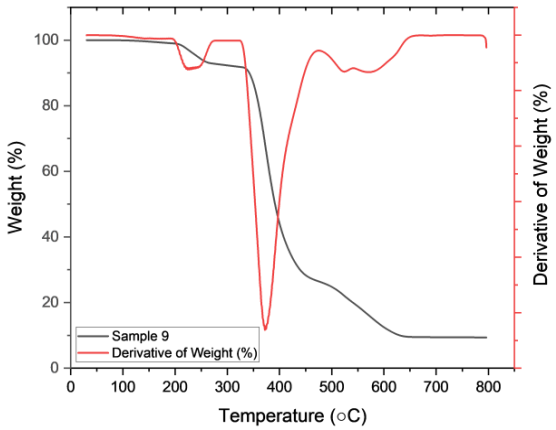

Figure 5.32 TGA and DTG Curve of composite Sample 9 (S9)

The comparison between samples with lower concentrations of APP in the epoxy resin (S2, S4, S6) and those with higher concentrations of APP (S3, S5, S7) reveals that higher APP levels significantly improve thermal stability and flame retardancy. S3 (high APP) shows a T_{max} of 376°C and 12.50% residual char, much higher than S2 (low APP) with 372°C T_{max} and 6.21% char. The higher APP content delays combustion more effectively and promotes more substantial char formation, providing better protection at higher temperatures.

The best thermal performance is seen in S5 (5% NaOH with high APP), which reaches a T_{max} of 431°C and 16.71% residual char. This demonstrates that combining moderate NaOH treatment with a high concentration of APP in both the fiber and resin provides the best balance of thermal protection and flame retardancy. In contrast, S4 and S6 (low APP) show moderate thermal stability but much lower char yields, highlighting the importance of APP concentration in enhancing the material's resistance to decomposition and combustion.

In summary, higher APP concentrations in the epoxy resin significantly improve the thermal stability and flame resistance of the composite materials, particularly when combined with NaOH-treated fibers. The increased APP content promotes char formation, delays decomposition, and protects both the fiber and resin matrix, resulting in composites that are more resistant to high temperatures and more suited for applications requiring enhanced flame retardancy.

The thermal decomposition data for the nine samples subjected to various treatments of NaOH and ammonium polyphosphate (APP) in fiber and epoxy resin reveal significant variations in thermal behavior has been represented Table 5.8. The key metrics—decomposition temperatures at 5% ($T_{95\%}$) and 50% ($T_{50\%}$) weight loss, maximum decomposition temperature (T_{max}), and ash yield—provide insight into how these treatments impact thermal stability and flame-retardant properties. Samples treated with APP in both water and epoxy resin generally exhibit earlier onset of degradation (lower $T_{95\%}$) but improved thermal resistance at higher temperatures, indicating the efficacy of APP as a flame retardant.

Table 5.8 Thermal Decomposition Parameters from TGA Analysis

Sample	$T_{95\%}$	$T_{50\%}$	T_{max}	Ash yield
	(ºC)	(ºC)	(ºC)	
S1	304	384	368	0.48
S2	243	388	372	6.21
S3	236	398	376	12.50
S4	234	385	372	4.27
S5	234	447	431	16.71
S6	297	387	372	1.44
S7	237	400	374	15.14
S8	301	389	378	2.49
S9	243	391	373	9.05

The untreated sample (S1) has a $T_{95\%}$ of 304°C, showing relatively high stability compared to the APP-treated samples. In contrast, samples with APP (S2, S3, and S5) exhibit earlier degradation at temperatures around 236°C–243°C. This earlier weight loss is attributed to the action of APP, which releases non-combustible gases and promotes char formation at lower temperatures. Notably, sample S5, with both NaOH and the highest concentrations of APP, exhibits the most delayed $T_{50\%}$ at 447°C, reflecting its improved resistance to major decomposition.

The maximum decomposition temperature (T_{max}) for most samples lies between 368°C and 378°C, showing limited variation. However, sample S5 again stands out with a significantly higher Tmax of 431°C, further demonstrating the enhanced thermal stability provided by the combination of NaOH and high APP content. The increased Tmax suggests that the presence of APP, particularly in the epoxy matrix, delays the peak decomposition rate and extends the material's resistance to heat. This finding highlights the role of APP in improving fire resistance by slowing down the material’s decomposition process.

Ash yield, which represents the residual material after decomposition at 800°C, further underscores the influence of APP. Untreated fibers (S1) have a very low ash yield of 0.48%, indicating nearly complete combustion, whereas samples with APP show significantly higher

residual weight, especially in S3 (12.50%), S5 (16.71%), and S7 (15.14%). This increase in ash yield is a clear indication of APP's flame-retardant action, as the formation of a protective char layer reduces further combustion, leaving more residual material. The higher the ash yield, the more effective the flame retardant action.

The thermogravimetric analysis of the treated samples clearly demonstrates the crucial role of APP in enhancing thermal stability and fire resistance, especially when combined with epoxy resin. APP promotes early degradation through char formation while improving the overall resistance to heat at higher temperatures, as seen in the delayed $T_{50\%}$ and increased Tmax values. NaOH treatment, while leading to early decomposition, improves long-term thermal stability when used alongside APP. These findings indicate that the combination of APP and NaOH, particularly in higher concentrations, significantly improves the fire-resistant properties of the composite materials.

5.7 Fire resistance of the composites

The effects of the three factors (A, B, and C) on the fire resistance properties of the composite, including tensile UL94 vertical burn test and cone calorimeter test are presented in this section.

5.7.1 UL94 vertical burn tests

The following table (Table 5.9) summarizes the flame ratings of various material samples evaluated using the UL94 standard flame test.

The UL94 vertical burn test results reveal distinct variations in flame resistance among the different samples, highlighting the impact of varying NaOH treatment levels, APP concentrations, and their combinations. Samples such as S3, S5, and S7 achieved the highest flame rating of V0, indicating superior flame retardancy. These samples consistently correspond to treatments combining higher APP concentrations (20%) and effective fiber pretreatment with NaOH, demonstrating the synergistic effect of these two modifications. The char formation and thermal stability induced by APP, coupled with the enhanced bonding provided by NaOH treatment, played a key role in their excellent performance.

Table 5.9 Flame Ratings of Material Samples Based on UL94 Test

Sample	Flame Rating
S1	No Rating
S2	V2
S3	V0
S4	No Rating
S5	V0
S6	V1
S7	V0
S8	V1
S8	V2

The UL94 vertical burn test results reveal distinct variations in flame resistance among the different samples, highlighting the impact of varying NaOH treatment levels, APP concentrations, and their combinations. Samples such as S3, S5, and S7 achieved the highest flame rating of V0, indicating superior flame retardancy. These samples consistently correspond to treatments combining higher APP concentrations (20%) and effective fiber pretreatment with NaOH, demonstrating the synergistic effect of these two modifications. The char formation and thermal stability induced by APP, coupled with the enhanced bonding provided by NaOH treatment, played a key role in their excellent performance.

In contrast, samples such as S1 and S4, which were either untreated or received minimal modifications, failed to achieve any flame rating, emphasizing the necessity of these chemical treatments to improve flame resistance. Intermediate ratings, such as V1 and V2 seen in samples like S6, S8, and S2, suggest a moderate level of flame retardancy. These samples benefitted from either NaOH or APP treatment alone but did not reach the optimal levels achieved with the combined treatments. Notably, S8 exhibits some variability, attaining both V1 and V2 ratings, which could be attributed to inconsistencies in treatment application or sample preparation. Overall, the results underscore that the combination of higher NaOH and APP concentrations consistently leads to the best flame ratings (V0), while untreated or minimally treated samples

exhibit the weakest performance, demonstrating the critical role of these treatments in achieving the desired fire safety standards for the developed materials.

5.7.2 Cone calorimeter tests

This table (Table 5.10) presents the cone calorimeter test results for nine composite samples, conducted under an Incident Heat Flux of 50kW/m². The table focuses on key four behavior metrics such as Peak Heat Release Rate (PHRR)**,** Average Heat Release Rate (AHRR)**,** and Total Heat Release**.** The AHRR and PHRR are critical indicators of how effectively each composite controls heat release during combustion. By comparing these values, the table allows for an assessment of the influence of different treatments, such as NaOH and APP, on the fire performance of the samples.

Table 5.10 Results of cone calorimeter test

Sample Number	Peak HRR Density (kW/m^2)		Avg HRR Density (kW/m^2)		Total Heat Release (MJ/m^2)		Total Heat Release/mass (MJ/kg)	
	Mean	St Dev.	Mean	St. dev.	Mean	St dev.	Mean	St dev.
S1	2274	57.40	277.67	28.36	73.19	0.31	833.61	0.56
S2	1255	17.90	172.33	5.51	101.86	0.40	485.16	0.88
S3	863	21.40	138.33	12.90	92.34	0.35	422.85	0.45
S4	1592	16.40	191.67	11.15	105.76	1.13	488.93	0.52
S5	1088	19.50	95.33	11.59	92.79	0.55	442.77	0.27
S6	1379	33.00	149.00	8.72	92.73	0.67	604.69	0.87
S7	1409	34.60	187.67	22.48	78.41	0.83	550.76	0.38
S8	1394	27.80	150.00	7.00	102.29	0.33	572.00	0.07
S9	937	7.40	96.33	10.07	100.35	0.74	470.13	1.58

The Average Heat Release Rate (HRR) results from the cone calorimeter test highlight significant differences between the samples based on their treatment with NaOH and ammonium polyphosphate (APP). S1, which has no NaOH or APP treatment, exhibits the highest Average HRR at 277.67 kW/m², indicating poor flame-retardant properties. This suggests that without any flame-retardant enhancements, the composite materials release heat quickly and combust at a

faster rate. In contrast, S5 and S9, which are treated with both NaOH and higher concentrations of APP in both the fibers and the resin, show the lowest Average HRR values of 95.33 kW/m² and 96.33 kW/m², respectively. These results demonstrate that the combination of NaOH treatment and APP significantly improves flame resistance by slowing down the heat release and combustion process

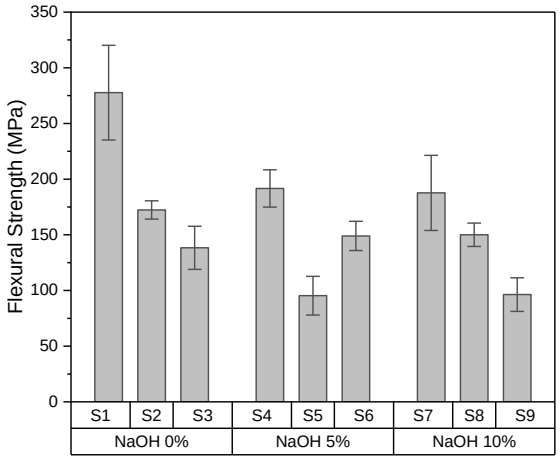

Figure 5.33 The variation in average heat release rate density of hemp fiber reinforced composites of different processing parameters.

When considering the impact of Factor A (NaOH treatment), it is clear that NaOH-treated samples generally show improved flame resistance (Figure 5.33). For instance, samples like S4 to S9, which include NaOH-treated fibers, exhibit lower Average HRR values compared to untreated samples like S1. The NaOH treatment removes hemicellulose and lignin from the natural fibers, which are more thermally unstable and tend to degrade at lower temperatures. This increases the crystallinity of cellulose in the fibers, thereby enhancing their thermal stability and slowing down combustion. The effect of NaOH treatment is especially evident in samples like S5 and S9, where NaOH works in conjunction with APP to further reduce heat release.

The role of Factor B (APP treatment in fiber) is also significant in reducing the Average HRR. APP acts as a flame retardant by promoting char formation during combustion, which insulates the material and slows down the release of heat. Samples with higher APP content in the fiber, such as S3, S6, and S9, demonstrate lower heat release rates compared to those with little to no

APP in the fibers, such as S1 and S4. However, the APP treatment in the fiber appears to be most effective when combined with APP in the resin, as seen in S9, which combines high APP concentrations in both the fiber and resin and shows excellent flame-retardant performance.

Finally, Factor C (APP treatment in resin) plays a crucial role in controlling heat release. Samples with APP in the resin, such as S2, S5, S7, and S9, generally show lower Average HRR values, as the presence of APP in the resin matrix enhances flame retardancy by further promoting char formation and slowing down combustion. The best-performing samples, S5 and S9, combine APP in both the fibers and the resin, along with NaOH-treated fibers, which provides maximum thermal stability and the most significant reduction in heat release. These results indicate that the combination of NaOH treatment with APP in both the fibers and the resin is the most effective strategy for reducing heat release and improving flame resistance in these composite materials.

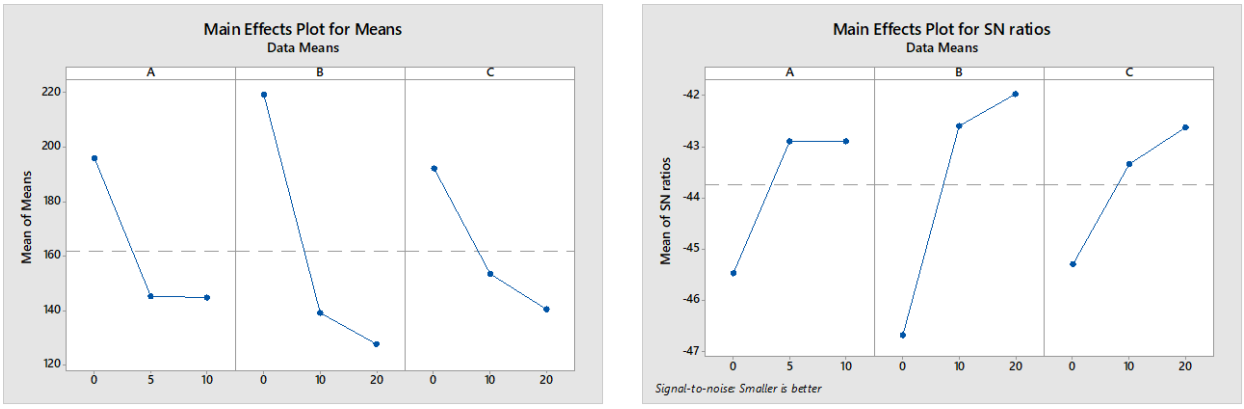

(a) (b)

Figure 5.34 Images of (a) Main effects plot of means for Avg HRR Density of biocomposite samples, (b) Main effects plot of signal-to-noise ratio for Avg HRR Density of biocomposite samples.

The main effects plot for means (Figure 5.34 (a)) illustrates the impact of the three factors on the Average Heat Release Rate (HRR). For Factor A (NaOH treatment), there is a sharp decrease in HRR when moving from 0% to 5% NaOH, indicating a significant reduction in HRR at lower NaOH concentrations. However, the curve levels off between 5% and 10%, suggesting that additional NaOH beyond 5% has diminishing returns on further reducing the HRR. For Factor B

(APP in fiber), there is a steep decline in HRR as APP concentration in the fiber increases from 0% to 20%, demonstrating that APP in the fiber is highly effective in reducing HRR and improving flame retardancy. Factor C (APP in resin) also shows a notable decrease in HRR as APP concentration in the resin increases, although the effect is slightly less pronounced compared to APP in the fiber.

The main effects plot for SN ratios (Figure 5.34 (b)) further reinforces these observations. For Factor A (NaOH treatment), the SN ratio improves significantly when NaOH concentration increases from 0% to 5%, with the improvement plateauing between 5% and 10%, indicating that 5% NaOH treatment is optimal. Factor B (APP in fiber) shows the most substantial improvement in the SN ratio, with a sharp rise from 0% to 20%**,** indicating that increasing APP concentration in the fiber greatly enhances the material's resistance to heat release and is the most influential factor in reducing HRR. Factor C (APP in resin) also contributes positively to the SN ratio, though the effect is slightly weaker compared to APP in the fiber.

In summary, Factor B (APP in fiber) has the most significant impact on reducing HRR and improving flame retardancy, followed closely by Factor C (APP in resin). Both factors show strong reductions in HRR with increased APP concentrations. Factor A (NaOH treatment) is effective at reducing HRR at 5% concentration, but further increases beyond 5% do not yield substantial additional benefits. These plots highlight the critical role of APP in both the fiber and resin in controlling heat release and enhancing fire resistance, with APP in the fiber having the most pronounced effect.

A regression model (Equation 5.7) has been developed to predict average heat release rate density based on the three factors: NaOH treatment (Factor A), APP treatment on fibers (Factor B), and APP in resin (Factor C).

$$Avg.HRR\ Density\ (kW/m^2) = 259.5 - 5.13A - 4.58B - 2.60C \qquad (5.8)$$

5.8 Optimization of the parameters

The presented table (Table 5.11) summarizes regression equations derived from the analysis of various test results for a developed material intended for use in ventilation ducts in underground mining applications. Each equation represents the relationship between different properties of the material and the influencing factors, with the corresponding R^2 values indicating the accuracy of the regression models. Among the listed equations, the ones for Energy Absorbed, Water Absorption, and Average HRR Density were chosen based on their relatively high R^2 values (56.99, 99.97, and 82.90, respectively) and their relevance to the material's performance. These equations were deemed most critical for optimization due to their importance in ensuring the safety, efficiency, and durability of the developed material in mining environments.

Table 5.11 Equations and corresponding R^2 values

Equations from Regression Analysis	R^2 Value
$Tensile\ Strength\ (MPa) = 36.41 - 0.087A + 0.158B + 0.586C$	42.90
$Young's\ Modulus\ (MPa) = 738 - 13.5A + 32.4B + 76.0\ C$	57.55
$Flexural\ strength\ (MPa) = 45.16 + 0.266A + 0.514B + 0.831C$	55.00
$Flexural\ modulus\ (MPa) = 6554 + 15A + 29B + 133C$	17.31
$Energy\ absorbed\ (kJ/m^2) = 4127.7 + 3.93A + 0.54B + 11.24\ C$	56.99
$Water\ absorption\ (\%) = 1.31105 - 0.65670A + 0.019912B + 0.12833C$	99.97
$Thermal\ conductivity\ (W/m.K) = 0.6744 - 0.001180A - 0.000215B - 0.000058C$	78.97
$Avg.HRR\ Density\ (kW/m^2) = 259.5 - 5.13A - 4.58B - 2.60C$	82.90

Using MATLAB's global optimization toolbox, a Genetic Algorithm (GA) was employed to optimize these selected equations, focusing on three primary parameters (A, B and C). This optimization process generated a dataset of 350 optimized combinations of these factors, which

are detailed in the appendix (Table A.1). The results of the optimization are illustrated by a Pareto front (Figure 5.35), which visually represents the trade-offs between the selected properties in the multi-objective optimization process. The Pareto front highlights the optimal solutions, providing a clear pathway to balance energy absorption, water resistance, and fire resistance for the material's intended application in underground mining environments.

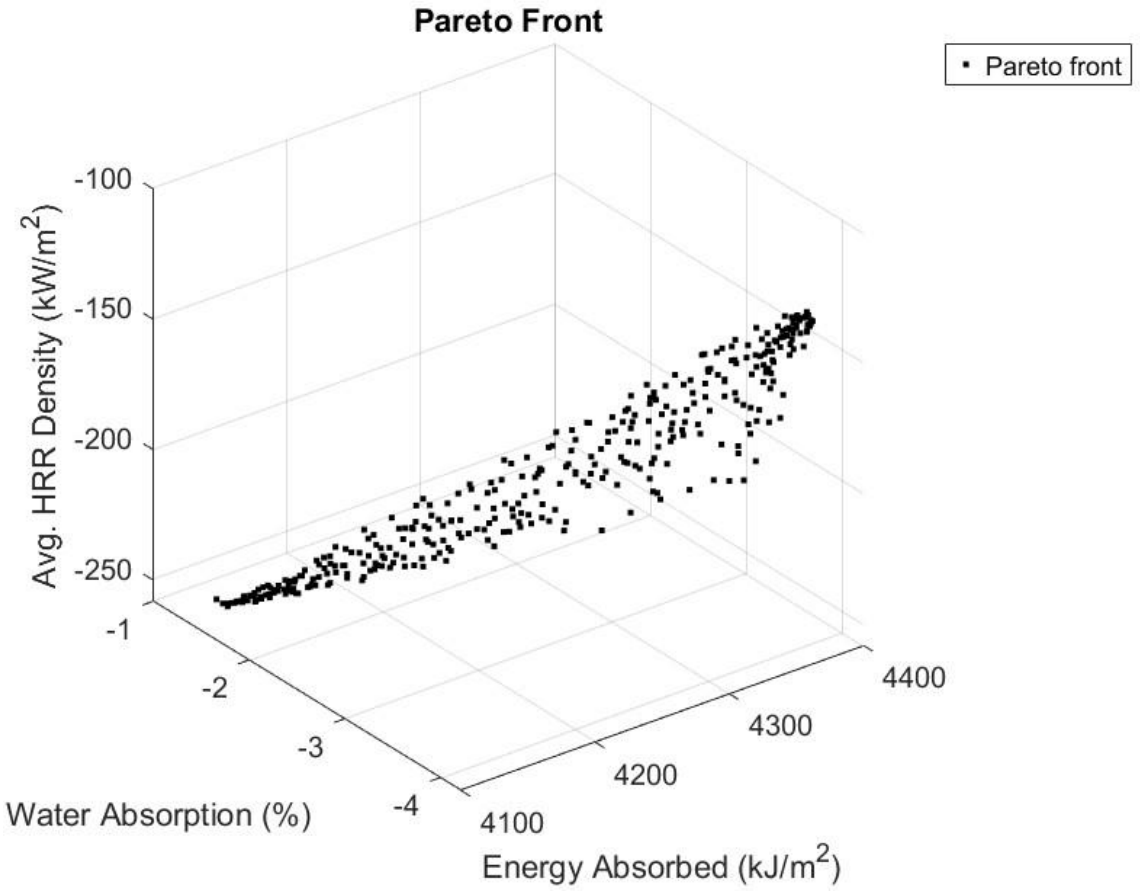

Figure 5.35 3D Pareto Front Representing Trade-Offs Among Water Absorption, Energy Absorbed, and Avg. HRR Density

CHAPTER 6

CONCLUSIONS AND RECOMMENDATIONS

This research successfully bridges the gap between agricultural waste management and sustainable industrial material development. By utilizing locally available hemp fibers and employing innovative chemical treatments, the study presents a cost-effective and environmentally friendly solution for mining ventilation systems.

6.1 Conclusions

i. This research successfully demonstrates the potential of agricultural byproducts, specifically hemp fibers, as a valuable resource for creating high-performance materials. The study highlights the economic and environmental benefits of converting waste into sustainable composites, supporting a circular economy.

ii. Alkali (NaOH) treatments were shown to significantly alter the hemp fiber surface, enhancing fiber-matrix bonding. Optimal treatment levels (5% NaOH) improved fiber purity and structural integrity, while excessive treatment (10% NaOH) led to fiber degradation and reduced performance

iii. Ammonium polyphosphate (APP) was identified as an effective flame retardant. Incorporating APP into both fibers and epoxy resin significantly enhanced the fire resistance of the composites, with 20% APP achieving optimal performance.

iv. A systematic approach using the hand layup method ensured consistent composite fabrication, achieving a 30:70 fiber-to-resin ratio. The methodology provided a reproducible way to produce bio-based composites suitable for industrial applications.

v. Taguchi's design of experiments (DOE) and genetic algorithm optimization facilitated efficient exploration of treatment parameters, identifying the best combination of fiber treatments for mechanical strength and fire resistance. The optimal combination of 5% NaOH and 20% APP delivered composites with superior tensile, flexural, and impact properties.

vi. Rigorous testing demonstrated the composites' ability to withstand the mechanical, thermal, and fire-resistance requirements of mining ventilation systems. SEM analysis

provided insights into fiber surface morphology and bonding, confirming the effectiveness of the chemical treatments.

vii. The research contributes to global sustainability efforts by reducing reliance on synthetic materials and offering an eco-friendly alternative for industrial applications. It provides a model for integrating agricultural waste management with industrial innovation, fostering environmental stewardship and economic growth.

viii. By using locally abundant hemp fibers, the study proposes an economical solution for managing agricultural waste. The findings are directly applicable to industries such as mining, where there is a growing demand for cost-effective, fire-resistant materials.

ix. The study offers a framework for developing bio-composites, paving the way for future research in sustainable materials. It highlights the potential of combining bio-based fibers with chemical treatments to enhance performance properties.

6.2 Recommendations for future work

The following are suggested for future work:

i. Develop prototypes of mining ventilation ducts using the optimized composite material. Conduct real-world testing in mining environments to evaluate long-term performance under operational conditions.

ii. Investigate large-scale manufacturing techniques to produce the composites economically. Collaborate with industries to transition from laboratory research to commercial applications.

iii. Extend the research to other agricultural byproducts to assess their suitability for bio-composite development. Compare performance metrics across different fiber sources to diversify applications.

iv. Utilize advanced techniques like X-ray diffraction and thermal analysis to further understand the microstructural and thermal behavior of the composites. Study the impact of fiber orientation and distribution on composite properties.

v. Evaluate the life cycle impact of the composite materials to ensure alignment with sustainability goals. Assess recyclability and end-of-life management strategies for the composites.

REFERENCES

Abdurohman, K., Satrio, T., Muzayadah, N. L., & Teten, N. (2018). A comparison process between hand lay-up, vacuum infusion and vacuum bagging method toward e-glass EW 185/lycal composites. *Journal of Physics Conference Series*, *1130*, 012018. https://doi.org/10.1088/1742-6596/1130/1/012018

Adapa, Tabil, Schoenau, Canam, & Dumonceaux. (2011). Quantitative Analysis of Lignocellulosic Components of Non-Treated and Steam Exploded Barley, Canola, Oat and Wheat Straw Using Fourier Transform Infrared Spectroscopy. *农业科学与技术：B*, *1*(2), 177 188. http://www.cqvip.com/QK/71212X/201102/38408484.html

Agriculture Sector Overview. (n.d.). https://www.saskatchewan.ca. Retrieved July 29, 2024, from https://www.saskatchewan.ca/business/agriculture-natural-resources-and-industry/agribusiness-farmers-and-ranchers/saskatchewan-import-and-export-information/resources-for-importers/agriculture-sector-overview#:~:text=Saskatchewan%20is%20the%20world's%20leading,berries%2C%20organic%20products%20and%20potatoes.

Agwa, M., Youssef, S. M., Ali-Eldin, S. S., & Megahed, M. (2020). Integrated vacuum assisted resin infusion and resin transfer molding technique for manufacturing of nano-filled glass fiber reinforced epoxy composite. *Journal of Industrial Textiles*, *51*(3_suppl), 5113S-5144S. https://doi.org/10.1177/1528083720932337

Ahmad, F., Choi, H. S., & Park, M. K. (2014). A Review: Natural Fiber Composites Selection in View of Mechanical, Light Weight, and Economic Properties. *Macromolecular Materials and Engineering*, *300*(1), 10–24. https://doi.org/10.1002/mame.201400089

Ajila, C. M., Brar, S. K., Verma, M., & Rao, U. J. S. P. (2011). Sustainable Solutions for Agro Processing Waste Management: An Overview. In *Springer eBooks* (pp. 65–109). https://doi.org/10.1007/978-94-007-1591-2_3

Akhtar, M. N., Sulong, A. B., Radzi, M. F., Ismail, N., Raza, Muhamad, N., & Khan, M. A. (2016). Influence of alkaline treatment and fiber loading on the physical and mechanical properties of kenaf/polypropylene composites for variety of applications. *Progress in Natural Science Materials International*, *26*(6), 657–664. https://doi.org/10.1016/j.pnsc.2016.12.004

Albrecht, W., Fuchs, H., & Kittelmann, W. (Eds.). (2003). *Nonwoven Fabrics: Raw Materials, Manufacture, Applications, Characteristics, Testing Processes*. John Wiley & Sons.

Alhaddi, H. (2015). Triple Bottom Line and Sustainability: A Literature Review. *Business and Management Studies*, *1*(2), 6. https://doi.org/10.11114/bms.v1i2.752

Amarakoon, M., Alenezi, H., Homer-Vanniasinkam, S., & Edirisinghe, M. (2022). Environmental Impact of Polymer Fiber Manufacture. *Macromolecular Materials and Engineering*, *307*(11). https://doi.org/10.1002/mame.202200356

Aravindh, M., Sathish, S., Raj, R. R., Karthick, A., Mohanavel, V., Patil, P. P., Muhibbullah, M., & Osman, S. M. (2022). A Review on the Effect of Various Chemical Treatments on the Mechanical Properties of Renewable Fiber-Reinforced Composites. *Advances in Materials Science and Engineering*, *2022*, 1–24. https://doi.org/10.1155/2022/2009691

Asim, M., Paridah, M. T., Chandrasekar, M., Shahroze, R. M., Jawaid, M., Nasir, M., & Siakeng, R. (2020). Thermal stability of natural fibers and their polymer composites. *Iranian Polymer Journal*, *29*(7), 625–648. https://doi.org/10.1007/s13726-020-00824-6

Asim, M., Paridah, M. T., Chandrasekar, M., Shahroze, R. M., Jawaid, M., Nasir, M., & Siakeng, R. (2020). Thermal stability of natural fibers and their polymer composites. *Iranian Polymer Journal*, *29*(7), 625–648. https://doi.org/10.1007/s13726-020-00824-6

Asma, B., Hamdi, L., Ali, B., & Youcef, M. (2020). Flexural Mechanical Properties of Natural Fibre Reinforced Polymer Composites — A Statistical Investigation. *Fibers and Polymers*, *21*(10), 2321–2337. https://doi.org/10.1007/s12221-020-1299-1

ASTM D570, Standard Test Method for Water Absorption of Plastics, ASTM Int. U.S.A 2022.

ASTM C518, Standard Test Method for Steady-State Thermal Transmission Properties by Means of the Heat Flow Meter Apparatus, ASTM Int. U.S.A 2021.

ASTM D256, Standard Test Methods for Determining the Izod Pendulum Impact Resistance of Plastics, ASTM Int. U.S.A 2024.

ASTM D2734, Standard Test Methods for Void Content of Reinforced Plastics, ASTM Int. U.S.A 2023.

ASTM D638, Standard Test Method for Tensile Properties of Plastics, ASTM Int. U.S.A 2022.

ASTM D790, Standard Test Methods for Flexural Properties of Unreinforced and Reinforced Plastics and Electrical Insulating Materials, ASTM Int. U.S.A 2017.

ASTM E1474, Standard Test Method for Determining the Heat Release Rate of Upholstered Furniture and Mattress Components or Composites Using a Bench Scale Oxygen Consumption Calorimeter, ASTM Int. U.S.A 2022.

Asyraf, M. R. M., Nurazzi, N. M., Norrrahim, M. N. F., Hazrati, K. Z., Ghani, A., Sabaruddin, F. A., Lee, S. H., Shazleen, S. S., & Razman, M. R. (2023). Thermal properties of oil palm lignocellulosic fibre reinforced polymer composites: a comprehensive review on thermogravimetry analysis. *Cellulose*, *30*(5), 2753–2790. https://doi.org/10.1007/s10570-023-05080-4

Atiqah, A., Jawaid, M., Sapuan, S. M., & Ishak, M. R. (2017). Mechanical and Thermal Properties of Sugar Palm Fiber Reinforced Thermoplastic Polyurethane Composites: Effect of Silane Treatment and Fiber Loading. *JOURNAL OF RENEWABLE MATERIALS*. https://doi.org/10.7569/jrm.2017.634188

Awasthi, M. K., Sindhu, R., Sirohi, R., Kumar, V., Ahluwalia, V., Binod, P., Juneja, A., Kumar, D., Yan, B., Sarsaiya, S., Zhang, Z., Pandey, A., & Taherzadeh, M. J. (2022). Agricultural waste biorefinery development towards circular bioeconomy. *Renewable and Sustainable Energy Reviews*, *158*, 112122. https://doi.org/10.1016/j.rser.2022.112122

Azman, M. A., Asyraf, M. R. M., Khalina, A., Petrů, M., Ruzaidi, C. M., Sapuan, S. M., Nik, W. B. W., Ishak, M. R., Ilyas, R. A., & Suriani, M. J. (2021). Natural Fiber Reinforced Composite Material for Product Design: A Short Review. *Polymers*, *13*(12), 1917. https://doi.org/10.3390/polym13121917

Babrauskas, V. (2015). The Cone Calorimeter. In *Springer eBooks* (pp. 952–980). https://doi.org/10.1007/978-1-4939-2565-0_28

Bachtiar, D., Sapuan, S., & Hamdan, M. (2008). The effect of alkaline treatment on tensile properties of sugar palm fibre reinforced epoxy composites. *Materials & Design (1980-2015)*, *29*(7), 1285–1290. https://doi.org/10.1016/j.matdes.2007.09.006

Bachtiar, E. V., Kurkowiak, K., Yan, L., Kasal, B., & Kolb, T. (2019). Thermal Stability, Fire Performance, and Mechanical Properties of Natural Fibre Fabric-Reinforced Polymer Composites with Different Fire Retardants. *Polymers*, *11*(4), 699. https://doi.org/10.3390/polym11040699

Bai, J. (2013). *Advanced Fibre-Reinforced Polymer (FRP) Composites for Structural Applications*. Woodhead Publishing.

Baroncini, E. A., Yadav, S. K., Palmese, G. R., & Stanzione, J. F. (2016). Recent advances in bio-based epoxy resins and bio-based epoxy curing agents. *Journal of Applied Polymer Science*, *133*(45). https://doi.org/10.1002/app.44103

Benin, S., Kannan, S., Bright, R. J., & Moses, A. J. (2020). A review on mechanical characterization of polymer matrix composites & its effects reinforced with various natural fibres. *Materials Today Proceedings*, *33*, 798–805. https://doi.org/10.1016/j.matpr.2020.06.259

Budd, R., & Cree, D. (2018). Effect of fire retardants on mechanical properties of a green bio-epoxy composite. *Journal of Applied Polymer Science*, *136*(16). https://doi.org/10.1002/app.47398

Cairns, D. S., & Shramstad, J. D. (2000b). *Evaluation of Hand Lay-Up and Resin Transfer Molding in Composite Wind Turbine Blade Manufacturing*. https://doi.org/10.2172/760737

Canada, N. R. (2024, October 21). *Minerals and the economy*. https://natural-resources.canada.ca/our-natural-resources/minerals-mining/mining-data-statistics-and-analysis/minerals-and-the-economy/20529

Chapple, S., & Anandjiwala, R. (2010). Flammability of Natural Fiber-reinforced Composites and Strategies for Fire Retardancy: A Review. *Journal of Thermoplastic Composite Materials*, *23*(6), 871–893. https://doi.org/10.1177/0892705709356338

Chaudhary, V., Bajpai, P. K., & Maheshwari, S. (2017). Studies on Mechanical and Morphological Characterization of Developed Jute/Hemp/Flax Reinforced Hybrid Composites for Structural Applications. *Journal of Natural Fibers*, *15*(1), 80–97. https://doi.org/10.1080/15440478.2017.1320260

Chen, H., Ginzburg, V. V., Yang, J., Yang, Y., Liu, W., Huang, Y., Du, L., & Chen, B. (2016). Thermal conductivity of polymer-based composites: Fundamentals and applications. *Progress in Polymer Science*, *59*, 41–85. https://doi.org/10.1016/j.progpolymsci.2016.03.001

Chen, R. S., Ahmad, S., Gan, S., Salleh, M. N., Ghani, M. H. A., & Tarawneh, M. A. (2016). Effect of polymer blend matrix compatibility and fibre reinforcement content on thermal stability and flammability of ecocomposites made from waste materials. *Thermochimica Acta*, *640*, 52–61. https://doi.org/10.1016/j.tca.2016.08.005

Cherney, J., & Small, E. (2016). Industrial Hemp in North America: Production, Politics and Potential. *Agronomy*, *6*(4), 58. https://doi.org/10.3390/agronomy6040058

Cong, H., Meng, H., Chen, M., Song, W., & Xing, H. (2023). Co-processing paths of agricultural and rural solid wastes for a circular economy based on the construction concept of "zero-waste city" in China. *Circular Economy*, *2*(4), 100065. https://doi.org/10.1016/j.cec.2023.100065

Davis, R., & John, P. (2018). Application of Taguchi-Based Design of Experiments for Industrial Chemical Processes. In *InTech eBooks*. https://doi.org/10.5772/intechopen.69501

Debnath, K., & Singh, I. (2017). *Primary and Secondary Manufacturing of Polymer Matrix Composites*. CRC Press.

Edwards, B. K. (2009). COMPOSITE MANUFACTURING OF SMALL WIND TURBINE BLADES. In *www.proquest.com*. California Polytechnic State University.

Elkington, M., Bloom, D., Ward, C., Chatzimichali, A., & Potter, K. (2015b). Hand layup: understanding the manual process. *Advanced Manufacturing Polymer & Composites Science*, *1*(3), 138–151. https://doi.org/10.1080/20550340.2015.1114801

Estrellan, C. R., & Iino, F. (2010). Toxic emissions from open burning. *Chemosphere*, *80*(3), 193–207. https://doi.org/10.1016/j.chemosphere.2010.03.057

Fitzpatrick, P., De Freitas Castro Fonseca, A., & McAllister, M. L. (2011). From the Whitehorse Mining Initiative Towards Sustainable Mining: lessons learned. *Journal of Cleaner Production*, *19*(4), 376–384. https://doi.org/10.1016/j.jclepro.2010.10.013

Fonseca, A., McAllister, M. L., & Fitzpatrick, P. (2014). Sustainability reporting among mining corporations: a constructive critique of the GRI approach. *Journal of Cleaner Production*, *84*, 70–83. https://doi.org/10.1016/j.jclepro.2012.11.050

Forsdyke, K. L., & Starr, T. F. (2002). *Thermoset Resins Market Report*. Rapra Technology Limited.

Friesen, B. (2019). Agricultural waste management in Canada, United States, New Zealand and Australia. *Acta Horticulturae*, *1252*, 93–96. https://doi.org/10.17660/actahortic.2019.1252.12

Fu, S. Y., & Lauke, B. (1996). Effects of fiber length and fiber orientation distributions on the tensile strength of short-fiber-reinforced polymers. *Composites Science and Technology*, *56*(10), 1179–1190. https://doi.org/10.1016/s0266-3538(96)00072-3

García, M., Hidalgo, J., Garmendia, I., & García-Jaca, J. (2009). Wood–plastics composites with better fire retardancy and durability performance. *Composites Part a Applied Science and Manufacturing*, *40*(11), 1772–1776. https://doi.org/10.1016/j.compositesa.2009.08.010

Gassan, J., & Bledzki, A. K. (1999b). Possibilities for improving the mechanical properties of jute/epoxy composites by alkali treatment of fibres. *Composites Science and Technology*, *59*(9), 1303–1309. https://doi.org/10.1016/s0266-3538(98)00169-9

Ghani, J., Choudhury, I., & Hassan, H. (2003). Application of Taguchi method in the optimization of end milling parameters. *Journal of Materials Processing Technology*, *145*(1), 84–92. https://doi.org/10.1016/s0924-0136(03)00865-3

Gholampour, A., & Ozbakkaloglu, T. (2019). A review of natural fiber composites: properties, modification and processing techniques, characterization, applications. *Journal of Materials Science*, *55*(3), 829–892. https://doi.org/10.1007/s10853-019-03990-y

Gholampour, A., & Ozbakkaloglu, T. (2019b). A review of natural fiber composites: properties, modification and processing techniques, characterization, applications. *Journal of Materials Science*, *55*(3), 829–892. https://doi.org/10.1007/s10853-019-03990-y

Gontard, N., Sonesson, U., Birkved, M., Majone, M., Bolzonella, D., Celli, A., Angellier-Coussy, H., Jang, G. W., Verniquet, A., Broeze, J., Schaer, B., Batista, A. P., & Sebok, A. (2018). A research challenge vision regarding management of agricultural waste in a circular bio-based economy. *Critical Reviews in Environmental Science and Technology*, *48*(6), 614–654. https://doi.org/10.1080/10643389.2018.1471957

Gorman, M. R., & Dzombak, D. A. (2018). A review of sustainable mining and resource management: Transitioning from the life cycle of the mine to the life cycle of the mineral. *Resources Conservation and Recycling*, *137*, 281–291. https://doi.org/10.1016/j.resconrec.2018.06.001

Greenhalgh, E. S. (2009). Failure analysis and fractography of polymer composites. In *Woodhead Publishing Limited eBooks*. https://doi.org/10.1533/9781845696818

Guan, Y. H., Huang, J. Q., Yang, J. C., Shao, Z. B., & Wang, Y. Z. (2015). An Effective Way To Flame-Retard Biocomposite with Ethanolamine Modified Ammonium Polyphosphate and Its Flame Retardant Mechanisms. *Industrial & Engineering Chemistry Research*, *54*(13), 3524–3531. https://doi.org/10.1021/acs.iecr.5b00123

H. Tamaki, H. Kita and S. Kobayashi, "Multi-objective optimization by genetic algorithms: a review," *Proceedings of IEEE International Conference on Evolutionary Computation*, Nagoya, Japan, 1996, pp. 517-522, doi: 10.1109/ICEC.1996.542653.

Hale, A., Macosko, C. W., & Bair, H. E. (1991). Glass transition temperature as a function of conversion in thermosetting polymers. *Macromolecules*, *24*(9), 2610–2621. https://doi.org/10.1021/ma00009a072

Hamann, R. (2003). Mining companies' role in sustainable development: The "why" and "how" of corporate social responsibility from a business perspective. *Development Southern Africa*, *20*(2), 237–254. https://doi.org/10.1080/03768350302957

Haque, F., Fan, C., & Lee, Y.-Y. (2023). From waste to value: Addressing the relevance of waste recovery to agricultural sector in line with circular economy. *Journal of Cleaner Production*, *415*.

Hassan, T., Jamshaid, H., Mishra, R., Khan, M. Q., Petru, M., Novak, J., Choteborsky, R., & Hromasova, M. (2020). Acoustic, Mechanical and Thermal Properties of Green Composites Reinforced with Natural Fibers Waste. *Polymers*, *12*(3), 654. https://doi.org/10.3390/polym12030654

Health Canada. (2018, November 7). *Hemp and the hemp industry Frequently Asked Questions*. Canada.ca. https://www.canada.ca/en/health-canada/services/drugs-medication/cannabis/producing-selling-hemp/about-hemp-canada-hemp-industry/frequently-asked-questions.html

Hocking, R. R. (2013). *Methods and Applications of Linear Models: Regression and the Analysis of Variance*. John Wiley & Sons.

Hörold, S. (1999). Phosphorus flame retardants in thermoset resins. *Polymer Degradation and Stability*, *64*(3), 427–431. https://doi.org/10.1016/s0141-3910(98)00163-3

Huang, C., Han, L., Liu, X., & Ma, L. (2010). The Rapid Estimation of Cellulose, Hemicellulose, and Lignin Contents in Rice Straw by Near Infrared Spectroscopy. *Energy Sources Part a Recovery Utilization and Environmental Effects*, *33*(2), 114–120. https://doi.org/10.1080/15567030902937127

Huang, Y., Gong, X., Peng, Y., Lin, X., & Kim, C. (2011). Effects of the ventilation duct arrangement and duct geometry on ventilation performance in a subway tunnel. *Tunnelling and Underground Space Technology*, *26*(6), 725–733. https://doi.org/10.1016/j.tust.2011.05.005

Huda, M. S., Drzal, L. T., Mohanty, A. K., & Misra, M. (2008). Effect of chemical modifications of the pineapple leaf fiber surfaces on the interfacial and mechanical properties of laminated biocomposites. *Composite Interfaces*, *15*(2–3), 169–191. https://doi.org/10.1163/156855408783810920

Ihsan, A., Widodo, N. P., Cheng, J., & Wang, E. (2024). Ventilation on demand in underground mines using neuro-fuzzy models: Modeling and laboratory-scale experimental validation. *Engineering Applications of Artificial Intelligence*, *133*, 108048. https://doi.org/10.1016/j.engappai.2024.108048

Iqbal, M. H., Verma, S. K., & Agrawal, A. P. (2024). Experimental Analysis of Hybrid Composite Sheets: Epoxy Resin Reinforced with Date Palm Fiber and Spent Alumina Catalyst. *Journal of the Institution of Engineers (India) Series D*. https://doi.org/10.1007/s40033-024-00791-9

Irshad, K., Habib, K., Thirumalaiswamy, N., & Saha, B. B. (2015). Performance analysis of a thermoelectric air duct system for energy-efficient buildings. *Energy*, *91*, 1009–1017. https://doi.org/10.1016/j.energy.2015.08.102

Islam, T., Chaion, M. H., Jalil, M. A., Rafi, A. S., Mushtari, F., Dhar, A. K., & Hossain, S. (2024). Advancements and challenges in natural fiber-reinforced hybrid composites: A comprehensive review. *SPE Polymers*, *5*(4), 481–506. https://doi.org/10.1002/pls2.10145

John, M. J., & Anandjiwala, R. D. (2007). Recent developments in chemical modification and characterization of natural fiber-reinforced composites. *Polymer Composites*, *29*(2), 187–207. https://doi.org/10.1002/pc.20461

John, M. J., & Anandjiwala, R. D. (2007). Recent developments in chemical modification and characterization of natural fiber-reinforced composites. *Polymer Composites*, *29*(2), 187–207. https://doi.org/10.1002/pc.20461

Kalia, S., Kaith, B., & Kaur, I. (2009). Pretreatments of natural fibers and their application as reinforcing material in polymer composites—A review. *Polymer Engineering and Science*, *49*(7), 1253–1272. https://doi.org/10.1002/pen.21328

Kamarudin, S. H., Basri, M. S. M., Rayung, M., Abu, F., Ahmad, S., Norizan, M. N., Osman, S., Sarifuddin, N., Desa, M. S. Z. M., Abdullah, U. H., Tawakkal, I. S. M. A., & Abdullah, L. C. (2022b). A Review on Natural Fiber Reinforced Polymer Composites (NFRPC) for Sustainable Industrial Applications. *Polymers*, *14*(17), 3698. https://doi.org/10.3390/polym14173698

Khalid, M. Y., Rashid, A. A., Arif, Z. U., Ahmed, W., & Arshad, H. (2021). Recent advances in nanocellulose-based different biomaterials: types, properties, and emerging applications. *Journal of Materials Research and Technology*, *14*, 2601–2623. https://doi.org/10.1016/j.jmrt.2021.07.128

Khalili, P., Liu, X., Tshai, K. Y., Rudd, C., Yi, X., & Kong, I. (2019). Development of fire retardancy of natural fiber composite encouraged by a synergy between zinc borate and ammonium polyphosphate. *Composites Part B Engineering*, *159*, 165–172. https://doi.org/10.1016/j.compositesb.2018.09.036

Khalili, P., Tshai, K., Hui, D., & Kong, I. (2017). Synergistic of ammonium polyphosphate and alumina trihydrate as fire retardants for natural fiber reinforced epoxy

composite. *Composites Part B Engineering*, *114*, 101–110. https://doi.org/10.1016/j.compositesb.2017.01.049

Koul, B., Yakoob, M., & Shah, M. P. (2022). Agricultural waste management strategies for environmental sustainability. *Environmental Research*, *206*, 112285. https://doi.org/10.1016/j.envres.2021.112285

Ku, H., Wang, H., Pattarachaiyakoop, N., & Trada, M. (2011). A review on the tensile properties of natural fiber reinforced polymer composites. *Composites Part B Engineering*, *42*(4), 856–873. https://doi.org/10.1016/j.compositesb.2011.01.010

Laurence, D. (2011). Establishing a sustainable mining operation: an overview. *Journal of Cleaner Production*, *19*(2–3), 278–284.

Lee, C. H., Khalina, A., & Lee, S. H. (2021). Importance of Interfacial Adhesion Condition on Characterization of Plant-Fiber-Reinforced Polymer Composites: A Review. *Polymers*, *13*(3), 438. https://doi.org/10.3390/polym13030438

Li, X., Tabil, L. G., & Panigrahi, S. (2007). Chemical Treatments of Natural Fiber for Use in Natural Fiber-Reinforced Composites: A Review. *Journal of Polymers and the Environment*, *15*(1), 25–33. https://doi.org/10.1007/s10924-006-0042-3

Lim, K. S., Bee, S. T., Sin, L. T., Tee, T. T., Ratnam, C., Hui, D., & Rahmat, A. (2016). A review of application of ammonium polyphosphate as intumescent flame retardant in thermoplastic composites. *Composites Part B Engineering*, *84*, 155–174. https://doi.org/10.1016/j.compositesb.2015.08.066

Losada-Pérez, P., Tripathi, C. S. P., Leys, J., Cordoyiannis, G., Glorieux, C., & Thoen, J. (2011). Measurements of Heat Capacity and Enthalpy of Phase Change Materials by Adiabatic Scanning Calorimetry. *International Journal of Thermophysics*, *32*(5), 913–924. https://doi.org/10.1007/s10765-011-0984-0

Lowell, S., Shields, J. E., Thomas, M. A., & Thommes, M. (2004). *Characterization of Porous Solids and Powders: Surface Area, Pore Size and Density*. Kluwer Academic Publishers.

Lu, Yingxiang, "Composites for hydraulic structures: a review" (2018). *Graduate Theses, Dissertations, and Problem Reports*. 4008. https://researchrepository.wvu.edu/etd/4008

Mann, G. S., Azum, N., Khan, A., Rub, M. A., Hassan, M. I., Fatima, K., & Asiri, A. M. (2023). Green Composites Based on Animal Fiber and Their Applications for a Sustainable Future. *Polymers*, *15*(3), 601. https://doi.org/10.3390/polym15030601

Marti, J., Idelsohn, S. R., & Oñate, E. (2018). A Finite Element Model for the Simulation of the UL-94 Burning Test. *Fire Technology*, *54*(6), 1783–1805. https://doi.org/10.1007/s10694-018-0769-0

Masud, M., & Chorzepa, M. G. (2016). Impact resilience of multiscale fibre reinforced composites. *Magazine of Concrete Research*, *68*(8), 379–390. https://doi.org/10.1680/jmacr.15.00184

Matkó, S., Toldy, A., Keszei, S., Anna, P., Bertalan, G., & Marosi, G. (2005). Flame retardancy of biodegradable polymers and biocomposites. *Polymer Degradation and Stability*, *88*(1), 138–145. https://doi.org/10.1016/j.polymdegradstab.2004.02.023

Mehdikhani, M., Gorbatikh, L., Verpoest, I., & Lomov, S. V. (2018). Voids in fiber-reinforced polymer composites: A review on their formation, characteristics, and effects on mechanical performance. *Journal of Composite Materials*, *53*(12), 1579–1669. https://doi.org/10.1177/0021998318772152

Menczel, J. D., & Prime, R. B. (Eds.). (2008). *Thermal Analysis of Polymers: Fundamentals and Applications*. John Wiley & Sons, Inc. https://doi.org/10.1002/9780470423837

Menczel, J. D., Judovits, L., Prime, R. B., Bair, H. E., Reading, M., & Swier, S. (2008). Differential Scanning Calorimetry (DSC). In *Thermal Analysis of Polymers: Fundamentals and Applications*. https://doi.org/10.1002/9780470423837.ch2

Meredith, J., Ebsworth, R., Coles, S. R., Wood, B. M., & Kirwan, K. (2011). Natural fibre composite energy absorption structures. *Composites Science and Technology*, *72*(2), 211–217. https://doi.org/10.1016/j.compscitech.2011.11.004

Middleton, B. (2016). Composites: Manufacture and Application. In *Elsevier eBooks* (pp. 53–101). https://doi.org/10.1016/b978-0-323-34061-8.00003-x

Minerals and the economy. (2024, October 21). Natural Resources Canada. https://natural-resources.canada.ca/our-natural-resources/minerals-mining/mining-data-statistics-and-analysis/minerals-and-the-economy/20529

Mishra, S. N., Mitra, S., Rangan, L., Dutta, S., & Singh, P. (2012). Exploration of 'hot-spots' of methane and nitrous oxide emission from the agriculture fields of Assam, India. *Agriculture & Food Security*, *1*(1). https://doi.org/10.1186/2048-7010-1-16

Mmereki, D., Baldwin, A., & Li, B. (2016). A comparative analysis of solid waste management in developed, developing and lesser developed countries. *Environmental Technology Reviews*, *5*(1), 120–141. https://doi.org/10.1080/21622515.2016.1259357

Mooleki, S. P., McVicar, R., Brenzil, C., Panchuk, K., Pearse, P., & Hartley, S. (2013). Hemp Production in Saskatchewan. Saskatchewan Ministry of Agriculture. https://publications.saskatchewan.ca/api/v1/products/75243/formats/84152/download

More, A. P. (2021). Flax fiber–based polymer composites: a review. *Advanced Composites and Hybrid Materials*, *5*(1), 1–20. https://doi.org/10.1007/s42114-021-00246-9

Mori, T. (2011). *Taguchi Methods: Benefits, Impacts, Mathematics, Statistics, and Applications*. Amer Society of Mechanical.

Mosaad, S., Issa, U., & Hassan, M. S. (2017). Risks affecting the delivery of HVAC systems: Identifying and analysis. *Journal of Building Engineering*, *16*, 20–30. https://doi.org/10.1016/j.jobe.2017.12.004

Murali, B., Yogesh, P., Karthickeyan, N., & Chandramohan, D. (2022). Multi-potency of bast fibers (flax, hemp and jute) as composite materials and their mechanical properties: A review. *Materials Today Proceedings*, *62*, 1839–1843. https://doi.org/10.1016/j.matpr.2022.01.001

Mutlur, S. (2004). Thermal Analysis of Composites Using DSC. In *Advanced Topics in Characterization of Composites*.

Nagendran, R. (2011). Agricultural Waste and Pollution. In *Elsevier eBooks* (pp. 341–355).

Nikafshar, S., Zabihi, O., Hamidi, S., Moradi, Y., Barzegar, S., Ahmadi, M., & Naebe, M. (2017). A renewable bio-based epoxy resin with improved mechanical performance that can compete with DGEBA. *RSC Advances*, *7*(14), 8694–8701. https://doi.org/10.1039/c6ra27283e

Nishino, T., Hirao, K., & Kotera, M. (2006). X-ray diffraction studies on stress transfer of kenaf reinforced poly(l-lactic acid) composite. *Composites Part a Applied Science and Manufacturing*, *37*(12), 2269–2273. https://doi.org/10.1016/j.compositesa.2006.01.026

Norouzi, A., & Zaim, A. H. (2014). Genetic Algorithm Application in Optimization of Wireless Sensor Networks. *The Scientific World JOURNAL*, *2014*, 1–15. https://doi.org/10.1155/2014/286575

Nurazzi, N. M., Asyraf, M. R. M., Rayung, M., Norrrahim, M. N. F., Shazleen, S. S., Rani, M. S. A., Shafi, A. R., Aisyah, H. A., Radzi, M. H. M., Sabaruddin, F. A., Ilyas, R. A., Zainudin, E. S., & Abdan, K. (2021). Thermogravimetric Analysis Properties of Cellulosic Natural Fiber Polymer Composites: A Review on Influence of Chemical Treatments. *Polymers*, *13*(16), 2710. https://doi.org/10.3390/polym13162710

Obileke, K., Nwokolo, N., Makaka, G., Mukumba, P., & Onyeaka, H. (2020). Anaerobic digestion: Technology for biogas production as a source of renewable energy—A review. *Energy & Environment*, *32*(2), 191–225. https://doi.org/10.1177/0958305x20923117

Painton, L., & Campbell, J. (1995). Genetic algorithms in optimization of system reliability. *IEEE Transactions on Reliability*, *44*(2), 172–178. https://doi.org/10.1109/24.387368

Parvez, A. M., Lewis, J. D., & Afzal, M. T. (2021). Potential of industrial hemp (Cannabis sativa L.) for bioenergy production in Canada: Status, challenges and outlook. *Renewable and Sustainable Energy Reviews*, *141*, 110784. https://doi.org/10.1016/j.rser.2021.110784

Phiri, R., Rangappa, S. M., Siengchin, S., Oladijo, O. P., & Ozbakkaloglu, T. (2024). Advances in lightweight composite structures and manufacturing technologies: A comprehensive review. *Heliyon*, *10*(21).

Phuong, N. L., & Ito, K. (2012). Experimental and numerical study of airflow pattern and particle dispersion in a vertical ventilation duct. *Building and Environment*, *59*, 466–481. https://doi.org/10.1016/j.buildenv.2012.09.014

Prabhu, L., Krishnaraj, V., Sathish, S., Gokulkumar, S., Karthi, N., Rajeshkumar, L., Balaji, D., Vigneshkumar, N., & Elango, K. (2021). A review on natural fiber reinforced hybrid composites: chemical treatments, manufacturing methods and potential applications. *Materials Today Proceedings*, *45*, 8080–8085. https://doi.org/10.1016/j.matpr.2021.01.280

Priya, A. K., Alagumalai, A., Balaji, D., & Song, H. (2023). Bio-based agricultural products: a sustainable alternative to agrochemicals for promoting a circular economy. *RSC Sustainability*, *1*(4), 746–762. https://doi.org/10.1039/d3su00075c

Rajak, D. K., Wagh, P. H., & Linul, E. (2022). A Review on Synthetic Fibers for Polymer Matrix Composites: Performance, Failure Modes and Applications. *Materials*, *15*(14), 4790. https://doi.org/10.3390/ma15144790

Rao, R. S., Kumar, C. G., Prakasham, R. S., & Hobbs, P. J. (2008). The Taguchi methodology as a statistical tool for biotechnological applications: A critical appraisal. *Biotechnology Journal*, *3*(4), 510–523. https://doi.org/10.1002/biot.200700201

Rodriguez, J. M., Molnar, J. J., Fazio, R. A., Sydnor, E., & Lowe, M. J. (2008). Barriers to adoption of sustainable agriculture practices: Change agent perspectives. *Renewable Agriculture and Food Systems*, *24*(1), 60–71. https://doi.org/10.1017/s1742170508002421

Rout, J., Misra, M., Tripathy, S., Nayak, S., & Mohanty, A. (2001). The influence of fibre treatment on the performance of coir-polyester composites. *Composites Science and Technology*, *61*(9), 1303–1310. https://doi.org/10.1016/s0266-3538(01)00021-5

Rout, J., Tripathy, S. S., Nayak, S. K., Misra, M., & Mohanty, A. K. (2000). Scanning electron microscopy study of chemically modified coir fibers. *Journal of Applied Polymer Science*, *79*(7), 1169–1177. https://doi.org/10.1002/1097-4628(20010214)79:7

Ruuska, T., Vinha, J., & Kivioja, H. (2016). Measuring thermal conductivity and specific heat capacity values of inhomogeneous materials with a heat flow meter apparatus. *Journal of Building Engineering*, *9*, 135–141. https://doi.org/10.1016/j.jobe.2016.11.011

Sahu, P., & Gupta, M. (2019). A review on the properties of natural fibres and its bio-composites: Effect of alkali treatment. *Proceedings of the Institution of Mechanical Engineers Part L Journal of Materials Design and Applications*, *234*(1), 198–217. https://doi.org/10.1177/1464420719875163

Sarstedt, M., & Mooi, E. (2018). Regression Analysis. In *Springer texts in business and economics* (pp. 209–256). https://doi.org/10.1007/978-3-662-56707-4_7

Saskatchewan Minerals: How mining benefited local and global communities in 2023. (2024). Saskatchewan Mining Association.

Saskatchewan Potash Nourishing the Earth: A snapshot of Saskatchewan's potash industry in 2023. (2024). Saskatchewan Mining Association. Retrieved November 11, 2024, from http://saskmining.ca/ckfinder/userfiles/files/SMA-Potash-Infographic-2024-Stats-WEB(1).pdf

Saskatchewan Uranium Energizing the World: A snapshot of Saskatchewan's uranium industry in 2023. (2024). Saskatchewan Mining Association. Retrieved November 4, 2024, from http://saskmining.ca/ckfinder/userfiles/files/SMA-Uranium-Infographic-2024-Stats-WEB(1).pdf

Schartel, B., & Hull, T. R. (2007). Development of fire-retarded materials—Interpretation of cone calorimeter data. *Fire and Materials*, *31*(5), 327–354. https://doi.org/10.1002/fam.949

Schartel, B., Bartholmai, M., & Knoll, U. (2005). Some comments on the use of cone calorimeter data. *Polymer Degradation and Stability*, *88*(3), 540–547. https://doi.org/10.1016/j.polymdegradstab.2004.12.016

Sherwani, S., Sapuan, S., Leman, Z., Zainudin, E., & Khalina, A. (2021). Effect of alkaline and benzoyl chloride treatments on the mechanical and morphological properties of sugar palm fiber-reinforced poly(lactic acid) composites. *Textile Research Journal*, *92*(3–4), 593–607. https://doi.org/10.1177/00405175211041878

Shriwas, M., & Pritchard, C. (2020). Ventilation Monitoring and Control in Mines. *Mining Metallurgy & Exploration*, *37*(4), 1015–1021. https://doi.org/10.1007/s42461-020-00231-8

Siedt, M., Schäffer, A., Smith, K. E., Nabel, M., Roß-Nickoll, M., & Van Dongen, J. T. (2021). Comparing straw, compost, and biochar regarding their suitability as agricultural soil amendments to affect soil structure, nutrient leaching, microbial communities, and the fate of pesticides. *Science of the Total Environment*, *751*, 141607. https://doi.org/10.1016/j.scitotenv.2020.141607

Sisti, L., Totaro, G., Vannini, M., Celli, A. (2018). Retting Process as a Pretreatment of Natural Fibers for the Development of Polymer Composites. In: Kalia, S. (eds) Lignocellulosic Composite Materials. Springer Series on Polymer and Composite Materials. Springer, Cham. https://doi.org/10.1007/978-3-319-68696-7_2

Stark, N. M., White, R. H., Mueller, S. A., & Osswald, T. A. (2010). Evaluation of various fire retardants for use in wood flour–polyethylene composites. *Polymer Degradation and Stability*, *95*(9), 1903–1910. https://doi.org/10.1016/j.polymdegradstab.2010.04.014

Sun, J., Xu, F., Sun, X., Xiao, B., & Sun, R. (2005). Physico-chemical and thermal characterization of cellulose from barley straw. *Polymer Degradation and Stability*, *88*(3), 521–531. https://doi.org/10.1016/j.polymdegradstab.2004.12.013

Taib, M. N. a. M., Hamidon, T. S., Garba, Z. N., Trache, D., Uyama, H., & Hussin, M. H. (2022). Recent progress in cellulose-based composites towards flame retardancy applications. *Polymer*, *244*, 124677. https://doi.org/10.1016/j.polymer.2022.124677

Tao, J., Ge, Y., Liang, R., Sun, Y., Cheng, Z., Yan, B., & Chen, G. (2022). Technologies integration towards bio-fuels production: A state-of-the-art review. *Applications in Energy and Combustion Science*, *10*, 100070. https://doi.org/10.1016/j.jaecs.2022.100070

Tator, K. B. (2015). Epoxy Resins and Curatives. In *Protective Organic Coatings* (Vol. 5B, pp. 63–79). ASM International. https://doi.org/10.31399/asm.hb.v05b.a0006077

Tiwari, A. K., & Pal, D. B. (2022). Nutrients contamination and eutrophication in the river ecosystem. In *Elsevier eBooks* (pp. 203–216). https://doi.org/10.1016/b978-0-323-85045-2.00001-7

UL 94, Tests for Flammability of Plastic Materials for Parts in Devices and Appliances, Published February 28, 2023

Ulrich, K. T., and W. P. Seering. 1988. “Function Sharing in Mechanical Design.” The Seventh National Conference on Artificial Intelligence 1: 342–370.

Umeda, Y., H. Takeda, T. Tomiyama, and H. Yoshikawa. 1990. “Function, Behaviour, andStructure.” In Applications of Artificial Intelligence in Engineering, V, edited by J. S. Gero, 177–193. Southampton: Computational Mechanics Publications and Springer-Verlag.

Van De Weyenberg, I., Ivens, J., De Coster, A., Kino, B., Baetens, E., & Verpoest, I. (2003). Influence of processing and chemical treatment of flax fibres on their composites. *Composites Science and Technology*, *63*(9), 1241–1246. https://doi.org/10.1016/s0266-3538(03)00093-9

Veiga, M. M., Scoble, M., & McAllister, M. L. (2001). Mining with communities. *Natural Resources Forum*, *25*(3), 191–202. https://doi.org/10.1111/j.1477-8947.2001.tb00761.x

Verma, D., & Goh, K. L. (2021). Effect of Mercerization/Alkali Surface Treatment of Natural Fibres and Their Utilization in Polymer Composites: Mechanical and Morphological Studies. *Journal of Composites Science*, *5*(7), 175. https://doi.org/10.3390/jcs5070175

Verma, D., & Goh, K. L. (2021). Effect of Mercerization/Alkali Surface Treatment of Natural Fibres and Their Utilization in Polymer Composites: Mechanical and Morphological Studies. *Journal of Composites Science*, *5*(7), 175. https://doi.org/10.3390/jcs5070175

Wang, R., & Schuman, T. (2014). Towards Green: A Review of Recent Developments in Bio-renewable Epoxy Resins from Vegetable Oils. In *Green Materials from Plant Oils* (pp. 202–241). Royal Society of Chemistry. https://doi.org/10.1039/9781782621850-00202

Wang, Y., Jow, J., Su, K., & Zhang, J. (2012). Development of the unsteady upward fire model to simulate polymer burning under UL94 vertical test conditions. *Fire Safety Journal*, *54*, 1–13. https://doi.org/10.1016/j.firesaf.2012.08.001

Wang, Y., Zhang, F., Chen, X., Jin, Y., & Zhang, J. (2009). Burning and dripping behaviors of polymers under the UL94 vertical burning test conditions. *Fire and Materials*, *34*(4), 203–215. https://doi.org/10.1002/fam.1021

Xiao, B., Yang, Y., Wu, X., Liao, M., Nishida, R., & Hamada, H. (2015). Hybrid laminated composites molded by spray lay-up process. *Fibers and Polymers*, *16*(8), 1759–1765. https://doi.org/10.1007/s12221-015-5298-6

Yan, L., Chouw, N., & Jayaraman, K. (2014). Flax fibre and its composites – A review. *Composites Part B Engineering*, *56*, 296–317. https://doi.org/10.1016/j.compositesb.2013.08.014

Yan, L., Chouw, N., Huang, L., & Kasal, B. (2016). Effect of alkali treatment on microstructure and mechanical properties of coir fibres, coir fibre reinforced-polymer composites and reinforced-cementitious composites. *Construction and Building Materials*, *112*, 168-182. https://doi.org/10.1016/j.conbuildmat.2016.02.182

Yang, B., Yao, H., & Wang, F. (2022). A Review of Ventilation and Environmental Control of Underground Spaces. *Energies*, *15*(2), 409. https://doi.org/10.3390/en15020409

Yang, X., & Zhang, W. (2018). Flame retardancy of Wood-Polymeric composites. In *Elsevier eBooks* (pp. 285–317). https://doi.org/10.1016/b978-0-12-815067-2.00011-1

Yeboah, D., Ackor, N., & Abrowah, E. (2023). Evaluation of Wind Energy Recovery from an Underground Mine Exhaust Ventilation System. *Journal of Engineering*, *2023*, 1–20. https://doi.org/10.1155/2023/8822475

Yu, B., Liu, X., Ji, C., & Sun, H. (2023). Greenhouse gas mitigation strategies and decision support for the utilization of agricultural waste systems: A case study of Jiangxi Province, China. *Energy*, *265*, 126380. https://doi.org/10.1016/j.energy.2022.126380

Yuan, Y., Lin, W., Xiao, Y., Yu, B., & Wang, W. (2024). Flame-retardant epoxy thermosets derived from renewable resources: research development and future perspectives. *Journal of Material Science and Technology*. https://doi.org/10.1016/j.jmst.2024.02.006

YÜKSEL, N. (2016). The review of some commonly used methods and techniques to measure the thermal conductivity of insulation materials. In *Insulation Materials in Context of Sustainability*. In tech Publication. https://doi.org/10.5772/64157

Zhang, L., Larsson, A., Moldin, A., & Edlund, U. (2022). Comparison of lignin distribution, structure, and morphology in wheat straw and wood. *Industrial Crops and Products*, *187*, 115432. https://doi.org/10.1016/j.indcrop.2022.115432

Zhang, L., Niu, K., Wang, H., Wang, J., Liu, M., Lei, Y., & Yan, L. (2024). Char formation and smoke suppression mechanism of montmorillonite modified by ammonium polyphosphate/silane towards fire safety enhancement for wood composites. *Wood Science and Technology*, *58*(2), 811–827. https://doi.org/10.1007/s00226-024-01546-1

Zhang, M., Anderson, S. L., Brym, Z. T., & Pearson, B. J. (2021). Photoperiodic Flowering Response of Essential Oil, Grain, and Fiber Hemp (Cannabis sativa L.) Cultivars. *Frontiers in Plant Science*, *12*. https://doi.org/10.3389/fpls.2021.694153

Zhang, W. J., Lin, Y., & Sinha, N. (2011). ON THE FUNCTION-BEHAVIOR-STRUCTURE MODEL FOR DESIGN. *Proceedings of the Canadian Engineering Education Association (CEEA)*. https://doi.org/10.24908/pceea.v0i0.3884

Zhang, W., & Wang, J. (2016). Design theory and methodology for enterprise systems. *Enterprise Information Systems*, *10*(3), 245-248. https://doi.org/10.1080/17517575.2015.1080860

Zhou, Y., Fan, M., & Chen, L. (2016). Interface and bonding mechanisms of plant fibre composites: An overview. *Composites Part B Engineering*, *101*, 31–45. https://doi.org/10.1016/j.compositesb.2016.06.055

APPENDIX

MATLAB code for genetic algorithm multi-objective optimization:

```
fun = @moo_objective_functions;
nvars = 3;
A = []; b = []; Aeq = []; beq = [];
lb = [0, 0, 0]; ub = [10, 20, 20];
nonlcon = @moo_const;
opts.PopulationSize = 1000;
[x,fval,exitflag,output,fg] = gamultiobj(fun,nvars,A,b,Aeq,beq,lb,ub,nonlcon,opts);
H = fval(:,1);
WA = fval(:,2);
HRR = fval(:,3);
scatter3(H,WA,HRR,'k.');
xlabel('Energy Absorbed (kJ/m^2)')
ylabel('Water Absorption (%)')
zlabel('Avg. HRR Density (kW/m^2)')
title('Pareto Front')
legend('Pareto front')



function [g_ineq, h_eq] = moo_const (x)

B = x(2); C = x(3);

g_ineq(1) = B - C;

h_eq = [];
end



function f = moo_objective_functions (x)
A = x(1); B = x(2); C = x(3);

f(1) = 4127.7 + 3.93*A + 0.54*B + 11.24*C;
f(2) = - (1.31105 - 0.65670*A + 0.019912*B + 0.12833*C);
f(3) = - (259.5 - 5.13*A - 4.58*B - 2.60*C);

end
```

Table A.1 Dataset of 350 optimized combinations

Serial No.	Optimal Solution			fval		
	A	B	C	Energy absorbed	Water absorption (%)	Avg. HRR Density (kW/m2)
1	0.0245	1.4643	2.6796	4158.7053	1.6680	245.7012
2	0.0259	0.1351	0.8832	4137.8022	1.4101	256.4518
3	0.0138	0.1291	2.8904	4160.3123	1.6755	251.3226
4	0.0187	0.2561	1.0448	4139.6548	1.4379	255.5148
5	0.0284	0.6213	0.8876	4138.1235	1.4187	254.2011
6	0.0072	17.5999	19.9922	4361.9448	4.2223	126.8756
7	0.0218	14.2523	18.9254	4348.2036	4.0092	144.9066
8	0.0187	0.7092	0.8885	4138.1433	1.4269	253.8457
9	0.0180	0.5736	1.9639	4150.1550	1.5627	251.6745
10	0.0559	15.8938	16.7596	4324.8804	3.7416	142.8449
11	0.0111	0.1638	1.3383	4142.8739	1.4788	255.2137
12	0.0437	12.3174	19.1423	4349.6824	3.9842	153.0924
13	0.0264	17.9880	19.3272	4354.7545	4.1321	126.7290
14	0.0004	0.5141	1.4454	4144.2250	1.5065	253.3855
15	0.0052	17.3927	19.9438	4361.2809	4.2134	127.9610
16	0.0191	0.0270	0.3427	4131.6417	1.3430	258.3870
17	0.0264	18.1130	19.8272	4360.4420	4.1988	124.8565
18	0.0544	16.4189	18.3546	4343.0859	3.9577	136.3004
19	0.0222	17.9630	19.6648	4358.5194	4.1778	125.9870
20	0.1429	0.1316	0.1826	4130.3852	1.2432	257.6890
21	0.0228	1.2993	3.5515	4168.4098	1.7777	244.1986
22	0.0094	17.7336	19.9073	4361.0713	4.2127	126.4731
23	0.0072	18.0999	19.4922	4356.5948	4.1681	125.8856
24	0.0577	0.1472	0.2307	4130.5989	1.3057	257.9302
25	0.0220	0.5125	3.2298	4164.3660	1.7213	248.6425
26	0.0259	0.6351	1.1332	4140.8822	1.4521	253.5118
27	0.0651	4.1955	8.2053	4222.4491	2.4049	218.6168
28	0.0410	2.9066	5.7060	4193.5655	2.0743	231.1420
29	0.0554	2.6928	3.4112	4167.7138	1.7660	238.0135
30	0.0072	17.8499	19.4922	4356.4598	4.1632	127.0306
31	0.0115	1.7583	5.5510	4191.0875	2.0509	236.9556
32	0.0054	0.3057	1.3227	4142.7535	1.4834	254.6335
33	0.0181	11.5351	14.1027	4292.5147	3.3387	169.9094

34	0.0255	1.1189	4.6188	4180.3190	1.9093	242.2363
35	0.0375	13.2267	14.6783	4299.9745	3.4334	160.5654
36	0.0157	16.0318	18.5442	4344.8559	3.9997	137.7787
37	0.0441	11.6844	19.0972	4348.8358	3.9655	156.1062
38	0.0266	0.2839	0.6795	4135.5957	1.3864	256.2963
39	0.0111	17.2630	19.4426	4355.6005	4.1426	129.8278
40	0.0085	17.2329	19.0797	4351.4950	4.0971	130.9223
41	0.0466	2.9289	3.6324	4170.2927	1.8049	236.4024
42	0.0127	0.3975	2.6444	4157.6871	1.6500	250.7391
43	0.0791	9.0176	9.7036	4241.9489	2.6839	192.5638
44	0.0464	13.2528	17.2803	4329.2689	3.7620	153.6356
45	0.0072	17.1564	19.9395	4361.1126	4.2068	129.0441
46	0.0305	1.0884	2.1173	4152.2063	1.5844	248.8537
47	0.0524	14.5562	17.5896	4333.4733	3.8238	146.8308
48	0.0324	0.4162	1.8359	4148.6872	1.5336	252.6542
49	0.0223	6.3633	14.7896	4297.4593	3.3210	191.7886
50	0.0172	16.5841	19.6664	4357.7735	4.1537	132.3237
51	0.0153	16.3292	18.7470	4347.2945	4.0319	135.8916
52	0.0229	12.6458	16.1256	4315.8709	3.6172	159.5381
53	0.0295	0.5410	1.2527	4142.1885	1.4632	253.6139
54	0.0367	13.6479	18.8252	4346.8096	3.9745	147.8588
55	0.0258	0.8187	1.2608	4142.4150	1.4722	252.3401
56	0.0345	16.9034	17.2981	4331.3944	3.8449	136.9303
57	0.0147	16.7273	19.8983	4360.4473	4.1880	131.0781
58	0.0962	13.9383	16.7277	4323.6239	3.6720	151.6768
59	0.0294	1.9390	4.4476	4178.8536	1.9011	238.9048
60	0.0245	13.7635	15.0241	4304.0993	3.4971	157.2747
61	0.0191	0.2770	0.3427	4131.7767	1.3480	257.2420
62	0.0197	0.3406	0.6891	4135.7069	1.3933	256.0475
63	0.0191	0.2770	0.4677	4133.1817	1.3640	256.9170
64	0.0212	0.5557	3.3021	4165.1994	1.7319	248.2604
65	0.0415	9.8543	18.8646	4345.2222	3.9009	165.1067
66	0.0292	11.6143	13.2979	4283.5544	3.2297	171.5822
67	0.0056	17.3395	19.1558	4352.3963	4.1109	130.2514
68	0.0313	3.4859	16.9056	4319.7237	3.5294	199.4196
69	0.0353	10.6341	18.1953	4338.0965	3.8346	163.3069
70	0.0484	13.8033	16.9839	4326.2427	3.7336	151.8743
71	0.0313	1.4428	3.8649	4172.0429	1.8152	242.6832
72	0.0197	16.5822	19.9132	4360.5564	4.1837	131.6781
73	0.0197	0.5914	2.4872	4156.0532	1.6290	250.2234

74	0.0762	14.7589	17.5665	4333.4164	3.8092	145.8403
75	0.0571	12.3376	18.8058	4345.9633	3.9326	153.8058
76	0.0502	6.8369	6.8900	4209.0334	2.2984	210.0153
77	0.0226	0.5566	4.0358	4173.4514	1.8252	246.3420
78	0.0315	1.9675	5.9079	4195.2904	2.0877	234.9672
79	0.0098	18.1087	19.6971	4358.9123	4.1929	125.2997
80	0.0337	2.4308	12.4923	4269.5584	2.9405	215.7140
81	0.0329	11.0218	11.8955	4267.4858	3.0355	177.9236
82	0.0404	2.8364	4.9249	4184.7462	1.9730	233.4975
83	0.0407	0.0771	1.6090	4145.9864	1.4924	254.7549
84	0.0340	16.0389	19.4486	4355.0970	4.1039	135.3010
85	0.0489	2.9959	8.5654	4225.7849	2.4378	223.2581
86	0.0180	0.8236	1.9639	4150.2900	1.5677	250.5295
87	0.0172	16.5841	19.1664	4352.1535	4.0896	133.6237
88	0.0592	14.4374	19.5712	4355.7096	4.0712	142.1877
89	0.0336	17.0717	19.4986	4356.2151	4.1312	130.4430
90	0.0157	16.5318	19.0442	4350.7459	4.0739	134.1887
91	0.0261	18.4261	19.7454	4359.6904	4.1947	123.6368
92	0.0264	17.6130	19.3272	4354.5520	4.1247	128.4465
93	0.0742	7.5527	18.8286	4343.7035	3.8290	175.5735
94	0.0664	6.6680	8.2249	4224.0098	2.4557	207.2353
95	0.0391	3.7796	10.4494	4247.3455	2.7016	214.8205
96	0.0461	7.2872	9.3269	4236.6509	2.6228	201.6382
97	0.0637	7.2431	11.0764	4256.3603	2.8348	197.2009
98	0.0385	13.5490	18.7552	4345.9764	3.9624	148.4843
99	0.0552	12.1260	14.6762	4299.4251	3.3996	165.5215
100	0.0349	5.6506	5.8238	4196.3477	2.1480	218.2993
101	0.0600	2.6982	11.2576	4255.9282	2.7701	217.5648
102	0.0496	0.0921	2.5164	4156.2287	1.6032	252.2812
103	0.0518	2.8106	8.9456	4229.9694	2.4810	223.1029
104	0.0277	1.3556	7.3237	4210.8593	2.2597	234.1078
105	0.0337	10.6299	16.9635	4324.2427	3.6775	166.5369
106	0.0575	7.2707	13.1328	4279.4643	3.1034	191.7601
107	0.0713	2.5717	7.5195	4213.8877	2.2804	227.8052
108	0.0418	1.8462	8.2719	4221.8367	2.3819	229.3234
109	0.0662	6.8740	8.6815	4229.2516	2.5186	205.1059
110	0.0452	5.1554	9.0129	4231.9664	2.5407	212.2230
111	0.1032	8.3181	16.3618	4316.5036	3.5086	178.3332
112	0.0394	15.2797	18.6335	4345.5463	3.9807	140.8699
113	0.0373	13.4920	15.7397	4312.0468	3.5751	156.5918

114	0.0297	11.7781	17.3895	4329.6343	3.7577	160.1916
115	0.0249	0.2631	0.6393	4135.1250	1.3820	256.5056
116	0.0541	10.1143	14.1724	4292.6723	3.2957	176.0509
117	0.0583	2.8916	7.3956	4212.6169	2.2794	226.7289
118	0.0115	16.3253	17.7682	4336.2752	3.9088	138.4741
119	0.0837	13.7975	14.4642	4298.0570	3.3870	158.2711
120	0.0234	2.4681	3.4470	4167.8691	1.7872	239.1141
121	0.0412	14.9109	18.4112	4342.8556	3.9436	143.1277
122	0.0382	2.0766	3.0036	4162.7325	1.7128	241.9835
123	0.0472	4.8144	9.6588	4239.0505	2.6154	212.0949
124	0.0137	14.7095	16.5537	4321.7609	3.7193	149.0209
125	0.0259	0.6351	2.1332	4152.1222	1.5804	250.9118
126	0.0041	18.4086	19.3542	4355.1983	4.1586	124.8466
127	0.0344	14.0092	18.3481	4341.6329	3.9220	147.4561
128	0.0111	1.1638	1.3383	4143.4139	1.4987	250.6337
129	0.0255	1.1189	5.6188	4191.5590	2.0377	239.6363
130	0.0185	5.3138	7.2753	4212.4162	2.3383	216.1523
131	0.0412	14.0295	18.6194	4344.7198	3.9527	146.6229
132	0.0519	10.9708	16.1285	4315.1123	3.5652	167.0536
133	0.0193	0.7227	3.3458	4165.7729	1.7421	247.3921
134	0.0523	5.4836	10.7232	4251.3956	2.7620	206.2363
135	0.0339	9.7639	11.1691	4258.6460	2.9166	185.5681
136	0.0294	13.3476	13.8127	4290.2779	3.3301	162.3042
137	0.0335	9.9510	16.1170	4314.3605	3.5555	171.8484
138	0.0354	2.1945	5.8240	4194.4858	2.0789	234.1250
139	0.0489	7.9635	15.3662	4304.9083	3.4094	182.8244
140	0.0350	13.3771	18.2381	4340.0571	3.8949	150.6345
141	0.0184	8.6662	19.2869	4349.2371	3.9466	169.5686
142	0.0158	8.9014	14.4393	4294.8662	3.3309	181.1081
143	0.0108	14.7058	15.2570	4307.1724	3.5547	152.4236
144	0.0380	18.1102	19.2465	4353.9592	4.1166	126.3194
145	0.0303	2.4560	5.2832	4188.5285	2.0181	234.3599
146	0.0768	3.4619	11.1251	4254.9172	2.7572	214.3253
147	0.0756	8.5870	9.9985	4245.0171	2.7155	193.7879
148	0.0496	11.8864	16.7194	4322.2391	3.6608	161.3354
149	0.0324	2.3154	3.9024	4172.9412	1.8367	238.5829
150	0.0116	17.3264	19.8524	4360.2424	4.1961	128.4697
151	0.0248	4.5501	11.4154	4258.5634	2.8503	208.8531
152	0.0852	10.3325	14.8743	4300.8012	3.3697	173.0668
153	0.0536	10.8247	19.6725	4354.8753	4.0159	158.4993

154	0.0552	0.9306	13.9973	4285.7494	3.0896	218.5618
155	0.0505	4.3426	6.4776	4203.0517	2.1956	222.5102
156	0.0287	3.4900	4.3395	4178.4732	1.9186	232.0858
157	0.0462	0.6316	8.3238	4221.7821	2.3614	234.7281
158	0.0427	6.7630	12.4475	4271.4293	3.0150	195.9427
159	0.0263	8.4030	15.7388	4309.2453	3.4809	179.9585
160	0.0237	5.1812	19.1491	4345.8266	3.8560	185.8606
161	0.0520	6.5207	14.6768	4296.3923	3.2902	191.2090
162	0.0566	14.9072	17.9437	4337.6592	3.8734	144.2812
163	0.0125	1.2507	3.3242	4165.7883	1.7544	245.0649
164	0.0625	5.9764	11.9930	4265.9737	2.9281	200.6257
165	0.0242	1.0451	1.8195	4148.8109	1.5495	249.8589
166	0.0440	1.9669	4.1244	4175.2939	1.8506	239.5421
167	0.0232	9.3480	15.1966	4303.6485	3.4322	177.0563
168	0.0381	4.3577	6.6942	4205.4451	2.2319	221.9417
169	0.0425	7.8528	11.0402	4256.1996	2.8563	194.6117
170	0.0551	9.3824	16.6986	4320.6753	3.6046	172.8299
171	0.0523	8.8756	14.2113	4292.4332	3.2772	181.6321
172	0.0222	6.5176	9.2120	4234.8492	2.6084	205.5844
173	0.0087	0.6959	2.6543	4157.9442	1.6598	249.3667
174	0.0188	16.6887	19.3924	4354.7567	4.1197	132.5490
175	0.0524	5.8268	12.8457	4275.4382	3.0411	199.1456
176	0.0506	11.8787	13.7974	4289.3962	3.2850	168.9627
177	0.0473	3.8215	15.5745	4305.0067	3.3547	201.2608
178	0.0343	15.1446	18.2090	4340.6817	3.9268	142.6181
179	0.0457	9.2676	13.4028	4283.5317	3.1855	181.9725
180	0.0145	6.1063	13.4415	4282.1373	3.1480	196.5107
181	0.0248	9.5064	15.6412	4308.7374	3.4913	175.1665
182	0.0340	6.4064	6.6465	4205.9993	2.2692	212.7033
183	0.0300	0.8653	6.7525	4204.1828	2.1751	237.8267
184	0.0351	3.4946	18.8989	4342.1484	3.7829	194.1779
185	0.0465	3.4923	9.6140	4237.8296	2.5838	218.2703
186	0.0526	11.6230	15.3199	4306.3795	3.4739	166.1649
187	0.0798	3.7363	17.8699	4330.8895	3.6263	195.5165
188	0.0568	11.3490	12.4611	4274.1143	3.0989	174.8314
189	0.0143	0.5035	1.6874	4146.9948	1.5282	252.7332
190	0.0404	0.7610	7.1307	4208.4191	2.2148	237.2675
191	0.0662	8.9756	10.5149	4250.9944	2.7957	190.7133
192	0.0197	1.3406	1.6891	4147.4869	1.5416	248.8675
193	0.0153	15.3292	18.7470	4346.7545	4.0120	140.4716

194	0.0218	13.2523	18.9254	4347.6636	3.9893	149.4866
195	0.0187	1.7092	2.8885	4161.1633	1.7035	244.0657
196	0.0223	6.3633	15.7896	4308.6993	3.4494	189.1886
197	0.0156	7.5651	10.3689	4248.3930	2.7820	197.8123
198	0.0520	7.5411	12.0524	4267.4454	2.9737	193.3588
199	0.0344	15.0092	17.3481	4330.9329	3.8136	145.4761
200	0.0211	18.4314	18.9269	4350.4745	4.0931	125.7659
201	0.0212	1.5557	2.3021	4154.4994	1.6235	246.2804
202	0.0331	1.8202	5.1552	4186.7574	1.9871	237.5900
203	0.0464	1.0944	7.8420	4216.6177	2.3087	233.8601
204	0.0912	1.3089	12.6577	4271.0380	2.9016	220.1274
205	0.0487	2.6217	10.8471	4251.2283	2.7232	219.0401
206	0.0556	6.4584	13.0709	4278.3233	3.0805	195.6509
207	0.0522	9.7472	11.3409	4260.6405	2.9262	185.1033
208	0.0282	1.1890	2.6828	4158.6078	1.6605	246.9344
209	0.0348	4.0593	5.1202	4187.5801	2.0261	227.4177
210	0.0242	0.2137	0.5641	4134.2506	1.3718	256.9307
211	0.1033	2.7745	9.3639	4234.8542	2.5001	221.9167
212	0.0633	11.4145	16.3768	4318.1881	3.5984	164.3170
213	0.0231	5.5857	12.9818	4276.7229	3.0730	200.0459
214	0.0947	3.5571	9.9176	4241.4666	2.5924	216.9370
215	0.0376	1.3756	5.6970	4192.6241	2.0449	238.1953
216	0.0174	6.6796	15.1943	4302.1587	3.3825	189.3131
217	0.0222	11.1404	15.1377	4303.9511	3.4609	169.0051
218	0.0465	3.7306	3.9816	4174.6502	1.8658	231.8232
219	0.0553	0.8721	5.5471	4190.7382	2.0040	240.7994
220	0.0365	15.0871	18.5426	4344.4091	3.9671	142.0029
221	0.0208	1.2373	1.5229	4145.5678	1.5174	249.7666
222	0.0814	4.8356	14.2380	4290.6666	3.1810	199.9164
223	0.0410	4.8438	6.7902	4206.7991	2.2520	219.4504
224	0.0549	2.5353	8.7052	4227.1306	2.4426	224.9735
225	0.0251	4.5664	10.3174	4246.2319	2.7095	211.6318
226	0.0282	8.2416	12.8538	4276.7377	3.1062	188.1890
227	0.0841	1.0003	10.1244	4242.3687	2.5750	228.1634
228	0.0329	14.4217	18.8881	4347.9190	4.0005	144.1706
229	0.0455	2.2020	14.9051	4296.6014	3.2378	210.4278
230	0.0937	8.8913	16.2466	4315.4813	3.5115	176.0559
231	0.0114	3.8000	18.2877	4335.3505	3.7261	194.4895
232	0.0439	9.0254	12.0816	4268.5428	3.0124	186.5266
233	0.0506	2.9315	9.4973	4236.2318	2.5550	221.1214

234	0.0295	4.3456	5.2787	4189.4949	2.0556	225.7211
235	0.0609	13.6746	16.0214	4315.4043	3.5994	154.9023
236	0.0639	10.9995	17.9717	4335.8932	3.7944	162.0678
237	0.0297	3.0446	3.8088	4172.2717	1.8409	235.5003
238	0.0326	4.9520	10.5172	4248.7154	2.7379	209.3082
239	0.0386	8.7454	13.1846	4280.7689	3.1518	184.9683
240	0.0358	1.2395	5.8907	4194.7213	2.0682	238.3237
241	0.0413	3.1825	11.5618	4259.5361	2.8310	214.6514
242	0.0490	2.3534	10.4667	4246.8089	2.6689	221.2567
243	0.0966	15.6528	16.3271	4320.0488	3.6546	144.8643
244	0.0370	11.4114	12.4849	4274.3374	3.1162	174.5855
245	0.0539	2.3726	10.2685	4244.6108	2.6407	221.6591
246	0.0207	6.6184	13.5264	4283.3917	3.1651	193.9133
247	0.0443	0.1543	5.2919	4187.4381	1.9641	244.8072
248	0.0461	1.3233	4.2248	4176.0821	1.8493	242.2183
249	0.0318	3.3584	5.4760	4191.1886	2.0598	229.7182
250	0.0183	11.1569	15.5802	4308.9182	3.5206	167.7988
251	0.0506	7.7659	12.1106	4268.2156	2.9866	192.1853
252	0.0255	4.0500	10.6895	4250.1373	2.7467	213.0272
253	0.0238	12.5776	14.7917	4300.8445	3.4441	163.3142
254	0.0617	0.1811	4.0749	4173.8418	1.7971	247.7595
255	0.0220	7.0989	15.2496	4303.0260	3.3949	187.2248
256	0.0246	2.0376	3.6949	4170.4276	1.8097	240.4352
257	0.0473	1.4820	8.4164	4223.2865	2.3896	230.5875
258	0.0524	15.3930	19.1249	4351.1821	4.0374	139.0062
259	0.0499	8.6415	15.8490	4310.7050	3.4843	178.4586
260	0.0199	3.2731	10.6695	4249.4705	2.7324	216.6668
261	0.0323	4.7196	7.6270	4216.1032	2.3626	217.8883
262	0.0196	12.2140	13.7988	4289.4714	3.3122	167.5823
263	0.0708	13.1026	18.8563	4346.9984	3.9453	150.1005
264	0.0505	16.2387	17.2657	4330.7333	3.8169	139.9771
265	0.0453	13.0904	17.2941	4329.3330	3.7613	154.3490
266	0.0473	7.0829	14.2111	4291.4431	3.2447	189.8690
267	0.0841	4.1395	8.2526	4223.0246	2.3973	218.6528
268	0.0380	6.7976	18.3817	4338.1303	3.7804	180.3797
269	0.0654	11.7221	17.8514	4334.9364	3.7924	159.0636
270	0.0518	10.9818	11.3581	4261.4984	2.9533	179.4065
271	0.0271	3.0918	15.8724	4307.8817	3.3917	203.9322
272	0.0485	14.4786	16.5599	4321.8427	3.6926	149.8837
273	0.0267	5.1911	9.9858	4242.8485	2.6784	209.6246

274	0.0434	2.0516	6.3468	4200.3167	2.1379	233.3792
275	0.0490	6.9172	14.3500	4292.9216	3.2581	190.2576
276	0.0219	0.1318	2.8343	4159.7149	1.6630	251.4149
277	0.0491	7.6188	11.1448	4257.2749	2.8607	195.3773
278	0.0583	17.5595	18.0494	4340.2872	3.9387	131.8494
279	0.0363	6.1062	7.8286	4219.1335	2.4134	210.9932
280	0.0179	2.8808	11.8098	4262.0680	2.8722	215.5089
281	0.0451	4.8995	4.9089	4185.6987	2.0090	224.0658
282	0.0259	6.1859	18.4185	4338.1664	3.7808	183.1476
283	0.0651	5.5699	11.1799	4256.6259	2.8139	204.5879
284	0.0540	12.6864	14.7703	4300.7807	3.4237	162.7165
285	0.0328	8.8258	14.4890	4295.4512	3.3246	181.2379
286	0.0231	0.2885	0.8129	4137.0831	1.4059	255.9466
287	0.0486	0.4443	7.4990	4212.4201	2.2503	237.7182
288	0.0272	1.6835	2.8370	4160.6038	1.6908	244.2741
289	0.0444	1.9269	9.7170	4238.1336	2.5672	225.1828
290	0.0984	7.2783	14.1826	4291.4297	3.2114	188.7858
291	0.0323	0.9829	6.2072	4198.1263	2.1060	238.6938
292	0.0223	1.1078	2.4644	4156.0855	1.6347	247.9047
293	0.0350	7.5359	8.4914	4227.3502	2.5278	202.7284
294	0.0374	1.3480	6.3007	4199.3946	2.1219	236.7526
295	0.0241	2.7377	7.9626	4218.7730	2.3716	226.1349
296	0.0231	10.1052	15.6273	4308.8982	3.5025	172.4686
297	0.0390	10.2189	13.3071	4282.9438	3.1966	177.8984
298	0.0361	4.3073	7.1598	4210.6438	2.2919	220.9719
299	0.0397	3.4078	6.4670	4202.3853	2.1827	226.8743
300	0.0514	5.0701	15.3421	4303.0852	3.3471	196.1257
301	0.0471	10.1598	13.5814	4286.0267	3.2253	177.4148
302	0.0401	3.6662	15.7294	4306.6363	3.3763	201.6062
303	0.0303	17.5195	18.7849	4348.4221	4.0507	130.2646
304	0.0250	10.2919	18.4726	4340.9878	3.8701	164.2058
305	0.0159	17.3783	19.4253	4355.4876	4.1395	129.3200
306	0.0468	1.6323	6.6782	4203.8288	2.1698	234.4204
307	0.0273	4.1206	7.8316	4218.0599	2.3802	220.1256
308	0.0328	7.0105	12.4041	4271.0371	3.0209	194.9728
309	0.0145	16.5111	18.9495	4349.6652	4.0621	134.5360
310	0.0553	1.8104	4.4529	4178.9452	1.8822	239.3473
311	0.0474	8.5257	16.8477	4321.8582	3.6118	176.4051
312	0.0242	1.6183	7.9338	4217.8456	2.3455	231.3357
313	0.0603	15.9050	16.3161	4319.9187	3.6820	143.9241

314	0.0491	7.3595	9.7049	4240.9505	2.6708	200.3087
315	0.0659	10.6205	14.2096	4293.4100	3.3027	173.5749
316	0.0172	3.8754	11.9281	4263.9320	2.9076	210.6494
317	0.0408	2.7820	6.8626	4206.4979	2.2203	228.7065
318	0.0491	2.3732	7.6904	4215.6142	2.3130	228.3840
319	0.0476	8.6370	18.5944	4341.5526	3.8380	171.3526
320	0.0565	9.9269	12.1711	4270.0859	3.0335	182.0998
321	0.0177	12.9058	14.5374	4298.1385	3.4220	162.5037
322	0.0365	0.5064	5.3033	4187.7263	1.9777	243.2049
323	0.0588	4.3579	6.2653	4200.7064	2.1632	222.9496
324	0.0468	13.1897	16.5805	4321.3705	3.6707	155.7421
325	0.0410	6.1817	7.1776	4211.8756	2.3283	212.3160
326	0.0350	4.3170	8.4599	4225.2579	2.4597	217.5527
327	0.0506	10.8787	13.7974	4288.8562	3.2651	173.5427
328	0.0412	0.6526	4.6883	4180.9108	1.8986	244.1098
329	0.0625	6.9764	10.9930	4255.2737	2.8197	198.6457
330	0.0218	15.2523	19.9254	4359.9836	4.1575	137.7266
331	0.0188	15.6887	19.3924	4354.2167	4.0998	137.1290
332	0.0531	16.2019	16.9195	4326.8324	3.7701	141.0323
333	0.0193	0.7227	2.3458	4154.5329	1.6138	249.9921
334	0.0566	15.9072	18.9437	4349.4392	4.0217	137.1012
335	0.0583	3.8916	7.3956	4213.1569	2.2993	222.1489
336	0.0431	7.1908	17.7464	4331.2222	3.7033	180.2043
337	0.0072	17.1564	18.9395	4349.8726	4.0784	131.6441
338	0.0422	2.8140	6.0355	4197.2248	2.1139	230.7032
339	0.0340	17.0389	18.4486	4344.3970	3.9955	133.3210
340	0.0742	8.5527	19.8286	4355.4835	3.9772	168.3935
341	0.0412	15.0295	19.6194	4356.4998	4.1010	139.4429
342	0.0415	8.8543	18.8646	4344.6822	3.8810	169.6867
343	0.0004	1.5141	2.4454	4156.0050	1.6547	246.2055
344	0.0259	0.1351	1.8832	4149.0422	1.5384	253.8518
345	0.0197	0.5914	3.4872	4167.2932	1.7574	247.6234
346	0.0236	6.6639	9.4710	4237.8452	2.6436	204.2334
347	0.0408	4.1904	6.7563	4206.0643	2.2347	222.5321
348	0.0543	2.9124	4.6598	4181.8625	1.9314	233.7672
349	0.0264	16.9880	19.3272	4354.2145	4.1122	131.3090
350	0.0191	0.0270	1.3427	4142.8817	1.4713	255.7870